Advancing novel cell-based therapies for the prevention of graft versus host disease (GVHD) and improvement of engraftment following bone marrow transplantation.

A DISSERTATION SUBMITTED TO THE FACULTY OF THE GRADUATE SCHOOL OF THE UNIVERSITY OF MINNESOTA BY

Steven Lorenz Highfill

IN PARTIAL FULFILLMENT OF THE REQUIREMENTS FOR THE DEGREE OF

DOCTOR OF PHILOSOPHY

Advisor: Bruce R. Blazar, M.D.

June 2010

Acknowledgements

I would first and foremost like to thank my mentor and dissertation advisor, Dr. Bruce R. Blazar. Dr. Blazar's guidance and support has been invaluable to the research outlined here. Despite his busy schedule, Dr. Blazar has always made himself available to me and was always ready and willing to discuss the progress of ongoing projects. Dr. Blazar sets the example as a world class researcher, while at the same time is possibly one of the most humble persons I know. I can only hope to become as successful and as respected as he is.

Secondly, I would like to thank Dr. Jakub Tolar. I have been especially lucky to have Dr.Tolar as a co-mentor. His empathetic demeanor toward his patients is only matched by his energy and enthusiasm for research. I thank him not only for his direct contributions toward this research, but also for the wise advice he continually bestowed upon me.

I have learned a great deal from those who have worked closely with me over these past 5 years and I gratefully acknowledge my debt to them, especially Dr. Christine Vogtenhuber, Dr. Ryan Kelly, Dr. Qing Zhou, Rachelle Veenstra, Michelle Smith, Dr. Pat Taylor, Ron McElmurry, Andy Price, Dr. Mark Osborn, Meghan Munger, Chris Lees, Nick Bade, Matt Weeres and all others in the Blazar lab. Their friendship and professional collaboration has meant a great deal to me and has given me the willpower and motivation to succeed.

I would also like to express my deepest thanks to the members of my thesis committee- Dr. Jeff Miller (committee chair), Dr.Angela Panoskaltsis-Mortari, and Dr. Walter Low. They have generously given their time and expertise to better my work. Were it not for their guidance, I would not have made it this far. Thank you for your excellent advice and encouragement over the years.

Last, and most importantly, I would like to give thanks to my parents, Rosemarie and Douglas Highfill, my brother, Richard Highfill, and my wife and daughter, Sarah and Kaitlyn, for their unfaltering love and support throughout my life.

Abstract

Bone marrow transplantation is a valuable treatment option for patients with underlying hematological disorders. Unfortunately, complications associated with this course of treatment, such as graft versus host disease and graft failure, results in significant morbidity and mortality. Current clinical methodology relies mainly on the use of corticosteroids and pan-T-cell depletion to restrain these complications, however, their global immunosuppressive attributes, toxicity and increased relapse rate of certain cancers has prompted the search for improved therapies. The research described herein investigates novel cell-based methods that may be used in place of current therapies. More specifically, we investigate the use of mutipotent adult progenitor cells (MAPCs) and myeloid-derived suppressor cells (MDSC) for ameliorating acute graft versus host disease (aGVHD) and the use of mesenchymal stem cells (MSCs) for enhancing bone marrow engraftment. For GVHD, we find that both MAPCs and MDSCs have the capacity to inhibit allo-T-cell reactions *in vitro* using two distinct mechanisms. However, we find that when these cells are applied to a murine model of aGVHD, only MDSC express the appropriate homing molecules that allows them to traffic to sites of allogeneic T-cell recognition and activation, and therefore, only MDSC decrease GVHD-related mortality when administered *i.v.* Another major concern following BMT is BM engraftment failure. Currently, MSCs are employed in the clinic as means to promote or enhance BM engraftment, however, there is no definitive mechanism of action identified to be responsible for this effect. We find that MSCs secrete copious amounts of a molecule known to have a positive influence on hematopoietic stem cell (HSC) survival and proliferation, prostaglandin E_2 (PGE_2). We show that the secretion of PGE_2 by MSCs increases the number and differentiation capacity of HSCs and also show that inhibiting the production of PGE_2 from MSCs by using COX inhibitors reverses these effects. These data are the first to define a mechanism of action that MSCs use to promote BM engraftment. In conclusion, the cutting edge preclinical research described here has advanced the field of cell therapies following BMT and will hopefully be used to design clinical regimes aimed at improving the lives of patients in need.

Table of Contents

Acknowledgments ..... *i*

Abstract ..... *ii*

Table of contents ..... *iii*

List of Figures ..... *v*

List of Abbreviations ..... *viii*

Chapter 1: Introduction

History of bone marrow transplantation and the recognition of graft versus host disease . 1

The Major Histocompatibility Complex and the allogeneic T-cell response 2

Dissection of acute graft versus host disease (aGVHD) 4

I. Incidence and diagnosis of aGVHD 4

II. Pathophysiology of aGVHD 5

III. Methods used to prevent aGVHD in mouse and man 8

Graft versus tumor effect 11

Cellular therapy for the treatment of GVHD and enhancement of bone marrow engraftment 12

Regulatory T-cells 12

Mesenchymal Stem Cells 16

Multipotent Adult Progenitor Cells 19

Myeloid-derived Suppressor Cells 20

Thesis Statement 22

Chapter 2: Multipotent adult progenitor cells can suppress graft vs. host disease via prostaglandin E_2 synthesis and only if localized to sites of allopriming

Foreward 29

Introduction 30

Methods 31

Results 36

Discussion 44

Figures 50

Chapter 3: Bone marrow myeloid-derived suppressor cells inhibit graft vs. host disease via an arginase-1 dependent mechanism that is upregulated by IL-13

Foreward 75

Introduction 76

Methods 78

Results 85

Discussion 93

Figures 101

Chapter 4: Mesenchymal stem cells production of prostaglandin E_2 amplifies hematopoietic stem cell differentiation and expansion

Forward 122

Introduction 123

Methods 125

Results 130

Discussion 134

Figures 139

Chapter 5: Concluding Statement 149

Bibliography 153

List of Figures

Chapter 1

Figure 1: The Major Histocompatibility Complex in mice and humans 24

Figure 2: Direct and indirect allorecognition during GVHD 25

Figure 3: Pathophysiology of acute GVHD 26

Figure 4: Diseases treatable by BMT and approximate incidences of new cases per year in the United States 27

Chapter 2

Figure 1: MAPCs potently inhibit allogeneic T-cell proliferation and activation 50

Figure 2: MAPC-mediated suppression in vitro is independent of Tregs 52

Figure 3: MAPCs mediate suppression via a soluble factor 54

Figure 4: MAPCs inhibit T-cell allo-responses by the secretion of PGE_2 56

Figure 5: The capacity of MAPCs to delay GVHD mortality and limit target tissue destruction is dependent on anatomic location of the cells and their production of PGE_2 58

Figure 6: MAPCs dampen T-cell proliferation and activation within the local environment 60

Figure 7: MAPCs affect costimulatory molecule expression on T-cells and DCs in the spleen 62

Supp Fig 1: Characterization of MAPC 64

Supp Fig 2: MAPC inhibit ongoing allo-responses 66

Supp Fig 3: Effects of PGE_2 and IDO on proliferation 68

Supp Fig 4: Persistence of MAPCs delivered intra-splenically 70

Supp Fig 5: Localization of MAPCs to the spleen after “in vivo MLR” 72

Chapter 3

Figure 1: Generation and phenotype of cultured MDSCs 101

Figure 2: MDSC inhibit allo-T-cell responses through the expression of arginase-1 103

Figure 3: MDSC migrate to sites of allo-priming in a GVHD setting 105

Figure 4: Cultured MDSC enhance GVHD survival in an arginase-1 dependent fashion 107

Figure 5: MDSCs negatively impact proliferation, activation, and effector function of donor T-cells 109

Figure 6: MDSC preserve the graft versus leukemia effect of allogeneic donor T-cells 111

Figure 7: PEG-arg1 has similar protective effects as MDSC IL13-tx 113

Supp Fig 1: IL-13 treated MDSC have significantly enhanced suppressive capacity 115

Supp Fig 2: MDSC IL13-tx elicit suppression mostly in a contact independent manner 117

Supp Fig 3: IL13-tx MDSC have enhanced suppressive capacity *in vivo* 119

Chapter 4:

Figure 1: Isolation and characterization of murine BM-derived MSC 139

Figure 2: MSCs produce cytokines that can positively influence BM engraftment 141

Figure 3: Treatment of whole BM ex vivo with MSCs increases HSC number and is partially dependent on PGE_2 143

Figure 4: MSC increase BM colony forming cells and differentiation capabilities 145

Figure 5: MSCs increase primitive CFU-S number and splenic weight post transplant 147

List of Abbreviations

Allo-HSCT: Allogeneic hematopoietic stem cell transplantation

APC: Antigen presenting cell

Arg-1: Arginase-1

BM: Bone marrow

BMT: Bone marrow transplantation

CCL: Chemokine C-C motif ligand (e.g., CCL19, CCL21)

CCR: Chemokine receptor (e.g., CCR7)

CD: Cluster of differentiation (e.g., CD4, CD8)

CFU: Colony forming unit

CFU-S12: Colony forming unit-spleen day12

c-kit/SCF: Cytokine stem cell factor

CTLA-4: Cytotoxic T-lymphocyte antigen 4

CXCL: Chemokine (C-X-C motif) ligand (e.g., CXCL12)

DC: Dendritic cell

DISC: Death-induced signaling complex

EGF: Epidermal growth factor

EP receptor: E family of prostaglandin receptors

FoxP3: Forkhead box P3

G-CSF: Granulocye stimulating factor

GI: gastro intestinal

GITR: Glucocorticoid-induced tumor necrosis factor receptor

GM-CSF: Granulocyte macrophage stimulating factor

GVHD: Graft versus host disease

GVL (GVT): Graft versus leukemia (graft versus tumor)

HGF: Hepatocyte growth factor

HLA: Human leukocyte antigen

HSC: Hematopoietic stem cell

HSCT: Hematopoietic stem cell transplant

HVEM: Herpes virus entry mediator

ICOS: Inducible T-cell costimulator

IDO: Indoleamine 2,3 dioxygenase

IFN-γ: Interferon gamma

IgG1: Immunoglobulin, isotype G1

IL-2: Interleukin-2

IL-4: Interleukin-4

IL-10: Interleukin-10

KGF: Keratinocyte growth factor

LIF: Leukemia inhibitory factor

LPS: Lipopolysaccharide

LSK: Lineage negative, stem cell factor positive, c-kit positive

MAPC: Multipotent adult progenitor cell

MDSC: Myeloid-derived suppressor cell

mHags: Minor histocompatibility antigens

MHC-I/II: Major histocompatibility complex I/II

MSC: Mesenchymal stem cell

NK cell: Natural killer cell

OX40/OX40L: Tumor necrosis factor superfamily member 4 / ligand

PB: Peripheral blood

PD-1/PD-L1: Programmed death-1 / Programmed death ligand-1

PDGF: Platelet-derived growth factor

PG: Prostaglandins

PGE_2: Prostaglandin E_2

qRT-PCR: Quantitative reverse transcriptase polymerase chain reaction

Sca-1: Stem cell antigen-1

SLO: Secondary lymphoid organ

TCR: T-cell receptor

TGF-β: Transforming growth factor beta

TNF-α: Tumor necrosis factor alpha

Treg: Regulatory T-cell

UCB: Umbilical cord blood

INTRODUCTION:

History of bone marrow transplantation and the recognition of graft versus host disease

The era of BMT began more than half a century ago in 1949 with the observation that shielding the spleens of experimental rodents with lead foil from external irradiation followed by the infusion of bone marrow cells could rescue animals from radiation-induced death.[1] In these early studies, emphasis was placed on the protective nature of BM cells and the success of the transplant was measured by 20 or 30 day survival periods. It wasn't until the mid-1950's that a secondary cause of mortality was first reported. Here, Barnes *et al*., reported that lethally irradiated mice receiving syngeneic (i.e., genetically identical) spleen cells were afforded long-term survival, whereas more than half of the mice receiving allogeneic (i.e., genetically disparate) spleen cells succumbed to a "wasting disease" before day 100.[2] Mice receiving allogeneic cells had very distinct clinical manifestations, including severe diarrhea, weight loss, retarded growth, liver abnormalities, and skin lesions. Lymphocytes were identified as the mediators of these effects by the observation that the severity of these manifestations directly correlated with the number of lymphocytes within the graft. In the 1960's the term graft versus host disease (GVHD) was coined by Billingham and Simonsen, and the minimum criteria for its development was put forth.[3,4] These criteria are: (1) immunocompetent donor cells must be transferred to the recipient; (2) there must be some degree of histoincompatibility between the donor and recipient; (3) the recipient must be incapable of destroying or inactivating the transplanted cells.[3] These criteria remain as the basis of our understanding of the disease today.

The Major Histocompatibility Complex and the allogeneic T-cell response

Arguably one of the most significant developments in the field of bone marrow transplantation was the discovery of the Major Histocompatibility Complex (MHC) molecules. MHC molecules, termed HLA in humans and H-2 in mice, are responsible for presenting foreign antigens to T-cells. Aside from the T-cells ability to recognize the antigen presented by the MHC as foreign, T-cells can also recognize the MHC itself as foreign. In syngeneic bone marrow transplantations, there is perfect histocompatibility, meaning the MHC loci are genetically identical between donor and recipient. In this case, the donor is fully tolerant of host tissue and there is no elicitation of an immune response following transplant. During allogeneic bone marrow transplants, however, differences in MHC (termed histo*in*compatable) are recognized as foreign antigens, which triggers a T-cell response. It is estimated that up to 10% of T-cells are alloreactive toward a given allogeneic MHC molecule.[5] This T-cell alloreactivity is responsible for much of the morbidity and mortality associated with graft rejection and graft versus host disease.

MHC molecules can be divided into two main subsets, class I molecules and class II molecules. Class I molecules are constitutively expressed by most nucleated cells and bind intracellular peptides derived from the cytosol for presentation to $CD8^+$ T-cells. These molecules are known as human leukocyte antigens (HLA)-A, -B, and –C in humans and H2-K, -D, and –L in mice. Class II molecules are constitutively expressed by bone marrow derived APC's (e.g., macrophages, B-cells, and DCs) and thymic epithelial cells, and present peptides to $CD4^+$ T-cells for the initiation of T-helper functions such as cytokine production. These molecules are known as HLA-DR, -DP, -and DQ in humans and I-A and –E in mice (Figure 1). The variability of the MHC locus is immense. In

humans, polymorphisms within HLA-A, -B, and –C result in approximately 1500 differing alleles.[6] These polymorphisms underscore the difficulty in identifying suitable donor/recipient pairs that will not induce a strong allogeneic T-cell response.

Allorecognition can occur via two distinct mechanisms: direct and indirect recognition (Figure 2). Direct allorecognition occurs when T-cells recognize and respond to differences within the MHC molecules themselves. During GVHD, direct allorecognition would be achieved by donor T-cells interacting with host APCs expressing disparate MHC on their surface. Although there is still some debate regarding the contribution of the presented peptide, it is generally believed that both peptide-independent and peptide-dependent allorecognition occur.[7] The degree of difference in MHC molecules between donor and host are thought to influence which factor plays the dominant role in recognition. For example, when the MHC is closely matched between donor and host, it is thought that much of the alloreactivity is directed toward epitopes of endogenous peptides presented on foreign MHC, however this becomes less peptide-dependent as the MHC becomes more disparate.[8] In contrast to this, the indirect pathway of allorecognition is entirely peptide-dependent. During GVHD, donor allospecific T-cells can recognize alloantigens shed from the host which are processed and presented by donor APCs in association with MHC class II molecules. This indirect allorecognition pathway is mediated by $CD4^+$ T-cells, and because alloantigen must be processed before being displayed by donor APCs, it is generally slower compared to the direct route of recognition.[9]

Adding to the complexity, even when a donor and host are matched for each MHC allele, differences in other proteins, known as minor histocompatibility antigens

(mHags), can lead to GVHD or graft rejection. Although any protein with a polymorphism can theoretically act as a mHag, T-cell responses in mice identified to date seem to be restricted to only a few epitopes, which are called immunodominant epitopes.[10] Probably the most studied mHags in relation to BMT are the male-specific H-Y antigens. Because the Y antigen is considered 'foreign' to female lymphocytes, it is well known that an appreciable alloresponse can occur in up to 50% of male recipients of female BM.[11]

Dissection of acute graft versus host disease (aGVHD)

I. Incidence and diagnosis of aGVHD

GVHD remains as a major complication following allogeneic BMT. Historically, aGVHD is defined as having occurred within 100 days of BMT and has distinctive pathological features usually afflicting the skin, liver and gut. This is opposed to chronic GVHD, which most often occurs >100 days post BMT and is characterized by multiorgan 'autoimmunity'. The incidence of aGVHD ranges from 26-32% in recipients of sibling donor BM and 42-52% in recipients of unrelated donor BM.[12] In 1974, Glucksberg established a clinical grading system for aGVHD that helped physicians diagnose the severity of the disease.[13] Confirmation of this diagnosis is performed through histological analysis of affected tissue for the presence of lymphocytic infiltrates and apoptotic and necrotic tissue. Our laboratory has established a similar histological grading system used to diagnose severity of aGVHD in experimental mice.[14] Here, Grade 0 indicates no acute GVHD; Grade 1 is mild aGVHD with minimal lymphocyte

infiltration in target organs; Grade 2 is moderate multi-organ disease; Grade 3 is severe multi-organ dysfunction; Grade 4 is life threatening multi-organ dysfunction.

Pathophysiology of aGVHD

Graft versus host disease has been described as a multi-phase phenomenon, which starts with host tissue damage leading to donor T-cell activation and target-tissue destruction by effector cells. The availability of inbred mice has made it possible to elucidate the mechanisms that we now understand to directly and indirectly contribute to aGVHD.

Phase I: Preconditioning-induced damage of the host.

Damage to the host epithelium, either from underlying disease or from chemo- or radio-therapy, incites a massive 'cytokine storm' which causes increased expression of molecules known to attract or activate donor T-cells. For example, it is well documented that there is a linear association of increased dosages of radiation with increased concentrations of proinflammatory cytokines such as TNF-α and IL-1, and also widely upregulated surface expression of costimulatory molecules and MHC antigens.[15] It is also noted that radiation damage to host epithelial cells lining the gastrointestinal tract induces apoptosis and allows for the translocation of microbial products into circulation.[16] Together, these processes serve to further amplify the activation state of host APCs and set the stage for the next phase of the cycle.

Phase II: Donor T-cell activation, cytokine secretion, and trafficking to target tissue.

The second phase of aGVHD is manifested by the activation of infused donor T-cells. In the setting of allogeneic BMT, donor T-cell activation occurs when T-cells recognize foreign MHC molecules presented on host APCs or peptides of host MHC molecules presented on donor APCs (as outlined above).

Costimulatory signals are also needed for maximum activation of T-cells. There are two major superfamilies of costimulatory molecules: 1) CD28 family members include CD28, cytotoxic T-lymphocyte antigen 4 (CTLA-4), inducible costimulatory (ICOS), and programmed death-1 (PD-1); 2) TNF receptor family members include CD40 ligand (CD154), 4-1BB (CD137), OX40 (CD134), and herpesvirus entry mediator (HVEM). While interaction of most of these molecules with their ligands located on APCs results in positive costimulation, at least two of these, CTLA-4 and PD-1, produce a negative costimulatory signal that results in an immune-dampening effect. Great effort has been made to determine the effects of blocking positive costimulatory signals or augmenting negative costimulatory signals for GVHD prevention.

Recognition of foreign MHC molecules and appropriate costimulatory molecules induces $CD4^+$ T-cells to secrete pro-inflammatory TH1 cytokines such as IFN-γ, IL-2, and TNF-α.[17] These cytokines, together with other pro-inflammatory chemokines, further amplify the immune response toward allo-antigens which leads to an increase in the surface expression of molecules known to be involved in cellular trafficking. After priming and activation in the secondary lymphoid organs (spleen and LN), donor T-cells migrate to GHVD target tissues to cause tissue destruction. Expression of distinct homing

molecules (selectins, integrins, and chemokines) direct the trafficking to specific target organs.[18] For example, the expression of the chemokine CCR6 on donor $CD4^+$ T-cells targets them to the gut and skin, while the expression of CXCR3 or CCR2 on donor $CD8^+$ T-cells targets these cells to the gut and liver in murine models.[19-21] Once they have arrived at their target, these T-cells complete the cycle by eliciting considerable tissue destruction.

Phase III: Target tissue destruction.

T-cells employ multiple effector mechanisms to cause GVHD. First, $CD4^+$ T-cells can induce tissue damage in a contact-independent manner through the secretion of pro-inflammatory cytokines such as TNF-α and IL-1. Upon their activation through donor or host APCs, they produce high concentrations of these molecules, which induces apoptosis and necrosis of host epithelium.[22] Although, clinical studies using anti-TNF-α mAbs have shown promise in reducing aGVHD, especially when gastrointestinal involvement is prominent, the vast majority of these patients develop viral, bacterial, and fungal infections, which limit their use.[23,24]

Secondly, $CD8^+$ T-cells and NK cells induce direct cell-cell mediated tissue damage through perforin/granzyme and Fas/FasL pathways. After allorecognition and activation, effector cells secrete the pore-forming molecule, perforin, into the cell membranes of target cells. This acts as a gateway that allows for the entrance of the serine protease, granzyme B. Catalytically active granzyme B cleaves BCL-2 family proteins, which results in the loss of mitochondrial membrane integrity and release of

cytochrome c, and finally, DNA fragmentation and apoptosis of the target cell.[25] Fas/FasL (CD95/CD95L) are members of the TNF-receptor superfamily. Fas expression on host tissue is increased in response to IFN-γ and TNF-α.[26] Fas becomes activated upon binding to FasL expressed on donor T-cells, which induces the formation of a death-inducing signaling complex (DISC) and subsequent activation of caspases and apoptosis of target cells.[27]

Each of these three phases has the potential to amplify the next and to feedback into previous stages resulting in a continuous cycle that leads to the clinical features of aGVHD (outlined in figure 3).

Methods of preventing aGVHD in mouse and man

Understanding the pathophysiology of aGVHD allows us to uncover new pathways that may be exploited to treat or prevent this disease. Next, I will outline some of the techniques used in experimental mice and in the clinic designed to target these specific pathways.

The GVHD cascade starts with damage to gut epithelium and release of microbial products into systemic circulation. This may be the most straightforward point of intervention and can be accomplished in a number of ways: 1) reducing irradiation, 2) reducing the load of bacteria in the GI tract, and 3) strengthening the epithelial cell barrier prior to preconditioning. Less intense irradiation doses have, in fact, proven effective in reducing GVHD in animal models. Hill *et al.,* showed that when irradiation dosage was decreased from 1,300 cGy to 900 cGy, there was decreased macrophage

priming due to less LPS-leakage from the GI tract. This resulted in significantly lower concentrations of pro-inflammatory TNF-α and less severe GVHD.[15] Secondly, studies using germ-free or completely decontaminated rodents showed that the absence or complete elimination of intestinal microflora prevented the development of aGVHD in allogeneic recipients.[28,29] To add to this, a retrospective clinical study was performed to determine the influence of intestinal bacteria decontamination on the occurrence of grade II-IV aGVHD.[30] After analysis of 194 patients, it was determined that patients with sustained growth suppression of, or completely decontaminated of anaerobic bacteria microflora had a markedly reduced risk of aGVHD.[30] Finally, growth factors such as keratinocyte growth factor (KGF) have been shown to prevent GI tract damage and subsequent inflammatory response. When KGF was given in an allogeneic murine BMT model, KGF-treated mice exhibited a significantly increased survival rate compared to untreated mice.[31] Upon histological analysis, it was found that treated mice had reduced tissue damage in nearly all aGVHD-target organs.[31]

TNF-α contributes to aGVHD progression in a number of ways. TNF-α activates APCs and donor T-cells, induces the expression of adhesion molecules and chemokines on host epithelium which promotes donor T-cell migration, and finally causes direct tissue damage by inducing apoptosis and necrosis.[22] It is not surprising, therefore, that methods have been developed to block TNF-α signaling with the hopes of halting aGVHD progression. One study in mice using a rat/mouse chimeric monoclonal antibody against TNF-α showed that $CD4^+$ T-cell mediated aGVHD was significantly improved (MST= 13 days control antibody vs. 100% survival in anti-TNF-α treated), while there was only a moderate effect on $CD8^+$ T-cell mediated aGVHD (MST= 29 days in control

antibody treated vs. 48 days anti-TNF-α treated).[32] Importantly, this study also demonstrated that anti- TNF-α therapy still allowed for an effective GVL response. Another chimeric mouse/human anti-TNF-α mAb (Infliximab) that blocks the interaction of TNF-α with its receptor and also causes lysis of TNF-α-producing cells has been produced for clinical purposes. Retrospective studies have been performed to determine the efficacy of Infliximab in minimizing the severity of aGVHD. Couriel and colleagues reported that 59% of 32 patients treated with Infliximab for steroid-refractory aGVHD had a complete response.[33] Unfortunately, because Infliximab also causes lysis of monocytes, there is an increased incidence of infections associated with its use.

Lastly, methods used to inhibit T-cell effector mechanisms have also been examined. One of the most studied of these is Fas/FasL pathway. Miwa *et al*. showed that administration of anti-Fas-L inhibitory mAb reduced GVHD-related weight loss and mortality in a P-F1 murine model of semi-allogeneic BMT.[34] Furthermore, when donor T-cells were isolated from B6 mice unable to express a functional ligand for Fas (*gld/gld*), GVHD lethality was completely abolished.[34] Taken together, these data demonstrate that by targeting specific mechanisms known to operate in the pathophysiology of aGVHD, we can have a positive impact on the outcome and severity of the disease.

Graft versus tumor effect

The first attempt to treat leukemia in mice using radiation therapy was performed using high dose radiation and syngeneic BM.[35] The authors immediately observed a recurrence of leukemic relapse and went on to postulate that a graft having a reaction against the leukemia may be needed. This graft versus leukemia (GVL; or graft versus tumor, GVT) theory was confirmed in 1979 when it was shown that human leukemia patients that underwent BMT were less likely to suffer relapse if they presented with aGVHD.[36] Furthermore, genetically identical twins that underwent BMT, and patients receiving T-cell depleted bone marrow grafts both demonstrated a reduced incidence of aGVHD, but an increased risk of leukemic relapse.[37,38] The evidence that GVT effect can occur independently of GVHD was described by Ringden *et al.* when he published a retrospective study of over 6000 BMT's over a 13 year period.[39] Here, he showed that recipients of bone marrow from HLA-identical siblings that had not presented with aGVHD had a lower risk of relapse and a better leukemia-free survival than recipients of autologous grafts.[39] Donor natural killer (NK) cells also exhibit GVT activity. Studies in this arena revealed that adoptive transfer of Ly49-mismatched, MHC-matched NK cells reduced pulmonary tumor burden while presenting with less GVHD.[40] Another study performed here at the University of Minnesota evaluated the use of NK cells for tumor therapy in a non-transplant setting. In this clinical trial, patients with acute myeloid leukemia were given infusions of NK cells from HLA-haploidentical related donors following a preparative regimen that included high-dose cyclophosphamide and fludarabine.[41] Results showed that 5 of 19 patients achieved a complete remission with no

sign of GVHD.[41] In light of these studies, research is now focused on augmenting beneficial GVT reactions, while dampening unwanted GVHD.

Cellular therapy for the prevention or amelioration of GVHD and enhancement of bone marrow engraftment

Although the corticosteroids prednisone and methylprednisone remain the first-line therapy for GVHD, their global immunosuppressive characteristics, toxicity, and the development of corticosteroid resistant forms of GVHD have set the foundation for the advancement of novel cell-based approaches that may be used in place of, or possibly in conjunction with, current methodology. In the next few sections, I will outline some of the key features of two well-defined suppressor cell types (regulatory T-cells and mesenchymal stem cells) as they relate to the treatment of acute GVHD and bone marrow graft failure. I will also introduce two additional cell types with suppressive capabilities that will be discussed in detail in chapters 2 and 3 (multipotent adult progenitor cells and myeloid-derived suppressor cells, respectively).

Regulatory T-cells

One cannot have a comprehensive discussion on the topic of cells with suppressor function without the inclusion of regulatory T-cells, or Tregs. Tregs are a subpopulation of $CD4^+$ T-cells that constitutively express the interleukin-2 receptor α-chain (CD25). These cells account for 5-10% of the normal CD4 T-cell compartment in mice and humans, and are phenotypically distinguished from activated CD4 T-cells (which also transiently express CD25) by the co-expression of the transcription factor FoxP3.[42] Tregs

are defined by their ability to mediate suppression of conventional $CD4^+$ or $CD8^+$ T-cells by preventing their activation and inducing anergy, which subsequently leads to limited effector functions in vivo.[43,44] In fact, mice harboring a loss-of-function mutation in the gene *FoxP3* are unable to restrain autoreactive T-cells and present with CD4 T-cell lymphoproliferative disease resulting from defective maintenance of T-cell tolerance.[42] The functional properties of Tregs appear to vary depending on the effector response being regulated, but cell surface molecules such as CTLA-4[45], Glucocorticoid-induced tumor necrosis factor receptor (GITR)[46], and PD-1[47], and suppressive cytokines such as IL-10[48] and transforming growth factor-beta (TGF-β)[49] have all been implicated as various mechanisms of action.

It wasn't long before it was realized that Tregs might be beneficial for prevention of GVHD. Accordingly, it was determined that when using either a partial or complete MHC-mismatched donor-recipient pair, Treg depletion from the donor innoculum or the host accelerated GVHD, while Treg repletion inhibited GVHD lethality.[50,51] Importantly, when Tregs were provided after the onset of the disease, they produced similar protective effects, indicating they may be used to ameliorate ongoing GVHD.[52] The mechanism of action of Tregs in this setting was elucidated further when it was shown that the population of Tregs responsible for these observations expressed the homing receptor L-selectin (CD62L). Here, the purified $CD62L^+$ subpopulation of Tregs efficiently migrated to the lymph nodes where they restricted the expansion of alloreactive T-cells and enhanced survival of recipient mice, whereas the $CD62L^-$ subpopulation had no such properties.[53] These studies also reaffirmed the previously held belief that the secondary

lymphoid organs are the primary site of allopriming and alloactivation of donor T-cells, and are therefore critical for GVHD progression.

The next important step forward for the application of Tregs in a clinical setting was to determine their effects on Teffector cells within the context of a tumor. As discussed above in detail, the ultimate goal of GVHD therapy is to dampen or eliminate the negative effects of GVHD while, at the same time, preserving the ability of allogeneic Teffector cells to eradicate residual tumor cells. Edinger *et al*. showed that when mice were given luciferase-tagged allogeneic A20 leukemia cells along with conventional GVHD-causing T-cells and Tregs, GVL activity was preserved with reduced GVHD.[54] This finding indicated that Tregs were capable of separating the beneficial effects of GVL from the detrimental effects of GVHD. The authors went on to determine that in this instance, perforin-mediated killing and FAS-FASL interactions were responsible for the observed GVL effects.[54]

The same T-cell inhibitory properties that allow Tregs to inhibit GVHD also allows them to influence donor bone marrow cell engraftment. Several reports have shown that Tregs promote donor cell engraftment in semiallogeneic (B6>B6D2F1) and fully MHC-mismatched models (B6>BALBc).[53,55-57] More specifically, work performed in our lab using a fully mismatched murine model of host-mediated graft rejection has shown that engraftment was significantly improved upon the addition of either donor-derived or host-derived Tregs.[53] In this model, sub-lethal irradiation of the host allows for residual T-cells to recognize and reject donor alloantigen by day 35 post transplant.[53] When mice were given as little as $3.5x10^6$ $CD62L^{high}$ Tregs, engraftment of donor bone

marrow was stable, multilineage, and long term (>3 months) in 10 out of 10 mice examined.[53]

Based on these exciting findings using animal models of BMT, clinical trials have begun to determine the maximum tolerated dose of $CD4^+CD25^+$ Tregs that can be safely administered to patients undergoing HLA-identical sibling donor peripheral blood progenitor cell transplantation.[58] Secondary outcome measures taken in this study are to evaluate the incidence of acute and chronic GVHD, relapse, and survival after the administration of Tregs.[58] In terms of assessing engraftment promotion, another phase I clinical trial is underway in which umbilical cord blood-derived Tregs are to be co-administered with umbilical cord blood progenitor cells.[59] Here, in addition to determining the maximum tolerated dose of Tregs capable of being administered, secondary outcome measures will determine the proportion of patients with sustained donor engraftment.[59] Results from these trials will establish whether the protective effect of Tregs, as demonstrated in experimental systems, can be effectively translated to a clinical setting.

Mesenchymal Stem Cells

Mesenchymal stem cells (*ie*, mesenchymal stromal cells, MSC) are a heterogeneous, nonhematopoietic, multipotent cell population capable of generating a wide variety of cells. MSCs have been isolated from a number of animals including human, mouse, rat, and sheep. The main source of MSC is the bone marrow, where they represent approximately 0.01-0.001% of mononuclear cells[60], but have also been isolated from umbilical cord blood[61], adipose tissue[62], peripheral blood[63], lung[64], and fetal liver[65]. Unfortunately, there are no specific cell surface markers that can be used to prospectively isolate MSCs and therefore isolation methods rely on their ability to adhere to plastic tissue culture dishes and propagate in vitro. Generally speaking, after a 3-4 week isolation period, MSCs express a number of cell surface antigens such as CD105 (SH2 or endoglin), CD73 (SH3 or SH4), CD106, CD34, CD166, CD44, Sca1 and CD29.[66] They lack the expression of common hematopoietic and endothelial markers such as CD90, CD11b, CD14, CD31, and CD45.[66] More commonly, MSCs are defined using functional criterion that requires them to be capable of differentiating in vitro into bone, fat, and cartilage.

Numerous experimental models highlight the immune-dampening effects of MSC in vitro. In these studies, MSCs suppressed T-cell proliferation induced by a variety of stimuli, including nonspecific mitogenic stimuli, allogeneic stimuli, and memory cell recognition of cognate antigen.[67,68] Most studies indicate that cell-cell contact was not necessary for suppression to occur. Soluble factors such as prostaglandin E_2 (PGE_2), IL-10, TGF-β, hepatocyte growth factor (HGF) and also the depletion of the essential amino acid tryptophan by the enzyme indoleamine 2,3-dioxygenase (IDO) have been described

to participate in suppression.[67,69,70] In vivo application of MSCs for the suppression of GVHD in rodent models have resulted in somewhat conflicting data. While most reports cite a reduction in the occurrence or severity of GVHD, at least one report shows that MSCs had no clinical benefit on the incidence or severity of GVHD in mice.[71] Although the MSCs used here possessed immune suppressive properties in vitro, when the cells were applied in vivo they were found to have migrated to the bone marrow, and only very few had established themselves within the LN and spleens.[71] This suggested that the ability of MSCs to influence GVHD may not only depend on their suppressive properties in vitro, but also on their capacity to traffic to sites of allorecognition and allopriming of donor T-cells.

Clinical trials using human MSCs for the treatment of GVHD are at various stages of completion. Lee *et al.* was the first to report that the injection of MSCs following T-cell depleted HLA haplotype-mismatched BMT not only suppressed GVHD following transplant, but also enhanced engraftment, and accelerated immune reconstitution.[72] Another completed trial was performed by the European Group for Blood and Marrow Transplantation Consortium for patients with steroid-resistant, severe, acute GVHD.[73] This group of clinicians treated 55 patients with bone marrow-derived MSCs at doses of 0.4-9x10^6 cells per kg bodyweight in one or multiple doses (up to 5). They found that 39 patients (71%) responded to treatment with MSCs; 30 of these patients had a complete response with no signs of GVHD, while 9 patients had a partial response.[73] Importantly, third party MSCs were as effective at producing a response as HLA-identical or haploidentical MSCs, indicating that third party MSCs can be selected for their immune suppressive properties and stored for the infusion of multiple patients

regardless of haplotype.[73] Another phase II clinical trial using a patented mixture of MSCs, termed PROCHYMAL™, isolated from the bone marrow of healthy adult donors to treat patients with newly diagnosed acute GVHD has recently been completed.[74] Here, it was reported that 29 of 31 patients (94%) had a positive response after receiving two infusions of MSCs, and 23 patients (74%) achieved a complete response with total clinical resolution of the disease.[75] These highly encouraging results have prompted a phase III study currently underway to evaluate the efficacy of using PROCHYMAL™ to treat pediatric patients with steroid-refractive acute GVHD.[76] In a recently issued release from Osiris Therapeutics Inc. it was stated that children receiving PROCHYMAL™ had an overall response rate of 63% compared with 36% of patients receiving placebo.[77] This resulted in a 30-point improvement in 100 day survival compared to placebo (79% vs. 50%).[77]

Although initial results regarding the use of MSCs to treat GVHD are promising, there have been conflicting results in terms of their ability to retain a GVL effect. Ning *et al.* treated 30 patients with hematological malignancies undergoing allogeneic BMT with HLA-identical donor derived MSCs. They found that only 10% of patients receiving MSCs developed grade II acute GVHD, compared to 53% of patients in the untreated group.[78] However, when they compared the relapse rate of treated versus untreated patients, they found there was a significant increase in patients given MSCs (60% vs. 20%).[78] While this study reinforced the idea that MSCs could have a beneficial impact on GVHD, it also cautioned their use in patients with underlying malignancies.

Multipotent Adult Progenitor Cells

Multipotent adult progenitor cells (MAPCs) are unique cells found in human and rodent postnatal bone marrow, muscle, and brain.[79] These cells are selected for by depleting adult bone marrow of hematopoietic cells expressing CD45 and glycophorin-A, followed by long term culture on fibronectin with the addition of epidermal growth factor (EGF) and platelet-derived growth factor (PDGF), all under low serum conditions. A homogenous population of MAPCs emerge from this culture after a period of about 3-4 months. Like embryonic stem (ES) cells, MAPCs express Oct-4, Rex-1, and SSEA-1, and when isolated from a rodent require the presence of leukemia inhibitory growth factor (LIF) in the culture media. MAPCs do not, however, express classical hematopoietic stem cell markers such as CD34 and c-kit, nor do they express MHC class I or MHC class II antigens. Surface markings show that a single MAPC can differentiate into cells representing all three germ layers in vitro and in vivo. This includes MSCs that produce cells of the limb-bud mesoderm derivation (osteoblasts, chondrocytes, adipocytes), endothelial cells which express vWF and CD31, and also cells of endodermal (hepatocytes being $HNF1^+$ and $albumin^+$) and ectodermal (neurons being $GFAP^+$ and $NF200^+$) origin.[79,80] Upon injection of MAPC's into irradiated (250 cGy) NOD/SCID mice, high levels of MAPC engraftment and differentiation were observed in radiosensitive organs known to be primary targets of GVHD (i.e., intestinal epithelium and liver).[80] Furthermore, it was found that MAPCs express telomerase and have long telomeres that do not shorten after a period of over 80 population doublings,[80] indicating that these cells do not undergo proliferative senescence. These features of MAPCs make

them an ideal cell type for the prevention or treatment of aGVHD. I will explore this possibility in depth in chapter 2.

Myeloid-Derived Suppressor Cells

Early studies of Bronte and colleagues described a suppressor cell population capable of inducing apoptosis of tumor-reactive cytotoxic T-cells.[81] In this report, it was shown that the depletion of $CD11b^{+}Gr1^{+}$ cells from tumor-bearing mice completely restored the capacity of these T-cells to mount a cytolytic reponse.[81] Morphologically, these suppressor cells are composed of a mixture of myeloid cells such as granulocytes, monocytes, and macrophages, and also myeloid precursor cells and were later given the classification of myeloid-derived suppressor cells (MDSCs). Since Bronte's seminal publication, there has been a flurry of primary research articles that demonstrate a clear linear association of MDSC number with tumor progression. In a wild type mouse, MDSCs represent approximately 2-4% of all nucleated splenocytes, whereas in tumor-bearing mice as much as 50% of the total splenocytes may be MDSCs.[82] The accumulation of these cells in tumor-bearing hosts suppresses antigen specific T-cell responses and therefore contributes to the failure of immune therapy in these patients. Although a number of mechanisms have been linked to the suppressive ability of these cells, including the production of TGF-β[83] and reactive oxygen species[84], the catabolism of the amino acid L-arginine appears to play a dominant role.[85]

L-arginine serves as a substrate for two distinct enzymes: nitric oxide synthase (NOS) and arginase. The catabolism of L-arginine by NOS produces nitric oxide (NO)

and citrulline. However, when L-arginine is present in low concentrations, NOS will produce more superoxide (O_2^-).[86] Superoxide can spontaneously be converted to H_2O_2 and oxygen, or combine with nitric oxide to form peroxynitrite ($ONOO^-$). Peroxynitrite is an oxidant that can inhibit T-cell activation, induce apoptosis and injure host epithelium.[86] Studies by Gabrilovich *et. al.,* implicated peroxynitrite-mediated mechanism for T-cell inhibition by MDSCs in tumor bearing mice.[87] Arginase is a major enzyme in the urea cycle and catalyzes the hydrolysis of L-arginine to urea and L-ornithine. Rodriguez *et. al.,* has demonstrated that when arginase-1 activity is increased and L-arginine availability is reduced, CD3ζ expression on T-cells is diminished, leaving the T-cells unable to respond.[85] Increased arginase activity in MDSCs results in local depletion of L-arginine and the accumulation of the byproduct urea. The combination of these effects is to alter the translation of mRNA in other cell types through kinase pathways involving general control non-depressible 2 (GCN2). The decrease in amino acid concentrations as a result of arginase activity results in an increased amount of uncharged tRNA, which subsequently activates GCN2.[88,89] GCN2 binds to uncharged tRNA and acts as a sensor for amino acid starvation and reacts to this by phosphorylating the serine residue at position 51 of the α-subunit of eukaryotic translation initiation factor 2 (EIF2α), and P-EIF2α turns off protein synthesis by impeding translation.[88-90]

These findings have led many to hypothesize that multiple types of cancers have evolved to utilize MDSCs as a means to evade T-cell-mediated clearance. While these cells represent a significant barrier to tumor-immunotherapy, the induction or isolation of these cells could signify a powerful tool useful in the control of autoimmunity, transplant

rejection, and GVHD. The use of MDSCs that have been generated from wild-type bone marrow as cellular therapy for aGVHD will be discussed in detail in chapter 3.

Thesis Statement

Any person with an immune or hematopoietic deficiency or pathology or that has a hematopoietic compartment which lacks the ability to produce an essential enzyme is a candidate for a bone marrow transplant (BMT). According to the National Marrow Donor Program (NMDP), there are approximately 20,000 BMTs, syngeneic and allogeneic, performed annually world-wide (the most common diseases requiring a BMT are included in figure 4). Although this is a proven life-saving procedure, it is not without significant risks. The focus of this dissertation is to identify new suppressor cell types that may hold clinical benefit for the treatment of aGVHD and the promotion of bone marrow engraftment. In the chapters that follow, I will employ the use of a fully MHC-mismatched model of murine allogeneic BMT. Chapter 2 explores the use of Multipotent Adult Progenitor Cells (MAPCs) for amelioration of aGVHD, and highlights the importance of cellular trafficking to T-cell priming sites to obtain the desired effects. In chapter 3, I discuss a novel culture method that I developed to generate myeloid-derived suppressor cells (MDSCs) from tumor-free mice. These MDSCs are then tested for their ability to inhibit allogeneic T-cell responses in vitro and in vivo, and the mechanism of action these cells use for suppressor function is determined. Lastly, in chapter 4, I use mesenchymal stromal cells (MSCs) as a means to promote bone marrow engraftment. It

is widely accepted that MSCs have the ability to promote engraftment in rodent models and in the clinic. However, the mechanism behind this phenomenon is still debated. We identify the soluble molecule prostaglandin E_2 (PGE2), which is secreted from MSCs, as the main factor responsible for mediating these beneficial effects. Collectively, the data presented in this thesis will shed light on novel cellular methods that one day may be used in a clinical setting to ameliorate the negative side effects of allogeneic BMT.

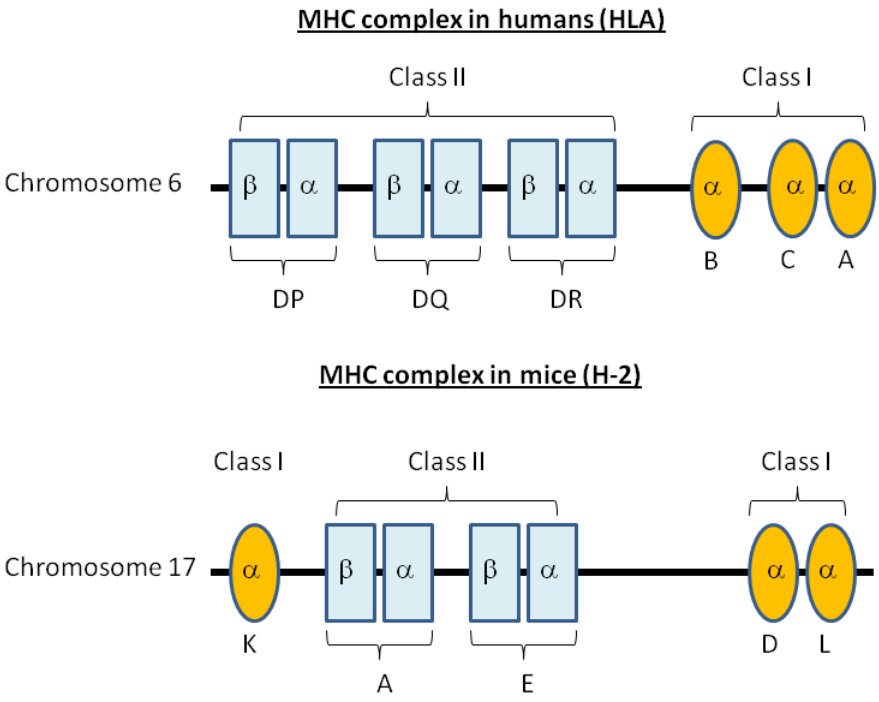

Figure 1: The major histocompatibility Complex (MHC) in mice and humans.

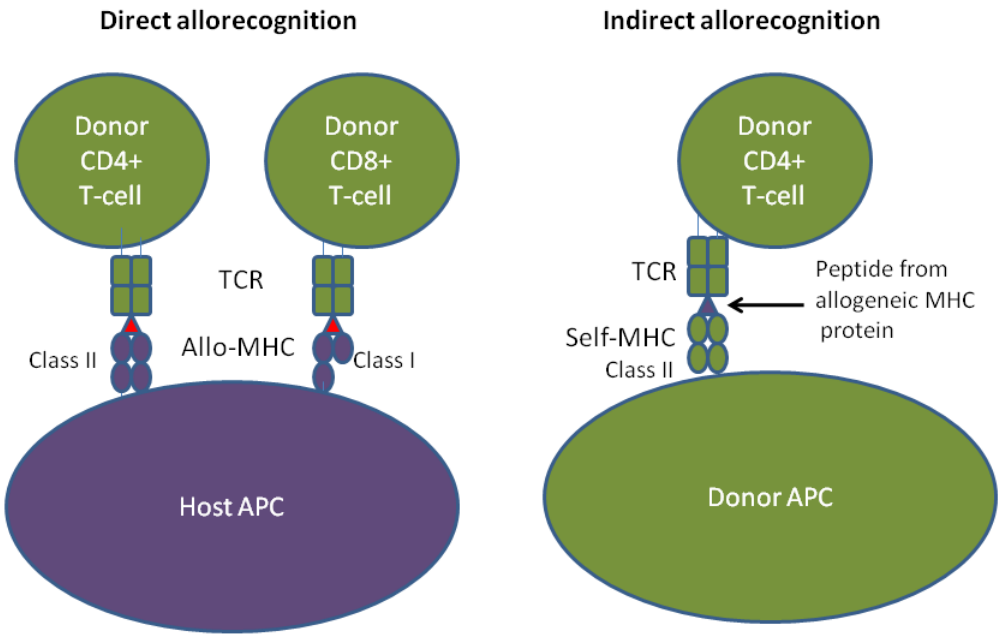

Figure 2: Direct and indirect allogeneic recognition during GVHD. Direct allorecognition occurs when donor T-cells recognize host MHC molecules as 'foreign'. Indirect allorecognition occurs when donor CD4 T-cells recognize peptides derived from allogeneic hosts which are presented on self MHC class II molecules.

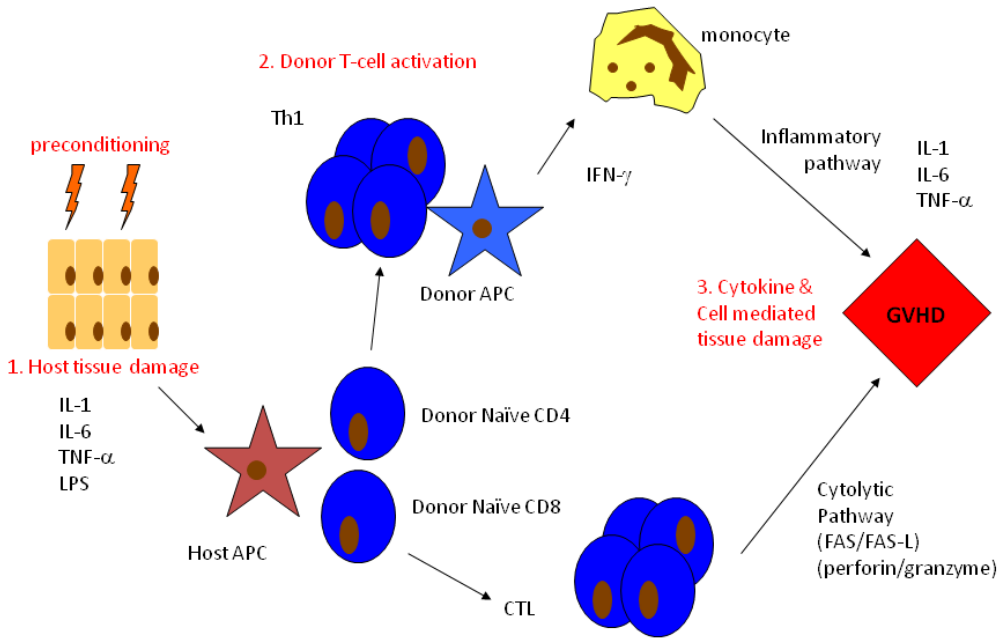

Figure 3: Pathophysiolgy of aGvHD. aGVHD occurs in three distinct stages. Stage 1: Intense conditioning regimes such as radiation and chemotherapy lead to tissue damage and the generation of large amounts of inflammatory cytokines which enhance HOST APC activation. Stage 2: Naïve donor CD8 cells are stimulated by residual host APC, which induce CTL priming. Naïve donor CD4 cells are stimulated by both host and donor APC presenting HOST-derived Ag, which drives Th1 biased cytokine production, promoting proliferation and monocyte/macrophage priming. Stage 3: Target tissue damage is induced by direct CTL cytotoxicity and indirect cytokine-mediated damage.

Figure 4

Disease's treatable by bone marrow transplantation and approximate incidences of new cases in the U.S. per year

Leukemia's and lymphoma's		
	Acute myelogenous leukemia	11,900
	Acute lymphoblastic leukemia	4,000
	Chronic myelogenous leukemia	4,600
	Juvenile myelomonocytic leukemia	25-50
	Hodgkin's lymphoma	14,000
	Non-Hodgkin's lymphoma	56,000
Multiple myeloma		16,000
	and other plasma cell disorders	
Severe aplastic anemia and other marrow failure states		
	Severe aplastic anemia	1,000
	Fanconi anemia	1,000
	Paroxysmal nocturnal hemoglobinuria (PNH)	100-500
	Pure red cell aplasia	
	Amegakaryocytosis	
Inherited immune disorders		
	Severe combined immune deficiency (SCID)	400
	Wiskott-Aldrich syndrome	600
Hemoglobinopathies		
	Beta thalassemia	
	Sickle cell disease	10,000
Inherited metabolic disorders		
	Hurler's syndrome (MPS-IH)	3,000
	Adrenoleukodystrophy	1,500
	Metachromatic leukodystrophy	3,000
Myelodysplastic and myeloproliferative disorders		
	Refractory anemia	
	Chronic myelomonocytic leukemia	
	Agnogenic myeloid metaplasia	3,000
Familial erythrophagocytic lymphohistiocytosis and other histiocytic disorders		
Other malignancies		

*Data taken from the National Marrow Donor Program and approximate incidences based on a population of 304×10^6 people living in the U.S. in 2008 (United States Census Bureau).

Chapter 2

Multipotent Adult Progenitor Cells (MAPC) can suppress graft-versus-host disease via prostaglandin E2 synthesis and only if localized to sites of allopriming

Steven L. Highfill[1], Ryan M. Kelly[1], Matthew J. O'Shaughnessy[1], Qing Zhou[1], Lily Xia[1], Angela Panoskaltsis-Mortari[1], Patricia A. Taylor[1], Jakub Tolar[1,*], Bruce R. Blazar[1,*]

[1]University of Minnesota Masonic Cancer Center and Department of Pediatrics, Division of Bone Marrow Transplantation, Minneapolis, MN 55455, USA

*equal contributors

Foreward

Multipotent adult progenitor cells (MAPCs) are non-hematopoietic stem cells capable of giving rise to a broad range of tissue cells. As such, MAPCs hold promise for tissue injury repair post-transplant. In vitro, MAPCs potently suppressed allogeneic T cell activation and proliferation in a dose-dependent, cell contact-independent and Tregulatory cell independent manner. Suppression occurred primarily through prostaglandin E_2 (PGE_2) synthesis in MAPCs, which resulted in decreased proinflammatory cytokine production. When given systemically, MAPCs did not home to sites of allopriming and did not suppress GVHD. To ensure that MAPCs would co-localize with donor T cells, MAPCs were injected directly into the spleen at BMT. MAPCs limited donor T cell proliferation and GVHD-induced injury via PGE_2 synthesis in vivo. Moreover, MAPCs altered the balance away from positive and toward inhibitory costimulatory pathway expression in splenic T cells and antigen presenting cells (APCs). These findings are the first to describe the immunosuppressive capacity and mechanism of MAPC-induced suppression of T cell alloresponses and illustrate the requirement for MAPC co-localization to site of initial donor T cell activation for GVHD inhibition. Such data have implications for the use of allogeneic MAPCs and possibly other immunomodulatory non-hematopoietic stem cells for preventing GVHD in the clinic.

Introduction

The wider application of BMT has been limited, in part, by graft-versus-host disease (GVHD) complications. Human and mouse mesenchymal stem cells (MSCs) have been shown to suppress allogeneic-induced and nonspecific mitogen-induced T cell proliferation in vitro (reviewed in detail [91,92]). Implicated suppressive mechanisms have included IL-10 [93], TGF-β, hepatocyte growth factor [67], indoleamine 2,3 dioxygenase (IDO) [94], nitric oxide [95], prostaglandin E_2 [69], increased Tregulatory cells (Tregs) [96], and activation of the PD-1 negative costimulatory pathway [97]. In vivo, there have been conflicting data regarding the potential of Mesenchymal Stem Cells (MSCs) to suppress GVHD [98,99,71].

Multipotent adult progenitor cells (MAPC) are non-hematopoietic stem cells that can be co-purified with MSCs from bone marrow cells. MAPCs express the pluripotent state-specific transcription factors Oct-3/4 and Rex1, and can differentiate into cell types representative of all three germ layers [79,80]; thus, MAPCs are generally believed to be a more primitive cell type than MSCs. MSCs kept for prolonged periods in culture tend to lose their differentiation capabilities and undergo senescence at ~20-40 population doublings [100,101]. In contrast to MSCs, MAPCs have an average telomere length remained constant for up to 100 population doublings in vitro [80]. Based upon their differential potential and reduced senescence, MAPCs have been considered as a potentially desirable non-hematopoietic stem cell source for use in allogeneic BMT.

In this study, we sought to determine whether MAPCs might be useful for GVHD prevention. We demonstrate that murine MAPCs are potently immune suppressive in vitro and can reduce GVHD lethality *in vivo* when present in the spleen, a site of initial

allopriming, early post-BMT. Furthermore, we identify the mechanism of action MAPCs employ to elicit T cell inhibition and reduce GVHD-induced tissue injury *in vivo*.

Materials and Methods

Mice. BALB/c ($H2^d$), C57BL/6 ($H2^b$)(termed B6) or B6-Ly5.2 (CD45 alleleic) mice were purchased from The Jackson Laboratory (Bar Harbor, ME) or the National Institute of Health (Bethesda, MD). B10.BR ($H2^k$) mice were purchased from The Jackson Laboratory. All mice were housed in specific pathogen-free facility in microisolator cages and used at 8-12 weeks of age in protocols approved by the Institutional Animal Care and Use Committee.

MAPC isolation and culture. MAPCs were isolated from B6 and BALB/c mice BM as described[80]. Briefly, BM was plated in DMEM/MCDB containing 10ng/ml EGF (Sigma-Aldrich, St.Louis, MO), PDGF-BB (R&D systems, Minneapolis, MN), LIF (Chemicon International, Temecula, CA), 2% FCS (Hyclone, Waltham, MA), 1x selenium-insulin-transferrin-ethanolamine (SITE), 0.2mg/ml linoleic acid-BSA, 0.8 mg/ml BSA, 1x chemically defined lipid concentrate, and 1x α-mercaptoethanol (all from Sigma-Aldrich). Cells were placed at 37C in humidified 5% O_2, 5% CO_2 incubator. After 4 weeks, $CD45^+$ and $Ter119^+$ cells were depleted using MACS separation columns (Miltenyi Biotech, Auburn, CA) and plated at 10 cells/well for expansion. For in vivo experiments in which cells were tracked, MAPCs were used that stably express red fluorescent protein (DSred2) and firefly luciferase transgenes (termed MAPC-DL)[102]. For

quality control, MAPCs were differentiated into cells representative of the mesodermal lineage, then subjected to in vitro trilineage (endothelium, endoderm, and neuroectodermal) differentiation to ensure multipotency[80]. MAPCs were analyzed for expression of CD90, Sca1, CD45, CD44, CD13, cKit, CD31, MHC class I, and MHC class II, CD3, Mac1, B220, and Gr1 and tested for expression of transcription factors Oct3/4 and Rex-1 by RT-PCR. Twenty metaphase cells were evaluated by G-banding. Results are found in supplemental Figure 1.

Mixed leukocyte reaction (MLR). Lymph nodes (LNs) were harvested from B6 mice and T cells were purified using by negative selection using PE-conjugated anti-CD19, anti-CD11c, anti-NK1.1 and anti-PE magnetic beads (Miltenyi Biotech). Purity was routinely >95%. Spleens were harvested from BALB/c mice, T cell depleted (anti-Thy1.1), and irradiated (3000 cGy). B6 T cells were mixed at a 1:1 ratio with BALB/c splenic stimulators and plated in a 96 well round bottom plate (10^5 T cells/well) or in the lower chamber of a 24 well plate TransWell insert (10^6 T cells/well). MAPCs were irradiated (3000cGy) and plated in a 96 well round bottom plate (10^4/well, 1:10) or in a 24 well TransWell plate (10^5/well, 1:10). Cells were incubated in "T cell media" in 200 μl/well (96 well) or 800 μl/well (24 well) of RPMI 1640 (Invitrogen, Carlsbad, CA) supplemented with 10% FCS, 50mM 2-ME (Sigma-Aldrich), 10mM HEPES buffer (Invitrogen), 1mM sodium pyruvate (Invitrogen), amino acid supplements (1.5mM L-glutamine, L-arginine, L-asparagine)(Sigma-Aldrich), 100U/ml penicillin, 100mg/ml streptomycin (Sigma-Aldrich). Cells were pulsed with ^{3}H-thymidine (1μCi/well) 16-18 hours prior to harvesting and counted in the absence of scintillation fluid on a β-plate

reader. To inhibit PGE_2 production, indomethacin (Sigma-Aldrich) resuspended in ethanol was diluted in T cell media to reach a final concentration of 5 μM per flask and incubated overnight at 37C, 5%CO2. The next day, cells were trypsinized and washed extensively with 2% FBS/PBS. Trypan blue exclusion was used to assess effects on live cells. In experiments evaluating the contribution of IDO, 1-methyl-D-tryptophan (1MT) (Sigma-Aldrich) was added to the culture media at a concentration of 200 μM.

Flow cytometry. Purified T cells purified were stained with 1μM carboxyfluorescein-succinimidyl-ester (CFSE, Invitrogen) for 2 minutes then washed. T cells or $CD11c^+$ DCs obtained from MLR cultures were stained for the expression of FoxP3, CD25, CD44, CD62L, CD122, PD-1, PDL1, PDL2, CTLA4, OX40, OX40L, 4-1BB, 4-1BBL, ICOS, ICOSL, CD80, CD86, CD40L, or CD40 antigens. All antibodies were purchased through Pharmingen (San Diego, Ca) or E-bioscience (San Diego, Ca) and stained according to manufacturer's instructions then analyzed using FACSCalibur or FACSCanto (Becton Dickinson, San Jose, Ca) and Flow Jo software (Treestar inc). Calculations to determine the proliferative capacity of T cells were performed as described [103].

Cytokines and PGE_2 quantification. Quantitative determination of prostaglandin E_2 (PGE_2) in cell culture supernatants was performed using PGE_2 assay kit (R&D Systems) by following manufacturer's instructions. Quantities of IL-10, TGF-β, IL-2, TNF-α, IFN-γ, and IL-12 were determined using Luminex technology and ELISA (R&D Systems).

In vivo MLR[104]. Host BALB/c stimulator mice were lethally irradiated using 850 cGy total body irradiation (TBI, ^{137}Cs), followed by intra-splenic injection of either PBS or 5 x

10^5 MAPC. The next day, purified responder T cells were labeled with 1μM CFSE and 15 x 10^6 cells were transferred into stimulator or syngeneic mice. After 96 hours, spleen and LNs were harvested for FACS analysis.

GVHD. BALB/c recipients were lethally irradiated using 850cGy TBI on day -1 followed by intra-splenic injection of either PBS or 5 x 10^5 MAPC. On day 0, mice were infused intravenously (i.v.) with 10^7 T cell depleted (TCD) donor BM. On day +1, mice were given 2 x 10^6 purified whole T cells (CD4 and CD8) depleted of CD25. Recipient mice were NK-depleted with anti-asialo GM-1 (Wako Corp., Richmond, VA) by intra-peritoneal (i.p.) injection of 25 μl on day -2, a dose previously determined to be highly effective for depletion of NK cells. Mice were monitored daily for survival and weighed twice weekly as well as examined for the clinical GVHD.

Tissue histology. On day 21, GVHD target organs (liver, lung, colon, skin, spleen) were harvested and snap-frozen in optimal cutting temperature (OCT) compound (Sakura, Tokyo, Japan) in liquid nitrogen. 6 μM sections were stained with hematoxylin and eosin and graded for GVHD using a semi-quantitative scoring system (0-4.0 grades in 0.5 increments)[14].

Immunofluorescence microscopy. Spleens taken from transplanted mice were embedded in OCT, snap-frozen in liquid nitrogen, and stored at -80°C. Cryosections (6 μM) were fixed in acetone for 10min, air dried, and blocked with 1% BSA/PBS for 1 hour at room temperature. Primary antibody was diluted in 0.3% BSA/PBS and incubated for 2 hours.

After 3 washes in PBS, sections were incubated with secondary antibody for 45 minutes. Sections were washed and mounted under a coverslip with 4,6-diamidino-2-phenylindole (DAPI) anti-fade solution (Invitrogen) and imaged on the following day at room temperature using an Olympus FluoView 500 Confocal Scanning Laser Microscope (Olympus, Center Valley, PA). Primary antibodies included anti-PGE synthase (Santa Cruz Biotechnology, Inc., Santa Cruz, CA) diluted 1:50, FITC-conjugated anti-Luciferase (Rockland Immunochemicals, Gilbertsville, PA) diluted 1:100. Goat-Cy3 secondary antibody (Jackson Immunoresearch Laboratories, West Grove, PA) was diluted to 1:200.

Bioluminescent imaging (BLI) studies. A Xenogen IVIS imaging system (Caliper Life Sciences, Hopkinton, MA) was used for live animal imaging and imaging of organs taken from transplanted mice. MAPC-DL bearing mice were anesthetized with 0.25 mL Nembutol (1:10 diluted in PBS). Firefly luciferin substrate (0.1mL, 30mg/ml, Caliper Life Sciences, Hopkinton, MA) was injected i.p. or added to the media containing tissues and imaging was performed immediately after substrate addition. Data were analyzed and presented as photon counts per area.

Statistical analysis. The Kaplan-Meier product-limit method was used to calculate survival curve. Differences between groups in survival studies were determined using log-rank statistics. For all other data, a Student's t-test was used to analyze differences between groups, results were considered significant if the P value was ≤ 0.05.

Results

MAPCs inhibit T cell proliferation and activation. Murine MAPCs were expanded under low oxygen conditions and had trilineage differentiation potential[105] (supplemental Fig. 1A, B). MAPCs were routinely $CD45^-$, $CD44^-$, $CD13^{lo/+}$, $CD90^+$, c-kit^-, Sca-1^+, $CD31^-$, MHC class I^-, and MHC class II^- (supplemental Fig. 1C). RT-PCR expression analysis confirmed that these MAPCs expressed Oct-3/4 and Rex-1 (supplemental Fig. 1D). G-banding analysis revealed that 90% of the 20 metaphase cells analyzed had a normal karyotype (supplemental Fig. 1E). The remaining two cells had a tetraploid complement, one with an additional deletion within the long arm of chromosome 6. The tetraploid complement is within the normal limits for cultures that have been passaged several times. The finding of a single cell with a structural abnormality is considered a nonclonal event, and this cytogenetic study was interpreted as normal.

We have previously reported that MAPCs do not stimulate a T cell alloresponse even when MAPCs have been pretreated with IFNγ to upregulate MHC class I, ICAM-1 and CD80 expression [106]. These studies did not address the possibility that MAPCs could actively suppress an immune response. To explore this possibility, B6 MAPCs were mixed with purified B6 T cells and added to irradiated BALB/c stimulators. A significant reduction in proliferation was observed in MAPC-treated MLR at all time points (Fig. 1A). On the peak of the response (day 5), there was a near complete inhibition of T cell alloresponses from MAPC co-cultures (91%, $P<0.001$ for 1:10; and 86%, $P<0.001$ for 1:100). To ensure the observed inhibitory effect was not dependent on this specific MAPC isolate or B6 strain of MAPC, BALB/c derived MAPCs were generated and mixed with BALB/c T cells and B6 irradiated stimulators. The percent T

cell inhibition on the day of peak response was 88% (P<0.001) for 1:10 co-cultures, and 85% (P<0.001) for 1:100 co-cultures (Fig. 1B). These data indicated that the MAPC immune suppressive properties are not dependent on isolate or strain. The presence of MAPCs in MLR cultures significantly reduced the percentage of activated (CD25+, CD44hi, CD62Llo, CD122+) $CD4^+$ (Fig. 1D) and $CD8^+$ (Fig. 1E) Teffectors on days 5 and 7 (P<0.001 for both time points for 1:10 and 1:100 co-cultures). Taken together, the data show that MAPCs potently inhibit the activation and proliferation of alloresponsive T cells *in vitro*.

To determine whether suppression was MHC-restricted, B6 MAPCs were added to purified BALB/c T cells and irradiated B10.BR splenic stimulators (Fig. 1C). Third-party MAPCs potently inhibit allogeneic T cell proliferation (89% and 80% average T cell inhibition at peak for 1:10 and 1:100, respectively, P<0.001 for both), indicating inhibition was not MHC restricted. To determine if MAPCs had differential effects on resting vs actively proliferating T cells, MAPCs were added on days 0, 1, 2, and 3 to an MLR consisting of B6 T cells and BALB/c stimulators. On both days 5 and 7, T cell proliferation was significantly diminished by MAPC (P<0.001) (supplemental Fig. 2A), indicating that MAPCs can suppress an ongoing alloresponse.

Several studies attribute the T cell inhibitory properties of MSCs to their ability to generate or regulate Tregs [96,107,108]. MLR-MAPC co-cultures were performed using T cells or CD25-depleted T cells to determine if the lack of Tregs at the priming stage of the allogeneic response would impact MAPC-induced suppression. No difference was seen in the suppression potency between Treg-depleted vs repleted cultures (Fig. 2A). $Foxp3^+$Tregs percentages did not increase in MAPC- vs control cultures through all time

points (day 5 shown) in cultures using CD25-replete vs depleted T cells at all points (Figs 2B, C and data not shown). We conclude that MAPC-mediated suppression neither depends upon Tregs in the responding T cell fraction and nor induces Tregs from the $CD25^-$ T cell fraction.

Murine MAPCs mediate suppression via PGE_2. MSCs are known to be capable of suppressing immune responses via release of soluble factors. To determine whether MAPCs could act similar to MSCs, we utilized a TransWell co-culture system in which B6 T cells and BALB/c splenic stimulators were placed in the lower chamber and B6-derived MAPCs were placed in the upper chamber of a TransWell. MAPCs inhibited T cell alloresponses in a contact-independent manner (Fig. 3A), producing an 85% inhibition of T cell proliferation on day 5 ($P<0.01$). No significant differences were seen due to the presence of a TransWell ($P=0.19$). To prove that MAPC-derived soluble factors were necessary and sufficient to induce immune suppression, cell-free supernatant from untreated and MAPC-treated MLR co-cultures were added in a 1:1 ratio with fresh media to a second MLR primary co-culture. MAPC-treated supernatant was equally as effective in inhibiting T cell proliferation as MAPCs placed in direct contact with responders (Fig. 3B; $P=0.20$). Supernatants were taken from B6>BALB/c MLR cultures and ELISAs were performed to determine effects on proinflammatory cytokine secretion. MAPCs decreased proinflammatory cytokine (TNFα, IL-12, IFN-γ, and IL-2) concentrations within these cultures at all time points (Fig. 3C). Although no significant increases in the amount of anti-inflammatory cytokines, IL-10 or TGF-β were observed,

there was a significant increase in PGE_2 concentrations within MAPC co-cultures (P<0.001) (Fig. 3D).

To determine if MAPCs were the source of PGE_2 and if the increase in PGE_2 was responsible for decreased T cell alloresponsiveness, MAPCs expression of PGE_2 synthase was verified, indicating they were capable of converting PGH_2 into PGE_2 (supplemental Fig. 3A). Overnight treatment of MAPCs with the COX1/2 inhibitor, indomethacin, potently inhibited the upstream synthesis of PGE_2 for the period of the MLR culture (9 days)(supplemental Fig. 3B) without adversely affecting MAPC viability (data not shown). When indomethacin-treated MAPCs were added to MLR co-cultures, they no longer inhibited T cell allo-responses (Fig. 4A). At the peak of the response (day 6), there was a 90% vs 13% inhibition in allogeneic T cell proliferation when untreated vs indomethacin-pretreated MAPCs were in co-culture (P<0.001). At all other days examined, pre-treatment of MAPC with indomethacin lead to >90% restoration of proliferation.

MAPCs were found to upregulate IDO upon activation with IFN-γ (data not shown). To determine if IDO could account for the remaining inhibitory properties of these cells (~10%), MAPCs were pre-treated with indomethacin and/or the MLR co-culture was treated with 1-Methyl-Tryptophan (1MT), a competitive inhibitor of IDO. The addition of 1MT to MLR co-cultures did not increase T cell proliferation (supplemental Fig. 3C) and there was little/no additive effect of indomethacin pre-treatment of MAPCs with 1MT treatment of the co-culture (supplemental Fig. 3C).

Murine MAPC can delay GVHD mortality and target tissue destruction if localized to the spleen early post-BMT. The prophylactic anti-GVHD efficacy of MAPC was tested in lethally irradiated BALB/c mice given B6 BM plus 2 x 10^6 B6 CD25-depleted T cells. Cohorts were given MAPC-DL or PBS via intra-cardiac (IC) injections since IC injections leads to a more widespread biodistribution and longer persistence of MAPC-DLs [106]. Despite their potent suppressive capacity *in vitro*, MAPC-treated mice vs control mice had virtually identical survival rates (Fig. 5A). BLI of these mice revealed that most cells had migrated to BM cavities (skull, femur, spine), rather than to T cell priming sites such as LNs or spleen (data not shown).

With the known short half life of PGE_2 *in vivo* [106], we speculated that sufficient quantities of this molecule might not be penetrating T cell allopriming sites such as LNs and spleen. Subsequent studies were performed in which untreated or indomethacin-treated B6 MAPCs were given via an intra-splenic (IS) injection. Controls were given BM alone plus sham surgeries or BM plus T cells and sham surgeries. BLI imaging of mice given MAPC-DL IS showed that these cells remained within the spleen for a period of up to 3 weeks (supplemental Fig. 4A and 4B). When compared to controls receiving BM+T-cells plus sham surgeries, mice given intra-splenic injections of untreated MAPCs have a significant improvement in survival (P <0.001), with two long-term survivors >55 days (Fig. 5B). MAPC-DLs present in the spleen continued to express PGE synthase as shown by co-staining (Fig. 5F). Indomethacin pretreatment of MAPCs precluded this protective effect (Fig. 5C) (MAPC vs MAPC-Indo, P=0.0058), indicating that PGE_2 is responsible for the suppressive potential of these cells *in vivo*. Mean body weights of these mice recapitulate these findings (supplemental Fig. 4C). On day 21 post-BMT,

there was significantly more infiltrating lymphocytes in the liver and lung, resulting in increased necrotic foci and perivascular and peribronchiolar cuffing (Fig. 5D, E) along with large numbers of infiltrating lymphocytes in the colons of GVHD control vs MAPC treated mice (Fig. 5D, E).

Therefore, MAPCs utilize PGE_2 as a mechanism in vivo that leads to a significant increase in survival of mice with GVHD, and importantly, these effects were dependent upon MAPC location.

MAPCs diminish T cell proliferation and activation within the local environment. The direct in vivo effects of PGE_2 on donor T cell proliferation and activation using the MAPC intra-splenic administration model was determined. BALB/c mice were lethally irradiated and given B6 MAPC-DL via intra-splenic injections on day 0, and B6 CFSE-labeled CD25-depleted T cells (15×10^6) on day 1. Controls were given labeled T cells alone plus sham injection. On day 4, LNs and spleens were analyzed by BLI. MAPCs were only located within the spleen and had not migrated out to the LNs (supplemental Fig. 5A). FACS analysis was performed to determine the percentage of T cells that had divided during this time period and the proliferative capacity (the number of daughter cells that each responder cell produced) was calculated. There was a significantly reduced number of $CD4^+$ and $CD8^+$ T cells that had undergone cellular division as determined by CFSE dilution in MAPC-treated vs control groups (Fig. 6A). In the LN of the same mice, there were no significant differences in either $CD4^+$ or $CD8^+$ T cells that had undergone cellular division. MAPCs resulted in a significantly reduced proliferative capacity of CFSE-labeled $CD4^+$ and $CD8^+$ T cells in the spleen (Fig. 6B). Each alloreactive CD4 T

cell that had divided gave rise to 15 vs 10 daughter cells in untreated vs MAPC-treated mice (P=0.0005). Each alloreactive CD8 T cell that divided gave rise to 10 vs 6 daughter cells, respectively (P=0.0004) (Fig. 6B). In the LN of the same mice, there were no significant differences in $CD4^+$ or $CD8^+$ T cell proliferative capacity between control- and MAPC-treated mice (Fig. 6C). Each $CD4^+$ T cell gave rise to an average of 9 and 9.4 daughter cells (P=0.25) and each $CD8^+$ T cell gave rise to 6.8 and 7.3 daughter cells in untreated vs MAPC-treated groups (P=0.061). More splenic T cells downregulated CD62L and upregulated CD25 in the control- vs MAPC-treated group (Fig. 6D). In LNs, no such effects were observed (Fig. 6E), indicating that MAPCs limit allogeneic T cell activation and expansion locally in vivo. Others have shown that PGE2 can influence the expression of co-stimulatory molecules [109]. Therefore, we tested T cells and DCs within this in vivo MLR setting using treated or un-treated MAPCs to determine if the PGE_2 effect on proliferation was due to its influence on co-stimulatory molecule expression. There were significantly more $CD4^+$ and $CD8^+$ T cells within MAPC-treated groups than the control groups that expressed the negative co-stimulatory molecules PD-1 on $CD4^+$ and $CD8^+$ T cells (Fig. 7A, B). Similarly, CTLA-4 was also expressed on a higher percentage of $CD4^+$ and $CD8^+$ T cells in MAPC vs control cultures. Also consistent with MAPC-induced suppression, the percentage of $OX40^+CD8^+$ T cells was significantly lower than controls, along with a trend toward less OX40 and 41BB expression on $CD4^+$ and $CD8^+$ T cells, respectively. These effects were reversed using MAPC treated with indomethacin prior to in vivo administration (Fig. 7). Within the MAPC vs control groups, there was a significant increase in the percentage of DCs expressing PD-L1 and CD86 (Fig. 7C) without significant differences in the percentage of DCs expressing other

costimulatory molecules (Fig. 7C). When using indomethacin-treated MAPCs, again, these effects were mostly reversed. There were no significant differences in the percentages of T cells and APCs expressing ICOS, ICOS-L, CD40 and CD40L between groups (data not shown). Taken together, these data indicated that PGE_2 accounts for the majority of the suppressive potential of MAPCs and has the downstream effect of increasing the percentage of cells expressing negative costimulatory regulators (PD1, PDL1, CTLA4), and decreasing the percentage of cells expressing positive costimulatory regulators (OX40, 41BB).

Discussion

We have shown that MAPCs inhibit the proliferation and activation of allogeneic T cells via the elaboration of PGE_2. *In vivo*, MAPCs did not home to lymphoid organs and were incapable of suppressing GVHD. Despite the contact-independence of MAPCs in suppressing alloresponse in vitro, MAPCs reduced GVHD only when injected into the spleen. MAPCs synthesis of PGE_2 *in situ* resulted in an unfavorable *in vivo* environment for supporting T cell activation. These data emphasize the importance of ensuring homing of immunomodulatory cell types to relevant tissue sites to dampen T cell priming and subsequent tissue injury.

Here we show that MAPCs are constitutive producers of PGE_2. Inhibiting MAPC synthesis of PGE_2 by treatment of the cells with a potent COX inhibitor restored in vitro T cell proliferation in an allo-MLR culture to >90% of the control. In contrast, precluding other known inhibitors of an immune response, IL-10, TGF-β or IDO, using IL-10 receptor knock-out T cells, anti-TGF-β antibodies or the competitive IDO inhibitor, 1MT, did not affect T cell proliferation in MLR cultures (Supplemental Fig. 3C and data not shown). Thus, of the several known soluble factors that have been shown to contribute to the suppression of T cells in MLR cultures in non-contact systems, PGE_2 appears to be the dominant secreted molecule involved in MAPC-induced suppression of an *in vitro* alloresponse. Similarly, *in vivo*, inhibition of GVHD required MAPC production of PGE_2 *in situ*.

PGE_2 can be produced by many cells [110] and influence the function of a wide array of immune cells including T cells [111], B cells [112], macrophages [113], and DCs[114]. MAPC synthesis of PGE_2 in vitro was associated with the upregulation of negative co-

stimulatory molecules and downregulation of positive costimulatory on T cells and APCs (data not shown). In contrast, a recent report has shown that human monocyte ($CD14^+$) and myeloid ($CD11c^+$) DCs upregulate positive costimulatory molecules (OX40L, CD70, 41BBL) if PGE_2 is added during the maturation process [115]. We speculate that the apparent discordance may be due to the differences in the maturation status of the DCs at the time of PGE_2 stimulation, although neither DC location (BM vs spleen) nor species-specific differences can be excluded as explanations. PGE_2 is known to have both stimulatory and inhibitory effects on DC activation, dependent upon the context in which PGE_2 is encountered. DCs encountering PGE_2 in the periphery have an increased activation and increased migratory abilities, whereas those encountering PGE_2 within secondary lymphoid organs leads to decreased activation and decreased effector function [114].

In this and our prior report [116], we have shown that donor MAPCs preferentially migrated to the BM after systemic delivery and are thus unlikely to directly interact with GVHD-causing donor T cells within lymphoid organs. Because the half-life of PGE_2 *in vivo* is extremely short (~30 sec)[117], we hypothesized that this mechanism of MAPC-mediated suppression may not penetrate secondary lymphoid organs to a sufficient degree to inhibit T cell activation and proliferation. MAPCs used in our studies did not express CD62L or CCR7, important for homing to secondary lymphoid organs (data not shown). To circumvent this problem, MAPCs were delivered directly into the spleens at the time of BMT, thereby restoring the capacity of MAPCs to suppress donor T cell activation and proliferation *in vivo*. As predicted, this MAPC-mediated effect was only observed in the spleens and not in the LNs of transplanted mice (Fig 6), confirming our

initial hypothesis that PGE_2 acts in a local manner. This suppressive effect on donor T cells in vivo improved the survival of mice experiencing severe GVHD, a process that was almost entirely dependent on PGE_2 production from MAPCs (Fig 5B, C). Although the overall survival was improved by MAPC injection into the spleen, most mice eventually succumbed to the disease with only a minority becoming long-term survivors. Therefore, despite the fact that ~8-fold more T cells migrate to the spleen than to LNs during a given time point[118], T cell activation within the LNs is sufficient, possibly along with residual T cell activation within the spleen, to cause to lethal GVHD. The importance of secondary lymphoid organs for GVHD initiation can be derived from studies in which mice that lack all secondary lymphoid organs are incapable of developing severe GVHD [119,120]. Because studies have shown that GVHD cannot be prevented by host splenectomy alone [121], our data suggest that MAPC-mediated suppression of donor T cells within the spleen is not equivalent to a splenectomy. This may be due to the functional alterations of donor T cells that are exposed to PGE_2 within the spleen in lymphoid replete recipients in contrast to the unrestrained activation and proliferation of a higher number of donor T cells that would traffic to the LNs of splenectomized hosts. Interestingly, MAPCs suppressed GVHD-induced tissue injury to a greater extent in the liver and lung as compared to the colon. Whether the influence of MAPCs on donor splenic T cell function as evidenced by the pattern of costimulatory molecule expression or the homing of donor T cells after exposure to MAPCs in the spleen would favor such a preferential organ-specific is unknown.

The requirement for homing of immune suppressive cells to secondary lymphoid organs to exert their maximum biological effect is not unique to MAPCs. For example,

previous studies using murine BM-derived MSCs have proven to be ineffective in altering GVHD lethality[71]. For Treg induced suppression of GVHD, high levels of CD62L expression was needed for optimal *in vivo* suppression of GVHD-induced lethality, though not for *in vitro* suppression [53,122]. Whereas CCR5 expression on Tregs was not required for *in vitro* suppression, CCR5 knockout Tregs were inferior to wild-type Tregs in suppressing GVHD lethality *in vivo*, which was associated with a reduced accumulation of Tregs in lymphoid and non-lymphoid GVHD target organs beyond the first week post-BMT [123]. In solid organ allograft studies, Tregs suppression of graft rejection requires the migration of Tregs from the blood to the allograft to the draining LN [124]. We conclude that the kinetics and homing patterns of immune modulatory cells to the sites of alloresponse are critical in determining the outcome of an alloresponse to foreign antigens and that GVHD inhibition by MAPCs requires homing to lymphoid sites that support GVHD initiation.

Although recent reports indicate that MAPCs can modify injury induced by vascular ischemia [125-127], the *in vitro* and *in vivo* immunosuppressive properties of MAPCs thus far are largely undefined. To our knowledge, only one recent report has described the immunosuppressive potential of rat-derived MAPCs[128]. Similar to our results, rat MAPCs inhibited alloresponses via a contact-independent mechanism. In contrast to our results, rat MAPC induced inhibition of T cell alloproliferation *in vitro* was dependent upon IDO expression since 1MT reverse the suppressive effects of rat MAPCs. Furthermore, rat MAPCs expressed MHC class I antigens, in distinction to both human- and mouse- derived MAPCs that are targeted by NK-mediated lysis [106]. Although neither the homing receptor expression nor the *in vivo* homing or suppressor cell mechanisms

responsible for GVHD inhibition were reported, similar to our study, MAPCs were effective in reducing GVHD lethality.

In summary, this is the first study to demonstrate the *in vitro* and *in vivo* immune suppressive capacity and mechanism of MAPCs in preventing GVHD. The direct demonstration that PGE_2 secretion is able to mediate donor T cell suppression suggests a mechanism by which other cell types such as MSCs and myeloid-derived suppressor cells may be able to suppress adverse alloresponses *in vivo* [129]. Further, these data suggest that pharmacological strategies toward achieving sufficient PGE_2 concentrations in relevant target organs during the acute initiation phase may be useful for GVHD prevention. Importantly, this is also the first study to demonstrate that location of MAPC immune suppressive, non-hematopoietic stem cells *in vivo* to lymphoid organs is a critical determinant of the efficacy of GVHD prevention. Future approaches to ensure the targeting of immune suppressive cells to allopriming sites may increase the efficacy of both non-hematopoietic stem cells and other immune suppressive populations with promise to inhibit GVHD.

Acknowledgements

The authors would like to thank Dr. Christine Vogtenhuber, Dr. Christoph Bucher, Rachelle Veenstra, Emily Goren, and Luna Liu for helpful discussions and technical assistance. We would also like to thank the University of Minnesota cytokine reference laboratory and Sophia Christoforides for technical assistance with cytokine analysis. This study was supported in parts by National Institute of Health (NIH) grants R01 AI34495, HL56067, and HL49997 (to BRB), and the Children's Cancer Research Fund (CCRF to SLH).

Figure 1. MAPC potently inhibit allogeneic T cell proliferation and activation. A MLR reaction was performed by mixing B6 purified T cells with irradiated BALB/c stimulators (1:1) and B6 MAPCs (1:10, 1:100)(A). These cultures were pulsed with ^{3}H-thymidine on the indicated days harvested 16 hours later. Proliferation was determined as a measure of radioactive uptake. A MLR reaction was performed as above using BALB/c T cells plus B6 stimulators and BALB/c MAPC (B), or BALB/c T cells plus B10.Br stimulators and B6 MAPCs (C). FACS analysis of B6>BALB/c MLR+B6 MAPC was performed on the indicated days and gated on CD4+ T cells (D) or CD8+ T cells (E) in conjunction with activation markers.

Figure 1

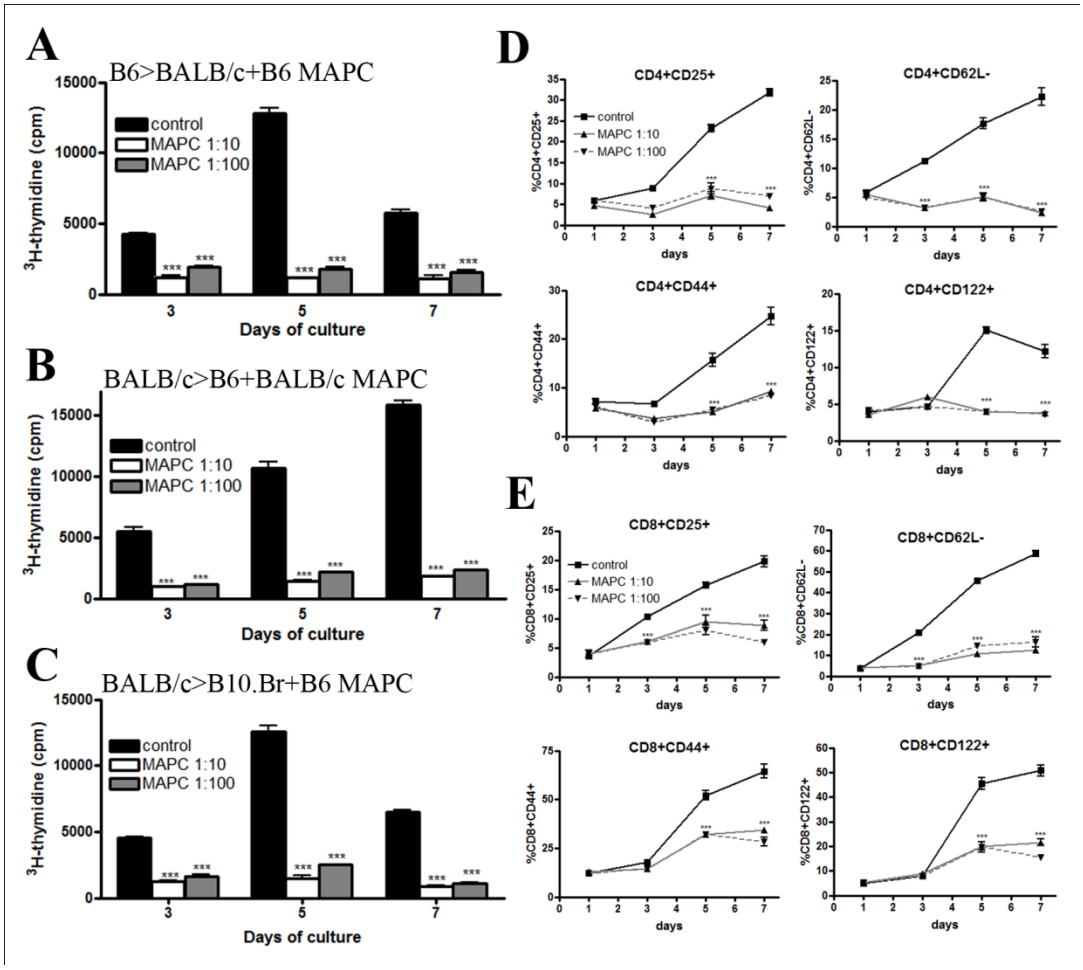
A
B6>BALB/c+B6 MAPC
control
MAPC 1:10
MAPC 1:100
^{3}H-thymidine (cpm)
Days of culture
B
BALB/c>B6+BALB/c MAPC
C
BALB/c>B10.Br+B6 MAPC
D
CD4+CD25+
CD4+CD62L-
CD4+CD44+
CD4+CD122+
%CD4+CD25+
%CD4+CD62L-
%CD4+CD44+
%CD4+CD122+
days
E
CD8+CD25+
CD8+CD62L-
CD8+CD44+
CD8+CD122+
%CD8+CD25+
%CD8+CD62L-
%CD8+CD44+
%CD8+CD122+

Figure 2. MAPC-mediated suppression in vitro is independent of Tregs. A B6>BALB/c MLR culture was performed using purified T cells or T cells that were CD25-depleted and MAPCs at 1:10 ratios. ^{3}H-thymidine was added on the indicated days and proliferation was measured (A). FACS analysis was performed on day 2 on the non-CD25-depleted (B) and the CD25-depleted (C) MLR co-cultures to determine the percentage of $CD4^{+}FoxP3^{+}$ T cells.

Figure 2

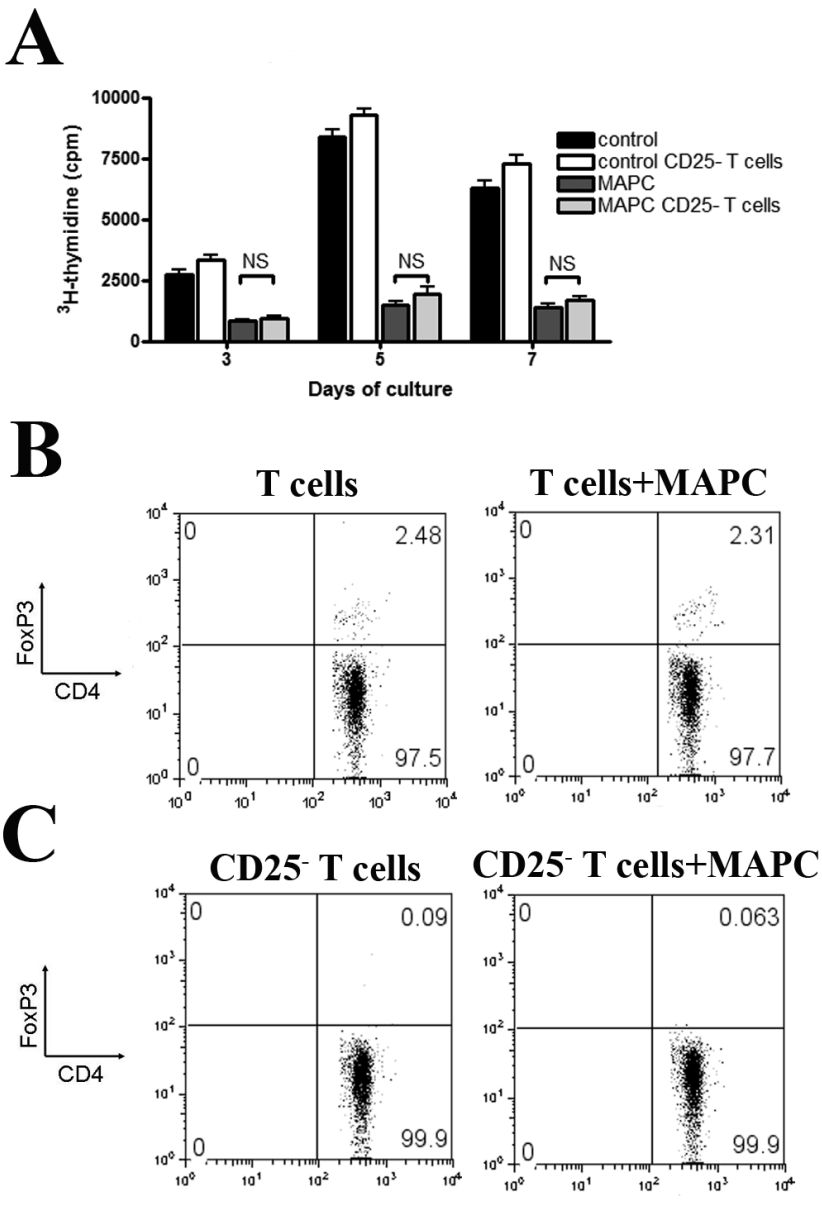
A
10000
7500
5000
2500
0
^{3}H-thymidine (cpm)
NS
NS
NS
3
5
7
Days of culture
control
control CD25- T cells
MAPC
MAPC CD25- T cells
B
T cells
T cells+MAPC
FoxP3
CD4
2.48
97.5
2.31
97.7
C
CD25$^-$ T cells
CD25$^-$ T cells+MAPC
0.09
99.9
0.063
99.9

Figure 3. MAPC mediate suppression via a soluble factor. A B6>BALB/c MLR plus MAPCs at 1:10 ratios were arranged by placing T cells and stimulators in the lower well of a TransWell insert and MAPCs in the upper chamber, or by placing MAPCs in direct contact with stimulators and responders (A). (B) Supernatant taken from MAPC or control co-cultures on day 3 were added in 1:1 ratio with fresh media to B6>BALB/c MLR. Results of MAPCs at 1:10 and 1:100 ratios in direct contact with responding T cells are shown for comparison. Proliferation was assessed using ^{3}H-thymidine uptake as above. ELISA or Luminex technology was performed on MLR supernatant harvested on the indicated day to determine the amount of proinflammatory (C) and anti-inflammatory (D) cytokines in culture with MAPCs at 1:10 and 1:100 ratios.

Figure 3

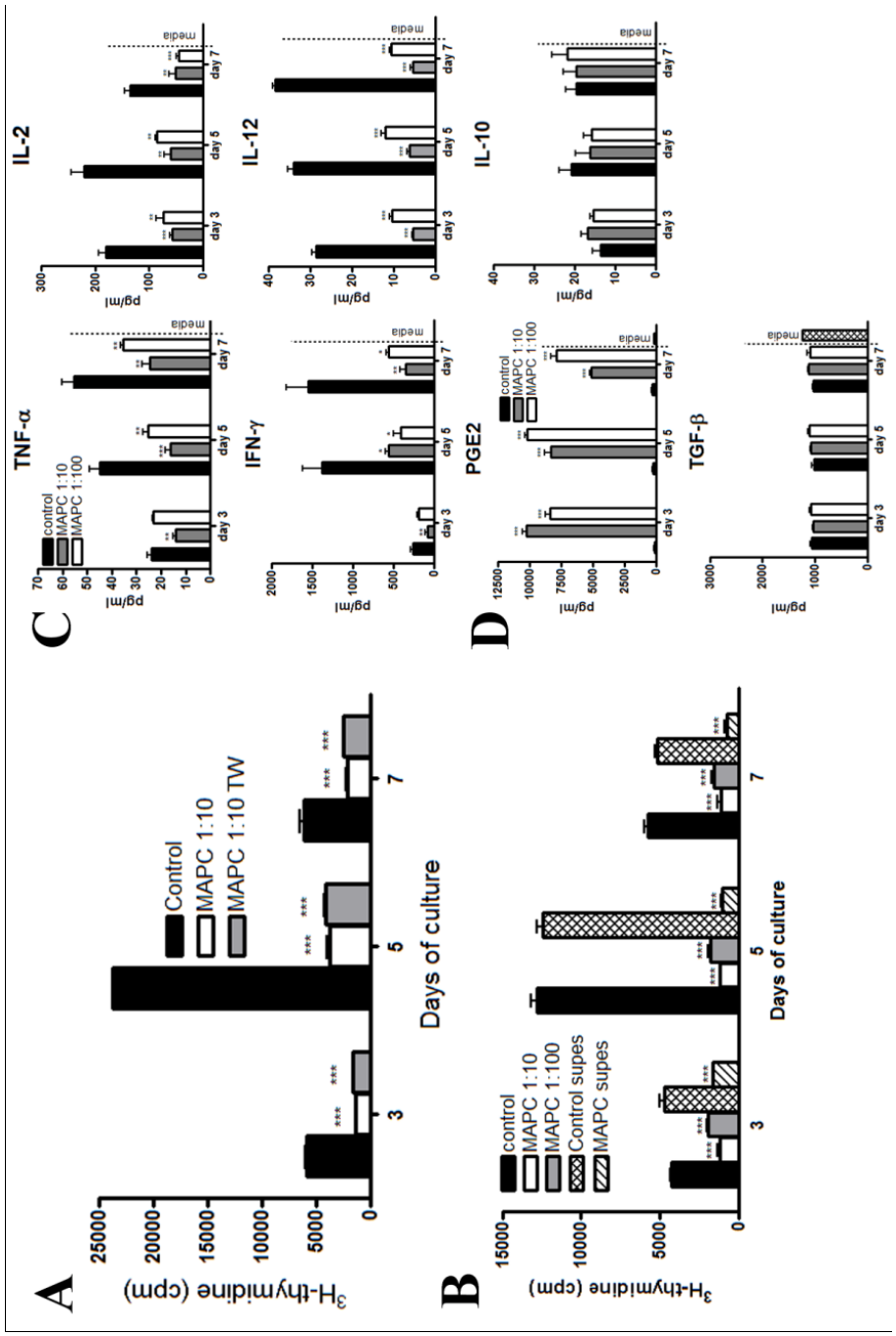
A
3H-thymidine (cpm)
Control
MAPC 1:10
MAPC 1:10 TW
Days of culture
B
3H-thymidine (cpm)
control
MAPC 1:10
MAPC 1:100
Control supes
MAPC supes
Days of culture
C
TNF-α
IL-2
IFN-γ
IL-12
D
PGE2
IL-10
TGF-β
pg/ml
media
day 3
day 5
day 7

Figure 4. MAPC inhibit T cell allo-responses through the secretion of PGE2.

B6>BALB/c MLR cultures were arranged as before. MAPCs, either untreated, treated overnight with 5uM indomethacin to inhibit production of PGE2, or treated with vehicle were titrated in at 1:10 ratios. Proliferation was assessed as above (A).

Figure 4

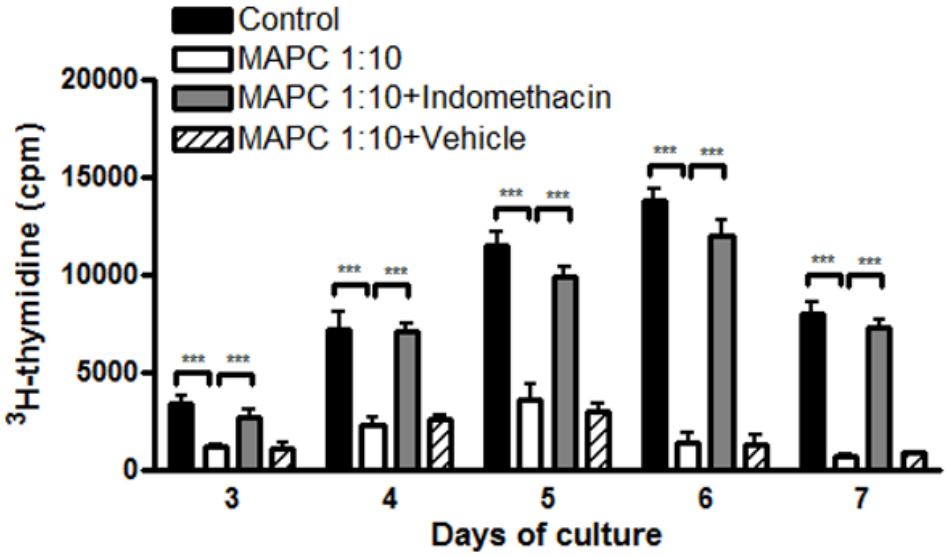
Control
MAPC 1:10
MAPC 1:10+Indomethacin
MAPC 1:10+Vehicle
^{3}H-thymidine (cpm)
20000
15000
10000
5000
0
***
3
4
5
6
7
Days of culture

Figure 5. The capacity of MAPCs to delay GVHD mortality and limit target tissue destruction is dependent on anatomical location of the cells and their production of PGE2.

BALB/c mice were lethally irradiated and then given 10^6 BM cells from B6 mice on day 0 followed by $2x10^6$ purified CD25-depleted whole T cells on day 2. On day 1, mice were given $5x10^5$ untreated B6 MAPCs or PBS delivered via intra-cardiac injections. Kaplan-Meier survival curve is representative of one experiment in which BM only and BM+T group had n=6, and MAPC group had n=8 (A). (B) BMT was performed as in (**A**) except mice were given PBS or $5x10^5$ MAPC intra-splenically (IS) on day 1. The survival curve is representative of 3 pooled experiments (BM only, n=18; BM+T, n=20; MAPC, n=26)(MAPC vs BM+T, $p<0.001$). (C) Survival curve representative of one experiment in which mice received BMT plus untreated MAPC or MAPC pre-treated overnight with indomethacin before IS injection (BM only, n=5; BM+T, n=5; MAPC, n=10; MAPC indo, n=10)(MAPC vs MAPC indo, $p=0.002$). Tissue taken from cohorts of mice from (B) were harvested on day 21 and embedded in OCT followed by freezing in liquid nitrogen. 6uM sections were stained with H&E and analyzed for histopathological evidence of GVHD. Representative images are shown (D)(magnification ×200). (E) The average GVHD score for BM only, BM+T, and BM+T+MAPC(IS) cohorts is shown. (F) Spleens were harvested from BMT plus MAPC IS transplanted mice on day 21 and snap frozen in OCT compound. Tissue sections were cut and stained using anti-luciferase and anti-PGE synthase antibodies. Confocal analysis reveals that MAPC are found in the spleen at this time point and retain their ability to produce PGE2. 5F *upper* shows luciferase alone, 5F *lower* shows colocalization of PGE synthase with luciferase

Figure 5

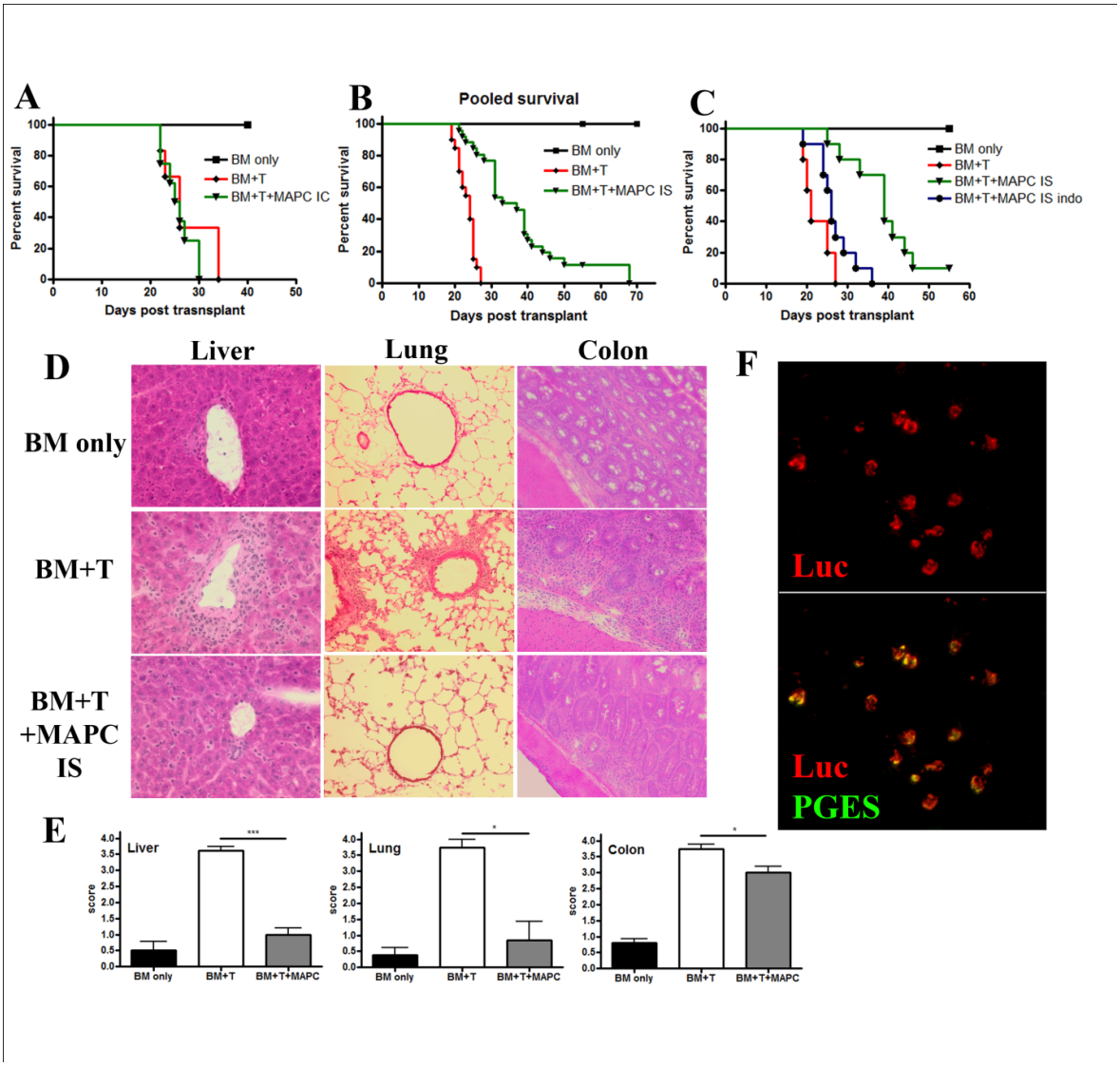
A
Percent survival
Days post trasnsplant
BM only
BM+T
BM+T+MAPC IC
B
Pooled survival
Percent survival
Days post transplant
BM only
BM+T
BM+T+MAPC IS
C
Percent survival
Days post transplant
BM only
BM+T
BM+T+MAPC IS
BM+T+MAPC IS indo
D
Liver
Lung
Colon
BM only
BM+T
BM+T +MAPC IS
F
Luc
Luc
PGES
E
Liver
Lung
Colon
score
BM only
BM+T
BM+T+MAPC

Figure 6. MAPCs dampen T cell proliferation and activation within the local environment.

"In vivo MLR" was performed by administering lethally irradiated BALB/c mice with $5x10^5$ B6 MAPCs IS (day 0) followed by $15x10^6$ B6 CFSE-labeled CD25-depleted T cells (i.v.)(day 1). Control mice were given labeled T cells alone plus sham surgeries. Spleens and LN were harvested on day 4 and analyzed via FACS for CD4 and CD8 expression and percent CFSE dilution (A). The proliferative capacity for $CD4^+$ and $CD8^+$ T cells in the spleen (B) and LN (C) of transplanted mice was calculated as previously published [103]. (D, E) Activation markers for $CD4^+$ and $CD8^+$ T cells in the spleen and LN were analyzed using FACS and graphed.

Figure 6

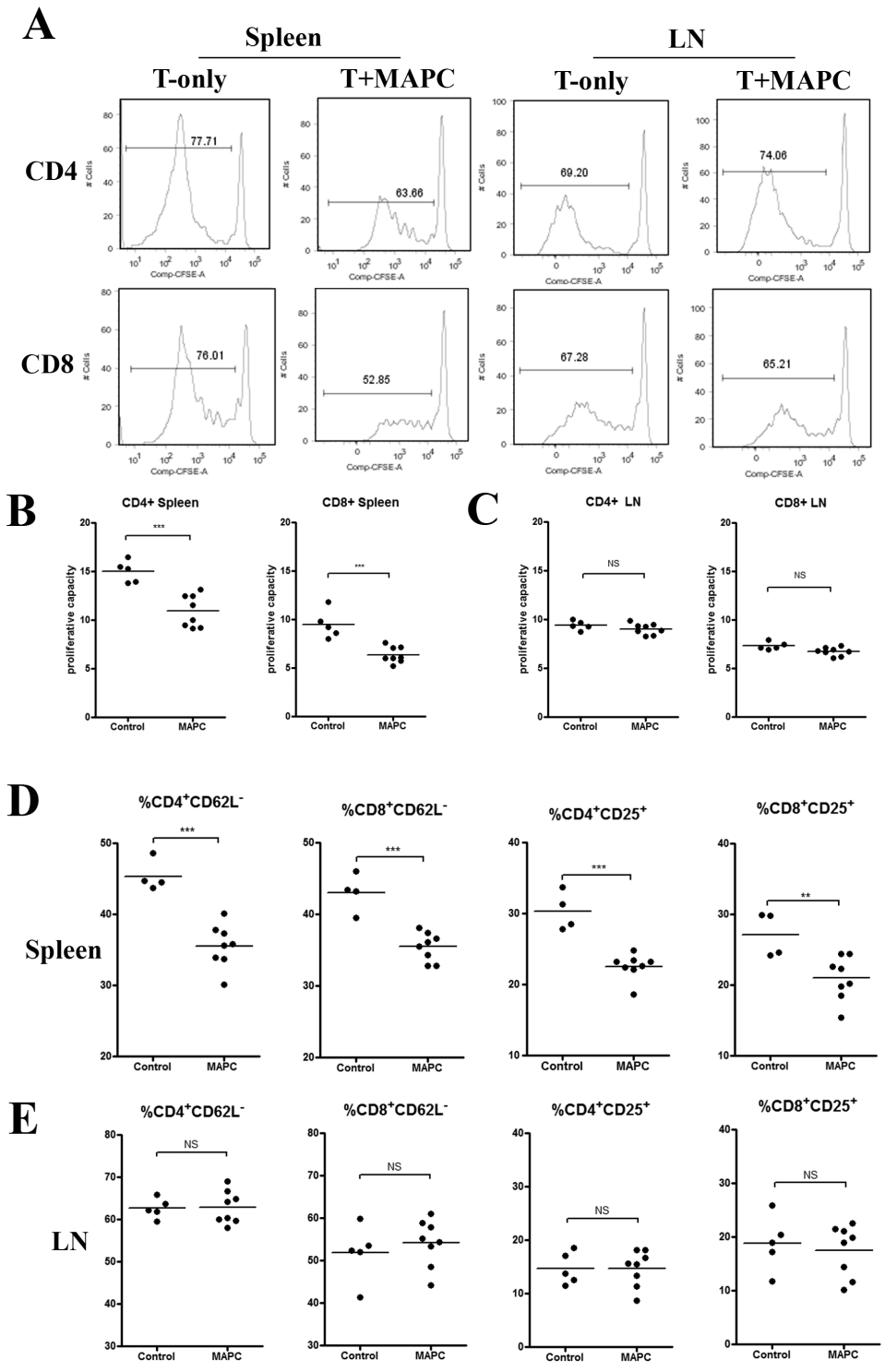
A
Spleen
LN
T-only
T+MAPC
T-only
T+MAPC
CD4
CD8
77.71
63.66
69.20
74.06
76.01
52.85
67.28
65.21
Cells
Comp-CFSE-A
B
CD4+ Spleen
CD8+ Spleen
C
CD4+ LN
CD8+ LN
proliferative capacity
***
NS
Control
MAPC
D
Spleen
%CD4+CD62L-
%CD8+CD62L-
%CD4+CD25+
%CD8+CD25+
**
E
LN

Figure 7. MAPCs affect costimulatory molecule expression on T cells and DCs in the spleen. FACS analysis of spleen cells harvested from transplanted mice on day 4 was performed to determine the percentage of $CD4^+$ (A), $CD8^+$ (B), and $CD11c^+$ (C) cells that expressed the indicated co-stimulatory molecules. In this transplant, MAPCs were untreated or pre-treated with indomethacin, as described, before their application.

Figure 7

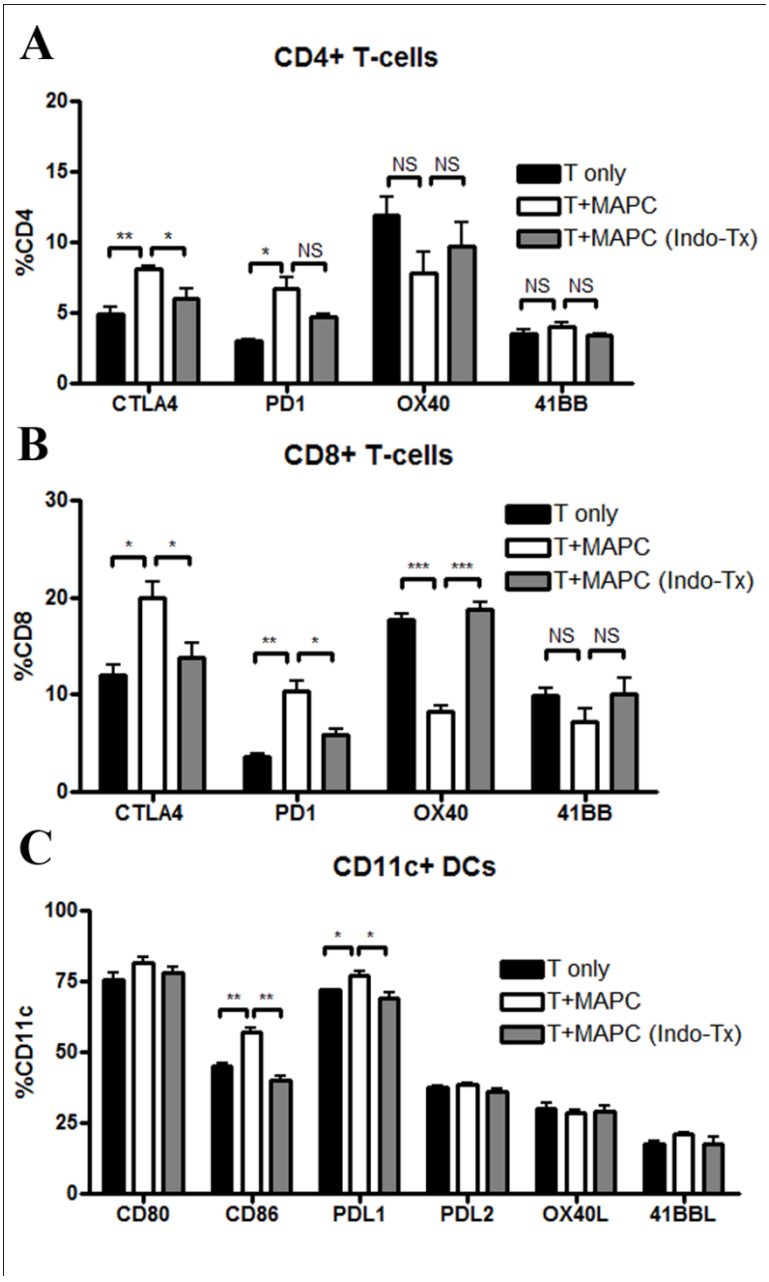
A
CD4+ T-cells
%CD4
20
15
10
5
0
**
*
*
NS
NS
NS
NS
NS
T only
T+MAPC
T+MAPC (Indo-Tx)
CTLA4
PD1
OX40
41BB
B
CD8+ T-cells
%CD8
30
20
10
0
*
*
**
*
***
***
NS
NS
T only
T+MAPC
T+MAPC (Indo-Tx)
CTLA4
PD1
OX40
41BB
C
CD11c+ DCs
%CD11c
100
75
50
25
0
**
**
*
*
T only
T+MAPC
T+MAPC (Indo-Tx)
CD80
CD86
PDL1
PDL2
OX40L
41BBL

Supplemental figure 1. Characterization of MAPC. (A) MAPCs isolated from B6 mice were differentiated into cells of mesodermal lineage and functionally tested for their ability to produce lipid droplets (adipocytes, Oil Red O), calcium deposition (osteocytes, Alizarin Red S), and accumulate collagen (chondrocytes, alkaline phosphatase). (B) Undifferentiated MAPCs (insert) or MAPCs directed to differentiate in vitro into cells representative of three germ layers, were stained for expression of CD31 and VWF (endothelium), HNF and albumin (endoderm), and GFAP and NF200 (neuroectoderm) and analyzed using confocal microscopy. In all images (except HNF) nuclear staining using DAPI is visualized as blue. (C) Undifferentiated MAPCs were examined for their expression of specific surface markers using flow cytometry. Isotype controls are shaded red. (D) RNA was isolated and cDNA was synthesized from undifferentiated MAPCs and murine embryonic stem cells. RT-PCR was used to examine the expression of Oct3/4 and Rex-1. No Template Control (NTC) and HPRT served as negative and positive controls, respectively. (E) Chromosomal analysis of MAPC shows a normal 40, XX karyotype.

Supplemental Figure 1

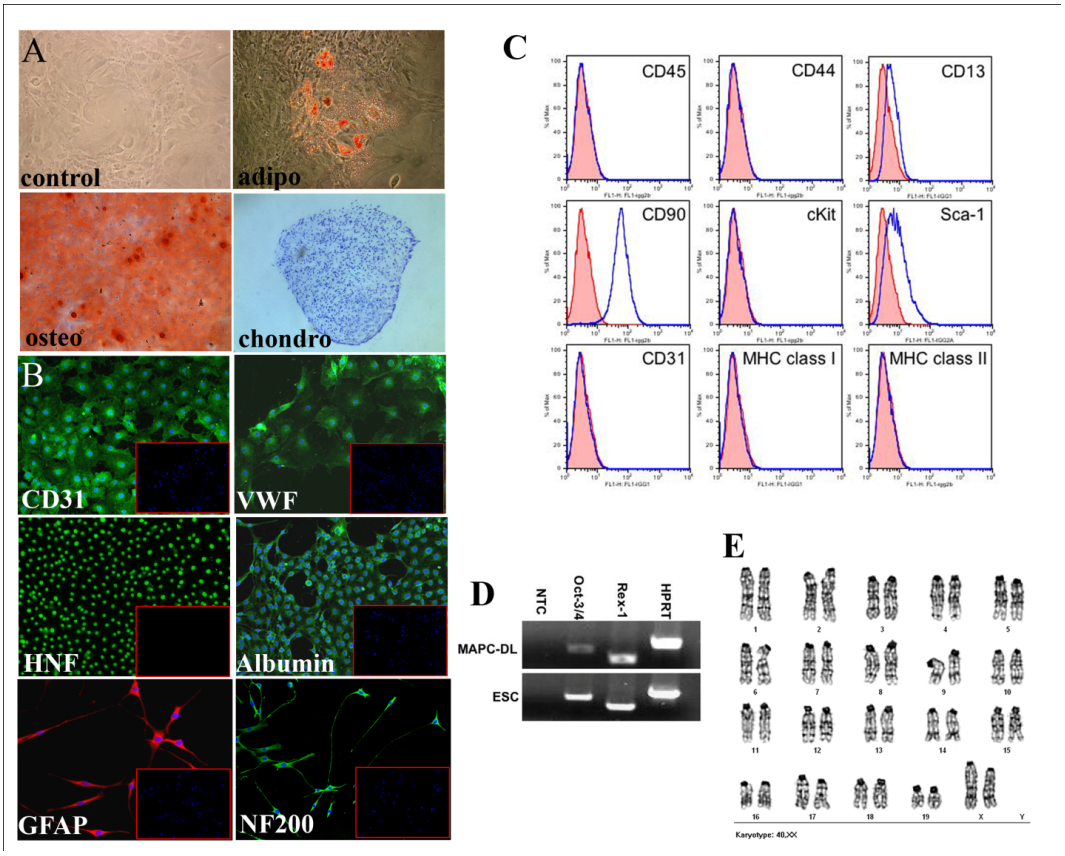

Supplemental figure 2. MAPC inhibit ongoing allo-responses. B6>BALB/c MLR cultures were performed and B6 MAPCs were titrated in at 1:10 ratios on days 0, 1, 2, and 3. Cultures were pulsed on the indicated days and harvested 16 hours later. Proliferation was assessed as a measure of ^{3}H-thymidine uptake.

Supplemental Figure 2

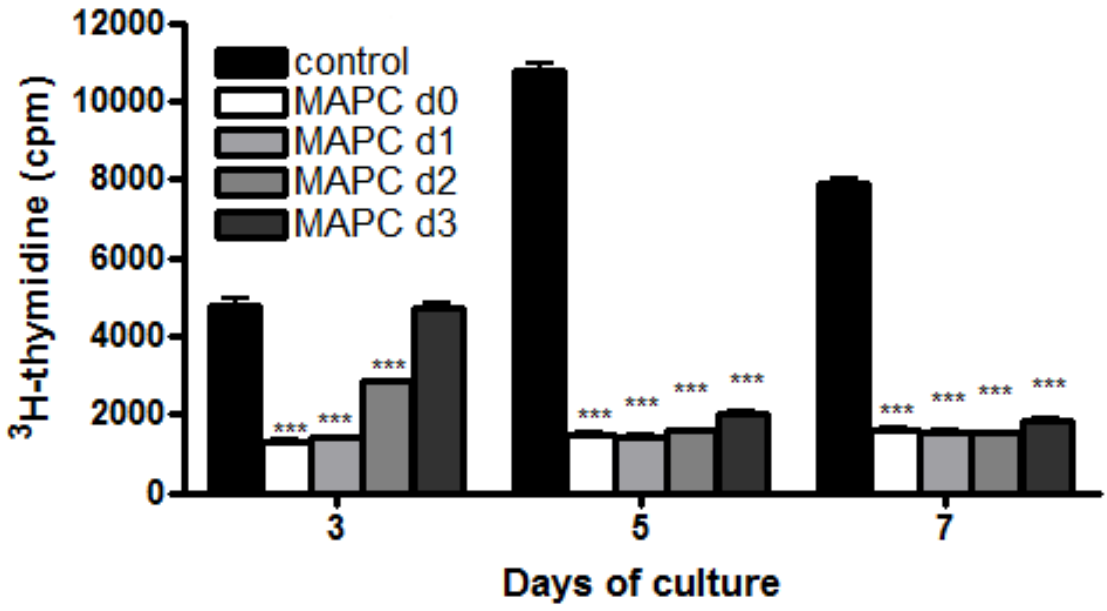

Supplemental figure 3. Effects of PGE2 and IDO on T cell proliferation. (A) RT-PCR verified that MAPC express PGE synthase. No template control (NTC) and HPRT were used as negative and positive controls. (B) Supernatant from MAPC cultures or MAPCs pretreated with 5uM indomethacin overnight and washed were analyzed for the production of PGE2 via ELISA (Day 7 shown). (C) MLR cocultures were arranged using 200 μM 1-methyl tryptophan and 5 μM indomethacin in the culture media either alone or in combination to assess the contribution of IDO and PGE2 on MAPC mediated suppression, respectively. MLR were pulsed with ^{3}H-thymidine on the indicated days and harvested 16 hours later.

Supplemental Figure 3

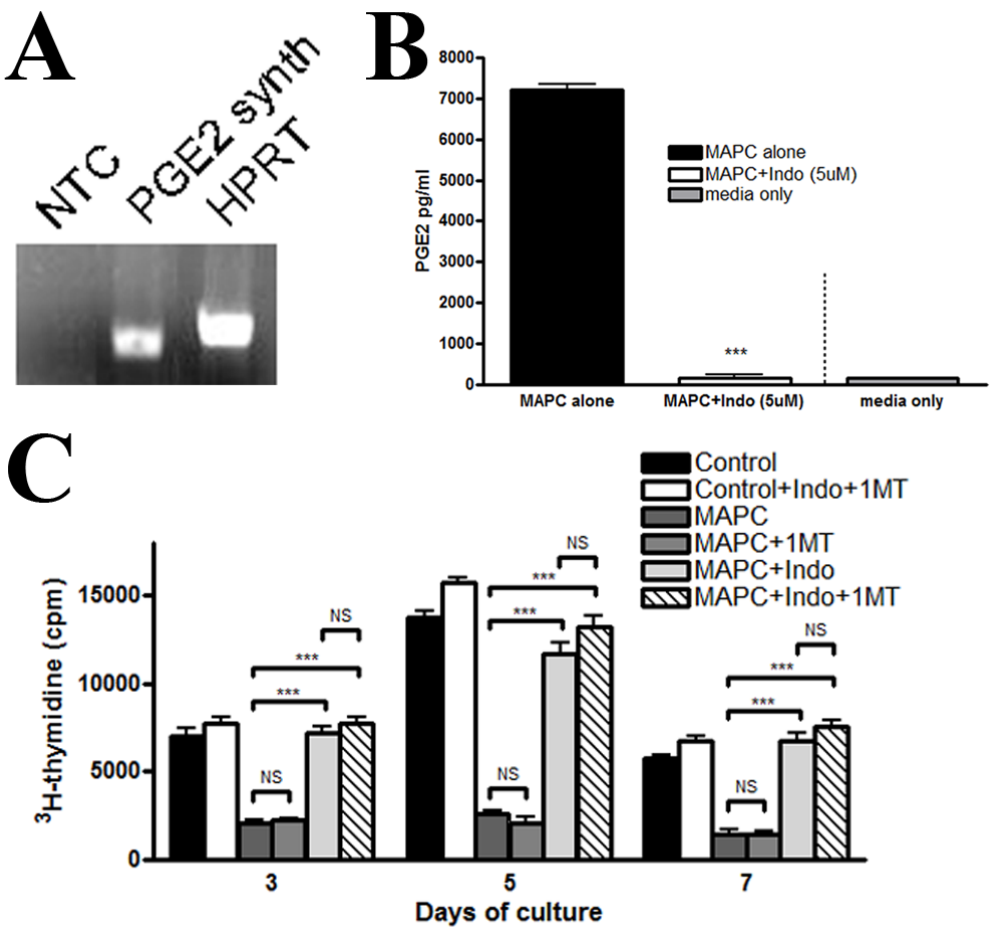

Supplemental figure 4. Persistence of MAPC delivered intra-splenically. (A) BALB/c mice were lethally irradiated and given 10^6 T cell depleted BM cells plus $5x10^5$ MAPC-DL IS. Individual mice and organs (top left-GI tract, top right-spleen, middle left-lung, middle right-LN, bottom left-femur, bottom right-liver) were monitored using bioluminescent imaging to determine the location of MAPCs on day 2, week 1, week 2, and week 3. (B) Weight curve from mice in figure 5C.

Supplemental Figure 4

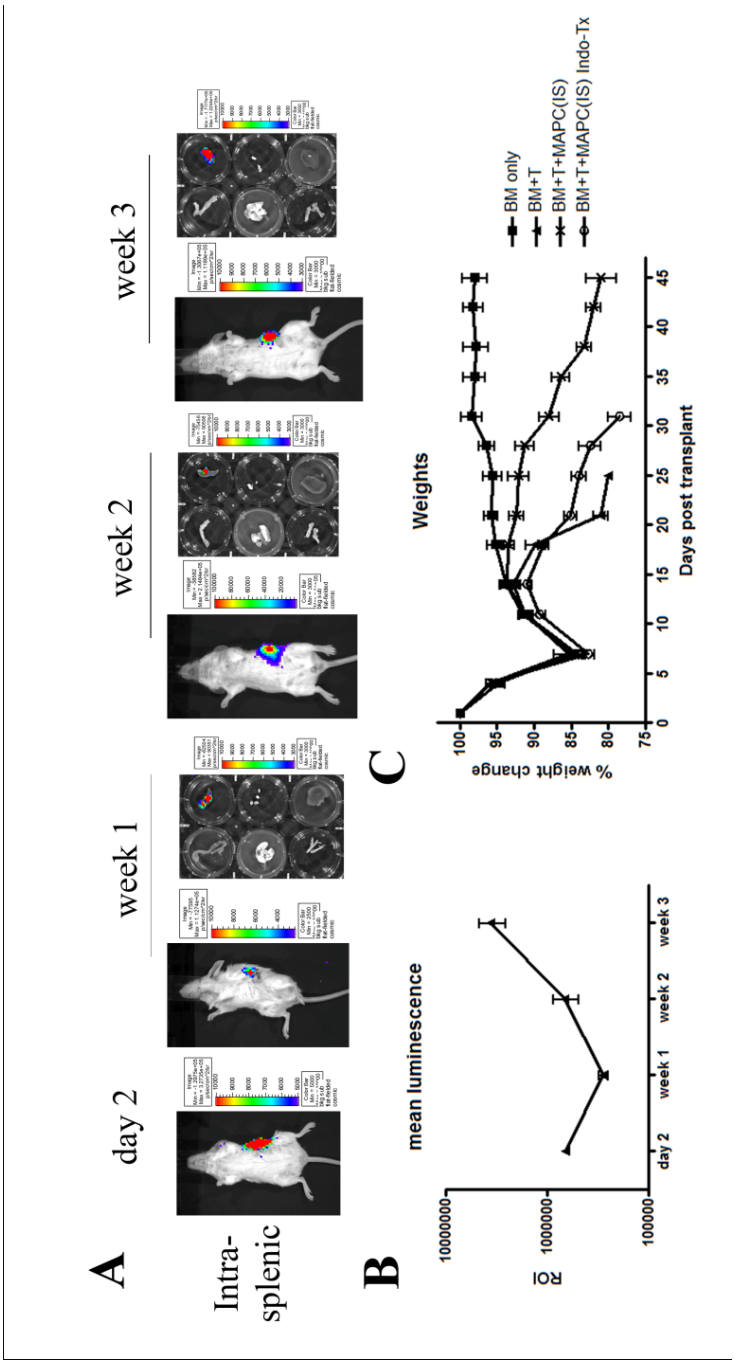

Supplemental figure 5. Localization of MAPC to the spleen after "in vivo MLR".

$5x10^5$ MAPC-DL were injected IS along with $15x10^6$ T cells. Day 4 bioluminescent imaging of spleens and lymph nodes from 6 mice revealed that MAPC remained within the spleen and had not migrated out to lymphoid tissue.

Supplemental Figure 5

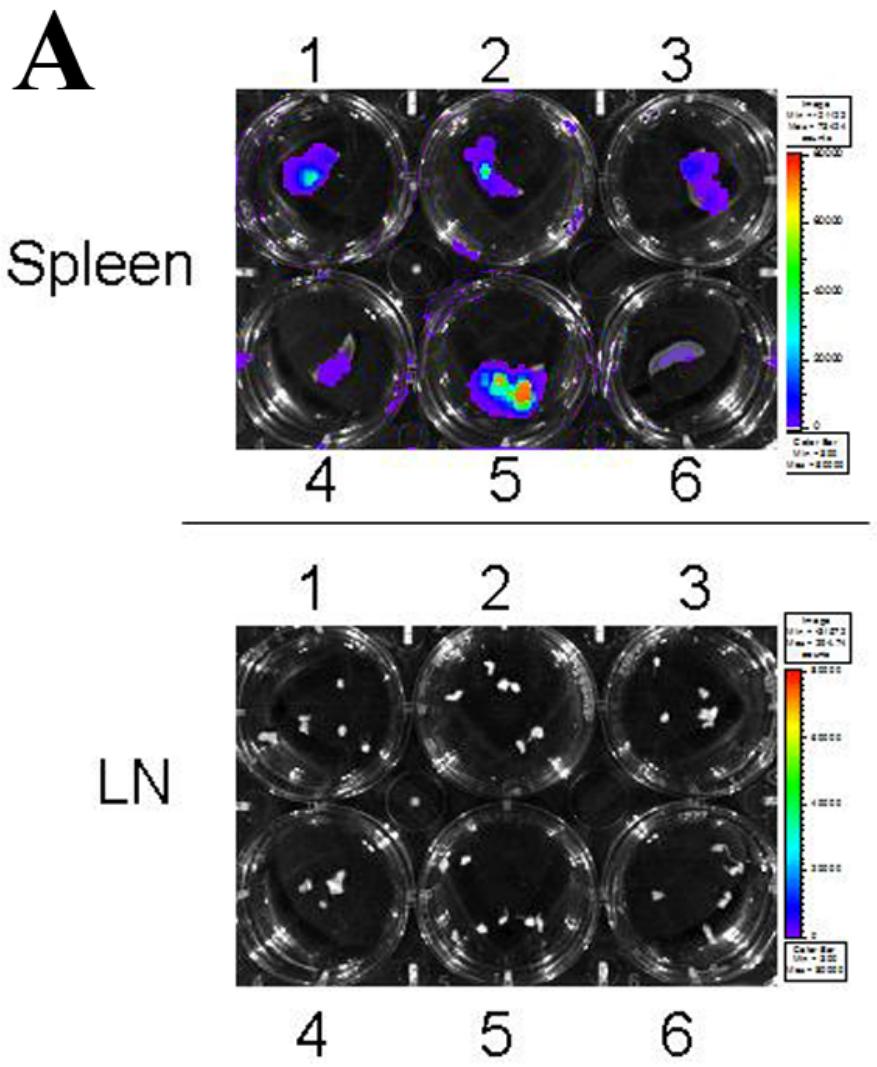

Chapter 3

Bone Marrow Myeloid-Derived Suppressor Cells (MDSC) Inhibit Graft-Versus-Host Disease (GVHD) via an Arginase 1 Dependent Mechanism that is Upregulated by IL-13

Steven L. Highfill,[1*] Paulo C. Rodriguez,[2*] Qing Zhou,[1] Christine A. Goetz,[1] Rachelle Veenstra,[1] Patricia A. Taylor,[1] Angela Panoskaltsis-Mortari,[1] Jonathan S. Serody,[3] David H. Munn,[4] Jakub Tolar,[1] Augusto C. Ochoa,[2#] Bruce R. Blazar [1#]

[1]University of Minnesota Masonic Cancer Center and Department of Pediatrics, Division of Blood and Marrow Transplantation, Minneapolis, MN 55455, USA

[2]Department of Microbiology, Stanley S Scott Cancer Center, Louisiana State University Health Sciences Center, New Orleans, Louisiana 70112, USA.

[3] Departments of Medicine, Microbiology and Immunology, and The Lineberger Comprehensive Cancer Center, The University of North Carolina at Chapel Hill, Chapel Hill, NC, 27599, USA

[4]Medical College of Georgia, Immunotherapy Center, Augusta, GA, 30912, USA

[*]S.L.H and P.C.R. contributed equally to this work.

[#]A.C.O. and B.R.B. contributed equally to this work.

Foreward

Myeloid-derived suppressor cells (MDSC) are a well-defined population of cells that accumulate in the tissue of tumor-bearing animals and are known to inhibit immune responses. Within 4 days, bone marrow cells cultured in G-CSF and GM-CSF resulted in the generation of $Gr1^{+}CD11b^{+}Ly6C^{+}$ MDSC, the majority of which are $IL4R\alpha^{+}$ and $F4/80^{+}$. Such MDSC potently inhibited *in vitro* allogeneic T-cell responses. Suppression was dependent on L-arginine depletion by arginase-1 activity. Adding IL-13 to cultures produced an MDSC subset (MDSC-IL13) that was more potently suppressive and resulted in arginase-1 but not inducible nitric oxide synthase (iNOS) upregulation. Suppression was reversed by L-arginine but not L-tryptophan or an iNOS inhibitor. Although both MDSC and MDSC-IL13 inhibited GVHD lethality, MDSC-IL13 were more effective. MDSC-IL13 migrated to sites of allopriming. GVHD inhibition was associated with limited donor T-cell proliferation, activation, and cytokine production. GVHD inhibition was greater with MDSC-IL13 than MDSC, and reduced when arginase-1 deficient MDSC-IL13 were used. MDSC-IL13 did not reduce the graft-versus-leukemia effect of donor T-cells. In vivo administration of a pegylated form of human arginase-1 (PEG-arg1) resulted in L-arginine depletion and significant GVHD reduction. MDSC-IL13 and PEG-arg1 represent novel strategies to prevent GVHD that can be clinically translated.

Introduction

Allogeneic hematopoietic stem cell transplantation is a commonly used option for those patients who lack a suitable matched donor. Although much progress has been made in this field over the last decade, there are still major limitations to this procedure. One of these limitations include the development of graft-versus-host disease (GVHD) due to donor-derived allogeneic T-cells which recognize host transplantation antigens. This T-cell mediated destruction of host tissue can sometimes be constrained with the long-term co-administration of multiple pharmacological agents or averted with the use of rigorously T-cell depleted donor grafts that may render the recipient T-cell lymphopenic for extended periods of time. However, these methods can predispose the recipient to opportunistic infections and relapse of host malignancy.

Myeloid-derived suppressor cells (MDSC) are a well-recognized population of cells known to accumulate in the lymph nodes, spleen, and liver of tumor bearing mice and humans where they may contribute to tumor evasion of cell-mediated immunity. In mice, MDSC have the surface phenotype of $CD11b^{+}$ (Mac-1) and $Gr1^{+}$ (Ly6G/Ly6C).[130] More recently, MDSC have been further subcategorized based on the differential expression of Ly6G and/or Ly6C. Granulocytic MDSC are defined as $CD11b^{+}Ly6G^{+}Ly6C^{low}$, while monocytic MDSC are defined as $CD11b^{+}Ly6G^{low/-}Ly6C^{hi}$.[131,132] Although these two distinct subsets can have varying function and distribution depending on their environment, their capacity to induce T-cell hypo-responsiveness are generally considered equal.[131,132] In addition, the suppressive capacity

of these cells has been linked to the expression of specific surface molecules including IL-4Rα[133] (CD124) and macrophage-colony stimulating factor receptor (CD115).[134]

Amongst the mechanisms proposed that may account for the immune suppressive properties of MDSC, L-arginine catabolism appears to be important in MDSC-induced T-cell dysfunction. MDSC can express both arginase-1 and inducible nitric oxide synthase (iNOS), both of which metabolize L-arginine and lead to the production of the byproducts urea, L-ornithine, and citrulline and nitric oxide, respectively.[135] Extensive studies by Rodriguez *et al*. have shown that L-arginine deprivation results in the loss of expression of the T-cell signaling molecule, CD3ζ, as well as T-cell cell cycle arrest.[136,137] Kerr and colleagues provided suggestive evidence that MDSC may be able to inhibit GVHD lethality in studies in which $SHIP^{-/-}$ recipients that have high numbers of MDSC had reduced GVHD lethality as compared to wild-type recipients.[129] More recently, the GVHD inhibitory effect of embryonic stem cell derived MDSC has been reported.[138]

In this study, we evaluated the efficacy of MDSC generated from a clinically applicable source, the bone marrow (BM) of non-tumor bearing donors, to inhibit GVHD lethality in a fully MHC-mismatched allogeneic model of BMT. We found that these MDSC inhibited T-cell alloresponses *in vitro* and *in vivo* and GVHD lethality *in vivo* through the depletion of L-arginine. The effect that limiting concentrations of L-arginine had on donor T-cells included a decrease in proliferation, a decrease in the expression of CD3ζ, and a decrease in IFNγ production. Despite these alterations in T-cell function, allogeneic T-cells retained their ability to eliminate lymphoma cells. Finally, we report

that the reduction in GVHD lethality by MDSC may be achieved by administration of a pegylated form of arginase-1 (PEG-argI) instead of MDSC cellular therapy.

Materials and Methods

Mice. BALB/c ($H2^d$) and C57BL/6 ($H2^b$)(termed B6) mice were purchased from Charles River (Wilmington, MA) or the National Institute of Health (Bethesda, MD). GCN2 knockout (KO) mice were generated as previously described.[139] B6 GFP transgenic (Tg) mice were generated as described and bred at the University of Minnesota.[140] All mice were bred and housed in a specific pathogen-free facility in microisolator cages and used at 8-12 weeks of age in protocols approved by the Institutional Animal Care and Use Committee.

MDSC generation and culture. BM was harvested from the tibia and femurs of B6 mice and plated at $2x10^5$ cells/ml in DMEM plus 10% FCS, 50 mM 2-ME (Sigma-Aldrich), 10mM HEPES buffer (Invitrogen), 1mM sodium pyruvate (Invitrogen), 100U/ml penicillin, 100mg/ml streptomycin (Sigma-Aldrich), and amino acid supplements (1.5 mM L-glutamine, L-arginine, L-asparagine)(Sigma-Aldrich). Recombinant methionyl human granulocyte colony-stimulating factor (G-CSF, Amgen Inc., Thousand Oaks, CA) was added to the culture at 100ng/ml. Recombinant mouse GM-CSF (R&D Systems, Minneapolis, MN) was added to the culture at 250U/ml. Cultures were incubated at 37ºC 10% CO_2 for a total of 4 days. On day 3 of culture, recombinant murine IL-13 (R&D Systems) was added at 80 ng/ml. On day 4 of culture, MDSC were harvested and purified

by positive selection of CD11b using Miltenyi technology (Miltenyi Biotech). Purified cells were routinely >95% double positive for CD11b and Gr1. B6 arginase-1 knockout bone marrow were obtained from the colony of Dr. Paulo Rodriguez and shipped overnight on wet ice before differentiation into MDSC using the above protocol.

RTPCR, QPCR and Western Blots. RNA was isolated from untreated BM, MDSC, and MDSC treated with IL-13 using RNAqueous 4 PCR kit (Applied Biosystems, Inc., Foster City, CA). cDNA was synthesized using Superscript III reverse transcriptase (Invitrogen). cDNA for non-quantitative RT-PCR was performed using specific primers for arginase-1 (sense, 5'-CAGAAGAATGGAA GAGTCAG-3'; antisense, 5'-CAGATTGCAGGGAGTCACC-3') and iNOS (sense, 5'-GCAAACGCTTCACTTCCAATGC-3'; antisense, 5'-AATCTCTGCCTATCCGTCTCGTCC-3') and amplified for 35 cycles. QRT-PCR Taqman primers/probe specific for arginase-1, iNOS and GAPDH were obtained through Applied Biosystems Inc. and used according to the manufacturer's protocol. For Western blots, whole cell lysates were made from BM only, MDSC, and MDSC IL13-tx cells that were differentiated *in vitro* over a 4 day time course (see above). Briefly, the cells were centrifuged, and the cell pellets were resuspended in 1x RIPA buffer containing protease and phosphatase inhibitors. Cell lysates were centrifuged and twenty micrograms of protein were fractionated on a 4-12% Bis-Tris SDS-PAGE gel and transferred to polyvinylidene difluoride membranes. The membranes were blocked in 5% milk, 1× TBS-0.05% Tween. Anti-arginase-1 monoclonal antibody (BD Biosciences) was incubated overnight at a 1:1000 dilution. The primary antibody was then washed off and

the secondary antibody (anti-mouse HRP; Cell Signaling) was incubated for 1h at a 1:1000 dilution. After 3x45 min washes with 1×TBS-Tween, the blot was developed with Pico ECL reagent from Pierce. Alpha-actin was used as a loading control.

Mixed leukocyte reaction (MLR). Lymph nodes (LNs) were harvested from B6 mice and T-cells were purified by negative selection using PE-conjugated anti-CD19, anti-CD11c, anti-NK1.1 and anti-PE magnetic beads (Miltenyi Biotech). Purity was routinely >95%. Spleens were harvested from BALB/c mice, T-cell depleted (anti-Thy1.1), and irradiated (1000 cGy). B6 T-cells were mixed at a 1:1 ratio with BALB/c splenic stimulators and plated in a 96 well round bottom plate (10^5 T-cells/well) or in the lower chamber of a 24 well plate TransWell insert (10^6 T-cells/well). Where indicated, MDSCs were plated in a 96 well round bottom plate (10^4/well, 1:10) or in a 24 well TransWell plate (10^5/well, 1:10). Cells were incubated in custom made RPMI 1640 that contained physiologic levels of L-arginine (150 μM)(Invitrogen, Carlsbad, CA) supplemented with 10% FCS, 50mM 2-ME (Sigma-Aldrich), 10mM HEPES buffer (Invitrogen), 1mM sodium pyruvate (Invitrogen), 100 U/ml penicillin, and 100 mg/ml streptomycin (Sigma-Aldrich). Cells were pulsed with ^{3}H-thymidine (1uCi/well) 16-18 hours prior to harvesting and counted in the absence of scintillation fluid on a β-plate reader. To inhibit arginase activity, N^w-hydroxy-nor-arginine (nor-NOHA) (Cayman Chemicals, Ann Arbor, MI) was resuspended at 5mg/ml in DMSO and further diluted to reach a final concentration of 30-300μM. In experiments where NOS was inhibited, L-N^G-monomethyl arginine citrate (L-NMMA)(Cayman Chemicals)was first re-suspended to 10mg/ml in PBS and used at a

final concentration of 300μM. Percent suppression was calculated by 100-((CPM of T-cells + stimulators + MDSC)/(CPM of T-cells + stimulators) x 100).

Flow cytometry. Purified T-cells were stained with 1μM carboxyfluorescein-succinimidyl-ester (CFSE, Invitrogen) for 2 minutes then washed. For CD3ζ, cells were stained using a digitonin-based method. Briefly, cells were incubated in digitonin at 500ng/ml for 30 minutes prior to the addition of anti-CD3ζ-PE (Abcam). Intracellular cytokine staining was performed after a 5 hour incubation of whole splenocytes with anti-CD3 and anti-CD28 with monensin at 37ºC 5% CO_2. All other antibodies were purchased through Pharmingen (San Diego, CA) or E-bioscience (San Diego, CA) and stained according to manufacturer's instructions. The samples were analyzed on a FACSLSRII or FACSCanto (Becton Dickinson, San Jose, CA) using Flow Jo software (Treestar inc).

Arginase activity and L-arginine quantification. Arginase activity, which measured the production of urea over a set time point, was determined using Quantichrom Arginase Assay Kit (Bioassay Systems, Hayward, CA) using the manufacturers protocol. L-Arg concentration in tissue culture medium was measured by high-performance liquid chromatography with electron capture detection using an ESA-CoulArray Model 540(ESA Inc., Chelmsford, MA) with an 80x3.2 column with 120A pore size. Briefly, supernatants were deproteinized in methanol. After centrifugation at 6000xg for 10 min at 4°C, the supernatant was derivatized with 0.2 M O-phtaldialdehyde containing

7 mM beta-mercaptoethanol. Fifty microliters of the sample were injected into the

column. Standards of L-Arg were prepared in methanol.

GVHD. BALB/c recipients were lethally irradiated using 600 cGy TBI from an X-ray source (X-RAD 320, Precision X-ray Inc., North Branford, CT) on day -1 followed by intravenous (*i.v.*) infusion of 10^7 T-cell depleted (TCD) B6 donor BM, $2x10^6$ purified B6 whole T-cells (CD4 and CD8) depleted of CD25, and either $2x10^6$ or $6x10^6$ CD11b positively-selected B6 MDSCs on day 0. Control mice were given BM alone or BM plus T-cells as negative and positive controls for GVHD induction, respectively. Mice were monitored daily for survival and weighed twice weekly. Migratory ability of MDSC was determined by generating MDSC from whole BM of GFP Tg B6 mice using the method described above. These cells were injected into lethally irradiated BALB/c mice at $6x10^6$ cells/mouse with 10^7 BM cells and $2x10^6$ whole T-cells. LNs (mesenteric, axillary, and inguinal) and spleens explanted from these mice on days 7 and 14 post-transplant were imaged using whole body fluorescent imager. Images were taken using a Magnafire color camera (Optronics, Goleta, CA) mounted onto a Leica MZFLIII stereomicroscope using a eGFP2-bandpass filter and a 0.63 x transfer lens (Leica Microsystems, Bannockburn, IL).

Assessment of graft versus leukemia effect of donor T-cells. A20 lymphoma cells were purchased from American Type Culture Collection (ATCC, Manassas, VA) and nucleoporated with a Sleeping Beauty transposon construct to permit the co-expression of dsred2 and *Renilla* luciferase (*Renilla reniformus*, termed $A20^{luc}$). On day 0, cohorts of lethally irradiated BALB/c recipients undergoing BMT received $3x10^5$ $A20^{luc}$. Groups

also received 10^7 BM only or BM plus $2x10^6$ $CD25^-$ B6 T-cells with and without $6x10^6$ B6 MDSC. A Xenogen IVIS imaging system (Caliper Life Sciences, Hopkinton, MA) was used for live animal imaging of transplanted mice. Mice were anesthetized with Isoflurane using a ventilator system. *Renilla* luciferin substrate (EnduRen, Promega, Madison, WI) was injected *i.p.* at 60 mM (final volume 0.1ml) and mice were imaged 5 minutes post injection. Data were analyzed and presented as photon counts per area.

Pegylation of human recombinant Arginase-1. O-[2-(N-Succinimidyloxycarbonyl)-ethyl]-O'-methylpolyethylene-glycol (PEG) 5000mw (Sigma-Aldrich, St. Louis, MO) was covalently attached to the human recombinant arginase-1 in a 50:1 molar ratio for 2.5 hours, as described by Cheng *et al*.[141] To determine the efficiency of the procedure, PEG-Arg1, recombinant arginase-1, and PEG 5000mw were electrophoresed in 10% Tris-Glycine gels (Invitrogen) and the gels were stained using GelCode Blue® Stain Solution (Thermo Scientific, Waltham, MA). The molecular weight of the PEG-Arg-1 ranged between 150-225kD, while the native unpegylated human recombinant arginase-1 was 36kD. Pegylation of arginase-1 was confirmed by staining of the gels in glutaraldehyde based stain solution, finding the presence of the PEG-Arg-1 between 150-225kD and the PEG 5000mw around 5kD. The specific activity of the native arginase and the PEG-arg-1 was about 400IU/mg protein. One international unit of arginase-1 is defined as the amount of enzyme that can produce 1 μmol urea/minute at 30°C, pH 8.5. In experiments using PEG-arg-1, reagent was administered *i.p.* into transplanted mice at 1mg/ml twice weekly for a period of four weeks.

Statistical analysis. The Kaplan-Meier product-limit method was used to calculate survival curve. Differences between groups in survival studies were determined using log-rank statistics. For all other data, a Student's t-test was used to analyze differences between groups. Results were considered significant if the *P* value was ≤ 0.05.

Results

In vitro generated MDSC inhibit T-cell alloresponses via arginase-1 expression, which is upregulated by IL-13. To generate MDSC, BM from WT B6 mice was incubated with G-CSF, GM-CSF, or both. After 4 days, cells were harvested and the surface phenotype determined (Figure 1). Cells incubated with GM-CSF had a more granulocytic morphology, as indicated by the increased forward scatter profile. The percentage of $CD11b^{+}Gr1^{+}$ cells increased from 29% in media to 35% with G-CSF, 34% with GM-CSF treated, 44% in the G-CSF+GM-CSF group, and 50% in G-CSF+GM-CSF+IL-13 group. Upon examination of the different subsets of MDSC, we observed a preferential expansion of the $CD11b^{+}$ $Ly6G^{-}Ly6C^{+}$ population of cells in all groups when compared to cells incubated in media only (24% vs. 39% vs. 59% vs. 69% vs. 73%). As compared to media or GM-CSF alone, $CD11b^{+}Gr1^{+}$ cells cultured with G-CSF, G-CSF+GM-CSF or G-CSF+GM-CSF+IL-13 had a marked increase in IL4Rα expression (28% vs. 49% vs. 78% vs. 62% vs. 64%, respectively). GM-CSF had a greater influence on the expression of CD115 (CSF-1R), and GM-CSF, GM-CSF+G-CSF, GM-CSF+G-CSF+IL-13 groups had increased expression of CD115 when compared to BM cells in culture media and cells treated with G-CSF alone (12% vs. 20% vs. 40% vs. 40% vs. 43%). GM-CSF also upregulated F4/80 expression from 31% (media) or 36% (G-CSF alone) to 65% (GM-CSF) or 66% (G-CSF+GM-CSF) and 63% (G-CSF+GM-CSF+IL-13). Cells were negative for CD11c, CD14, and MHC class II molecules in all cultures, and there was no change in MHC class I observed between the groups (Figure 1A, data not shown). Based on the cell surface phenotyping and *in vitro* suppression data (see below), all subsequent MDSC cultures were performed in the presence of G-CSF+GM-CSF+IL-13. As shown in

Figure 1B and C, H/E-stained cytospin preparations demonstrated that MDSC produced in this fashion were highly homogeneous and had mononuclear morphology with a large nuclear to cytoplasm ratio. Thus, cells with a phenotype consistent with MDSC can be generated from whole BM through simple culture techniques in as little as 4 days.

To enrich MDSCs, CD11b positive selection was performed on day 4 of culture. More than 95% of CD11b selected cells expressed both CD11b and Gr1 (data not shown). RT-PCR analysis of CD11b selected cells shows that MDSCs expressed both arginase-1 and iNOS (Figure 2A). The addition of IL-13 (80ng/ml) on day 3 of culture resulted in the upregulation of arginase-1 expression in MDSCs (Figure 2A). To quantify the degree of increased expression, real time PCR was performed using specific Taqman primer/probe sets (Figure 2B). As compared to the BM control, the relative expression of arginase-1 was increased 20-fold in MDSC and increased to a significantly greater extent to 350-fold in MDSC-IL13 cultures. The expression of iNOS was increased in MDSC but was not significantly increased higher in MDSC-IL13 (5-fold vs. 7-fold increased, respectively, vs. BM controls) (Figure 2B). Western blot analysis of arginase-1 (Figure 2C) and arginase-1 activity determination (Figure 2D) using a urea-based detection method indicated that the increase in the expression levels of arginase-1 in MDSC and MDSC-IL13 correlated with the downstream increase in protein levels and activity.

Next, studies were performed to determine the *in vitro* suppressive capacity of MDSC in an allogeneic MLR culture. B6 purified $CD4^+$ and $CD8^+$ T-cells ($2x10^5$) were co-cultured with irradiated BALB/c T-cell-depleted stimulators ($2x10^5$) and B6 MDSC ($2x10^4$). Cells were plated in complete media containing physiological concentrations of L-arginine (150 μM) and incubated for 3-7 days. The percent suppression by MDSC

ranged from 50-60% at a 1:10 ratio of T-cells to MDSC (Supplementary Figure 1). MDSC-IL13 were significantly more suppressive at each time point of the assay, ranging from 65-75%. Since the *in vitro* suppression and *in vivo* GVHD inhibition (see below) was superior with MDSC-IL13 vs. MDSC, subsequent studies were performed with MDSC-IL13.

The suppressive capabilities of MDSC were dominantly cell-contact independent (Supplemental Figure 2) when using a semi-permeable membrane to separate MDSC from T-cells and stimulators. To determine the extent to which MLR suppression was dependent upon the arginase pathway, the arginase inhibitor (nor-NOHA) was added to MDSC-IL13 cultures. Nor-NOHA significantly reduced MDSC suppression of an *in vitro* MLR response to levels of 18-35% at a nor-NOHA concentration of 300μM, an effect that was titratable at lower concentrations (Figure 2E, F). Inhibition of NOS by L-NMMA alone resulted in a slight reduction in suppression at the peak of the response (day 5; 72% in control vs 64% in L-NMMA treated) and the addition of L-NMMA to nor-NOHA was not more effective in reducing suppression than nor-NOHA alone.

The stress response pathway, GCN2, can sense essential amino acid starvation. Therefore, GCN2 knockout T-cells were used as responders in an MLR culture to which MDSC-IL13 were added. Consistent with the possibility that L-arginine and perhaps other essential amino acids were depleted by MDSC-IL13, the percent suppression by MDSC-IL13 significantly decreased using wildtype (WT) vs. GCN2 KO responders from 60% to 25% at the peak of the response (day 5, P=0.01) (Figure 2G). The addition of excess L-arginine (5mM) to the MLR:MDSC-IL13 co-culture also resulted in a 60% reduction in suppression (day 4, P=0.001) (Figure 2H). This effect was specific for L-

arginine because the addition of excess tryptophan, a different essential amino acid depleted by the indoleamine 2,3 dioxygenase pathway, had no such effect. Together, these results indicate that in vitro generated MDSC-IL13 inhibit T-cell alloresponses by starving T-cells of L-arginine.

Donor MDSC-IL13 cells migrate to sites of allopriming shortly after BMT and reduce GVHD lethality. We then determined if MDSC-IL13 migratory patterns were such that it allowed for them to traffic to secondary lymphoid organs, sites of allorecognition and priming, and thus have the potential to suppress GVHD. MDSC-IL13 cells expressed the secondary lymphoid organ selectin/adhesion molecules, CD62L and LFA-1, as well as CCR9 (small intestine and colon homing) but not alpha4beta7 (Peyer's patches and lamina propria) or CCR7 (LN; afferent lymphatics) (Figure 3A). Lethally irradiated BALB/c recipients were given 10^7 B6 BM cells plus $2x10^6$ purified B6 T-cells. A cohort also received MDSC-IL13 ($6x10^6$ cells/mouse) expanded from eGFP transgenic B6 donors BM. On day 7 and 14 post-BMT, LN and spleen were explanted and imaged using a whole-body fluorescent imager. A bright fluorescent signal emanated from the spleen and from the mesenteric, axillary, and inguinal LNs on days 7 and 14 (Figure 3B). As indicated by flow cytometry analysis, eGFP expressing cells in the LN and spleen increased from day 7 to day 14 (LN, 3.3 vs. $11x10^4$; spleen, 6.5 vs. $15x10^4$) (Figure 3C). On day 7, 75% of donor $CD11b^+$ cells co-expressed Gr-1 (Figure 3D). These results demonstrated that MDSC-IL13 efficiently migrate to sites of alloactivation in a GVHD setting and increased in numbers over time.

Next, we wanted to determine if MDSC-IL13 had a beneficial impact on GVHD survival. As above, lethally irradiated BALB/c recipients were given 10^7 B6 BM cells plus $2x10^6$ purified B6 T-cells. Some cohorts received $2x10^6$ or $6x10^6$ B6-derived $CD11b^+$ selected MDSC-IL13 at the time of transplant. As shown in Figure 4A, mice given either $2x10^6$ or $6x10^6$ MDSC-IL13 had significantly improved survival compared to controls ($P<0.001$). Recipients of higher vs. lower MDSC-IL13 had a trend toward increased survival ($P=0.06$). Mice given MDSC-IL13 at either dose lost significantly less weight than mice without MDSC-IL13, albeit weight loss was greater than the BM only group indicating that MDSC-IL13 mice were not GVHD-free (Figure 4B). In other studies and consistent with the *in vitro* MLR data, recipients of MDSC-IL13 had increased survival as compared to those receiving MDSC ($P=0.001$) (Supplemental Figure 3), validating the choice of MDSC-IL13 for further analysis.

MDSC-IL13 suppress donor T-cell activation, proliferation and IFNγ production and GVHD lethality via an arginase-1 dependent mechanism. Because the MDSC-IL13 expression of arginase-1 was essential to achieve maximum suppression of a T-cell alloresponse *in vitro*, we sought to determine if the same mechanism of action was involved *in vivo*. MDSC-IL13 were isolated from WT or arginase-1 KO mice and applied to our GVHD model described above. Survival analysis indicated that WT MDSC-IL13 significantly enhanced survival when compared to mice receiving BM+T alone (BM+T vs. BM+T+$6x10^6$ WT MDSC-IL13, $P=0.05$). Arginase-1 contributed to the GVHD inhibitory effect of MDSC-IL13 since arginase-1 KO MDSC-IL13 were not sufficiently potent in reducing GVHD to reach statistical significance with 12 mice/group (BM+T vs.

BM+T+6x10^6 arginase-1 KO MDSC, *P*=0.08). (Figure 4C). Again, weight loss substantiated survival data (Figure 4D). These data confirm arginase-1 expression as a contributing mechanism for MDSC-IL13 inhibition of GVHD lethality.

To further investigate the direct effects MDSC had on donor T-cell alloresponses *in vivo*, CFSE-labeled B6 T-cells (15x10^6) and T-cells plus MDSC-IL13 (10x10^6; 1:0.67 ratio) were given to lethally irradiated mice. As compared to the GVHD group, there is a significant reduction in the percent of both $CD4^+$ and $CD8^+$ donor T-cells that had divided on day 4 post-BMT when MDSC-IL13 were co-administered (40.2±7 vs. 17.3±1 for CD4, *P*=0.01; 51.5±13 vs. 16.1±1 for CD8, *P*=0.01) (Figure 5A). L-arginine deprivation has been shown to be associated with a decrease in the expression of CD3ζ on $CD4^+$ and $CD8^+$ T-cells. As compared to controls, a decrease in CD3ζ expression was observed in donor $CD4^+$ and $CD8^+$ T-cells when MDSC-IL13 was co-administered (86±2% vs. 56±3% for $CD4^+$ T-cells, *P*<0.001; 85±1% vs. 68±1% for $CD8^+$ T-cells, *P*<0.001) (Figure 5B). The activation status of donor T-cells was assessed by examining the expression of CD25 and L-selectin (CD62L) (Figure 5C). As compared to controls, $CD8^+$ T-cells co-administered with MDSC-IL13 had a less activated phenotype, indicated by a lower frequency of $CD25^+$ cells (32±2% vs. 19%±1, *P*<0.001). There was no statistical difference on $CD4^+$ T-cells between the two groups when CD25 expression was examined (37±3% vs. 33±1%, *P*=0.3). However, both $CD4^+$ and $CD8^+$ T-cells have fewer $CD62L^-$ cells when MDSC-IL13 are co-administered (74±2% vs. 50±3% for $CD4^+$ T-cells, *P*<0.001; 77±4% vs. 41±3% for $CD8^+$ T-cells, *P*<0.001). When comparing no MDSC-IL13 to MDSC-IL13 co-administration, there was a significant reduction in the percentage of cells expressing IFN-γ in both $CD4^+$ and $CD8^+$ T-cell populations (37±5%

vs. 24±2% for $CD4^+IFN\gamma^+$, P=0.04; 30±4% vs. 15±1% for $CD8^+IFN\gamma^+$, P=0.007) (Figure 5D). Cumulatively, these results show that MDSC-IL13 diminish donor T-cell activation, proliferation, and proinflammatory cytokine production which is associated with reduced GVHD lethality.

MDSC-IL13 preserve the GVL effect of allogeneic T-cells. To determine whether the reduction of GVHD lethality upon co-administration of MDSCs would impair a GVL effect, we used an A20 lymphoma model known to be sensitive toward T-cell mediated elimination. Irradiated BALB/c recipients were given BM with or without purified whole T-cells ($2x10^6$) from B6 donors. Other cohorts received MDSC-IL13 ($6x10^6$) and/or $A20^{luc}$ cells ($3x10^5$) on day 0 (Figure 6). Again, co-administration of MDSC on day 0 resulted in a significant reduction of GVHD induced mortality (BM+T vs. BM+T+MDSC-IL13, P<0.001)(Figure 6A) and weight loss compared to mice receiving T-cells alone (Figure 6B). Recipients of T-cells plus $A20^{luc}$ cells all eventually succumbed to GVHD. However, recipients of T-cells/$A20^{luc}$/MDSC-IL13 had a significantly improved survival and 37% of mice survived long-term (BM+T+A20 vs. BM+T+A20+MDSC-IL13, P<0.001)(Figure 6C, D), in marked contrast to mice receiving BM+$A20^{luc}$ cells, that all succumbed to lymphoma by day 25 (Figure 6C). Despite a reduction in GVHD, recipients of MDSC-IL13 and T-cells were capable of eliminating $A20^{luc}$ cells to the same extent as recipients of T-cells only (Figure 6E). These data show that the dampening of GVHD by MDSC-IL13 does not hinder the ability of donor T-cells to mediate a GVL effect when given at the time of allo-BMT.

PEG-arg1 administration has similar GVHD inhibitory properties as MDSC-IL13.

Arginase-1 expression contributed to the MDSC-IL13 suppression of alloresponses *in vitro* and reduction of GVHD lethality *in vivo*. To determine if arginase-1 itself was sufficient to inhibit GVHD lethality generation, arginase-1 was conjugated to PEG (PEG-arg1) to prolong its half-life *in vivo*. Lethally irradiated BALB/c mice were given 10^6 BM cells plus $2x10^6$ $CD25^-$ B6 T-cells. Cohorts were given PEG-arg1 *i.p.* at 1mg/mouse 2 times weekly for a total of 4 weeks. Other cohorts received $6x10^6$ B6 BM-derived MDSC-IL13 as a comparison. Mice receiving PEG-arg1 had a significant improvement in survival compared to mice receiving BM+T alone (P=0.003) (Figure 7A), which was comparable to mice receiving $6x10^6$ MDSCs (P=0.4)(Figure 7A). Notably, the most impressive survival differences between PEG-arg1 and T-cell only control was evident while PEG-arg1 continued to be administered with 75% of treated mice vs. 0% of controls surviving. The precipitous loss of mice from GVHD in the PEG-arg1 treated group occurred upon discontinuation of PEG-arg1 treatment *i.e.* between days 30-62. Weights of these mice demonstrated that mice receiving PEG-arg1 were comparable and different than the T-cell only controls (Figure 7B). When we quantify the concentration of L-arginine in peripheral blood from these animals at day 14, we observed a significant decrease of this amino acid in mice given $6x10^6$ MDSC and PEG-arg1 (Figure 7C). These data indicate that PEG-arg1 administration was able to inhibit GVHD-induced lethality, especially during the time period of continued injections.

Discussion

We report a novel cellular therapy using MDSC-IL13 generated within 4 days from the BM of tumor-free animals using G-CSF+GM-CSF followed by the addition of IL-13 to upregulate arginase-1 expression. MDSC-IL13 were more potent in inhibiting *in vitro* alloresponses and *in vivo* GVHD lethality than MDSC generated without IL-13. MDSC-IL13 limited the proliferation, activation, and IFNγ secretion of donor T-cells exposed to allogeneic stimuli *in vivo*. Additionally, the GVL alloreactivity of donor T-cells was preserved. Arginase-1 expression was critical for GVHD reduction. Conversely, the administration of PEG-arg1 inhibited GVHD lethality.

Several studies have proposed a link between the increased production of tumor-derived G-CSF and GM-CSF with increasing numbers of MDSCs.[142-144] We have utilized these cytokines to develop a culture system in which we are able to produce $CD11b^{+}Gr1^{+}$ MDSC from whole BM. Phenotypic analysis revealed these cells express IL4Rα and CD115, both have previously been linked to enhanced suppressive capacity of MDSC.[133,134] MDSC also expressed both Ly6C and F4/80, placing them within the monocytic subset of MDSC described earlier.[130,132] The addition of IL-13 to the culture for the last 24 hours markedly increased arginase-1 expression (Figure 2B), which proved to be vital to the suppressive effects of MDSC-IL13.

Successful prevention of GVHD using cellular approaches is dependent on migration of suppressor cells to areas which harbor alloreactive donor T-cells. Our laboratory has previously shown that regulatory T-cells (Tregs) expressing high levels of CD62L ($CD62L^{hi}$) efficiently migrated to SLO and potently inhibited GVHD and BM

graft rejection, while $CD62L^-$ Tregs had no such effect.[53] More recent studies using multipotent adult progenitor cells further elucidated the need for suppressor cells to be located within the vicinity of alloreactive T-cells. Only when multipotent progenitor cells were administered within the splenic microenvironment through direct splenic injections was there was a positive effect on GVHD survival that resulted from decreased activation and expansion of donor T-cells *in vivo*.[145] In the current study, we have shown that *in vitro* generated MDSC and MDSC-IL13 express appropriate homing molecules that guide them to SLO, CD62L being one of these. Furthermore, we show that the absolute number of MDSC-IL13 in the LN and spleen increases from day 7 to 14, indicative of *in vivo* proliferation of MDSC-IL13. Because most of the injected MDSC retained their cell surface phenotype of $CD11b^+Gr\text{-}1^+$ at 7 days post transplant, MDSC-IL13 adoptively transferred *in vivo* should continue to have the capacity to modulate immune responses.

Recently, Zhou *et al.* have described a culture system, which generates $CD115^+Ly6C^+$ MDSC from embryonic stem cells (ES) and purified hematopoietic stem cells (HSC).[138] The suppressive capacity of their MDSC used is in line with our current report, although there are significant differences worth mentioning. First, the length of time needed to generate MDSC is longer than ours (17 days for ES-MDSC, 8 days for HSC-MDSC) and employs the use of a larger array of reagents/cytokines (c-kit ligand, IL-6, IL-3, thrombopoietin, VEGF, Flt3L and M-CSF) increasing the logistics of translation into the clinic.[138] Although the MDSC derived from Zhou *et al* and those described in the current paper have a similar cell surface phenotype, there is an apparent discordance in the suppressive mechanism utilized. For example, these investigators demonstrated that inhibiting arginase-1 had minimal effects on the suppressive capacity

of MDSC *in vitro*, and show data which indicate iNOS, IL-10 and the induction of Tregs as the mediators of T-cell inhibition.[138] In contrast, our data show a more important role for arginase-1. Furthermore, in our studies, T-cell production of IL-10, the induction of Tregs, or the inhibition of iNOS did not differ in the *in vitro* MLR suppression assay between conditions that contained or did not contain MDSC-IL13 (data not shown). We speculate that these differences may be due to the addition of IL-13 in our culture system, which is known to increase arginase-1 activity at the expense of iNOS.[146] Secondly, the effect of ES-MDSC on GVHD was tested using $5x10^5$ allogeneic T-cells as GVHD inducers whereas we used $2x10^6$ T-cells that were CD25 depleted T-cells, thereby eliminating the possibility that donor Tregs within the donor innoculum contributed to the GVHD inhibitory effect of MDSC-IL13. Lastly, the ratio of MDSC to T-cells administered *in vivo* differed between the studies. Zhou *et al.* administered 3 total treatments of $2x10^6$ MDSCs each, effectively making MDSC:input T-cell ratio 12:1.[138] Our model used $2x10^6$ T-cells with one treatment of $6x10^6$ MDSCs, which is a 3:1 MDSC:input T-cell ratio. Taken together, these differences may explain the decreased survival we observed in our system. Consistent with data not shown but mentioned by Zhou *et al.* is that the GVL activity of donor T-cells remained intact in mice given $CD115^+Gr\text{-}1^+F4/80^+$ MDSC. We now report that MDSC-IL13 preserve the GVL response as analyzed by a day 0 challenge of BMT recipients with a luciferase tagged lymphoma cell line (A20). Allogeneic T-cells given with MDSC-IL13 retained their GVL activity and were equally effective at eradicating tumor as T-cell given alone. The net result of MDSC-IL13 was to reduce GVHD lethality, efficiently eliminate A20

lymphoma cells, and permit survival of 37% of recipients vs 0% of controls not given MDSC-IL13 or allogeneic T-cells alone.

Amino acid starvation results in T-cell dysfunction. Perhaps the best studied enzyme that induces this effect is IDO. IDO degrades the essential amino acid tryptophan and activates the GCN2 stress-kinase pathway.[147] This, in turn, results in the phosphorylation of eIF2α which initiates cell cycle arrest and T-cell anergy.[147] Munn *et al.* have shown that GCN2 KO T-cells bypass this pathway and can proliferate in the absence of tryptophan.[139] L-arginine deprivation also induces the GCN2 kinase pathway in T-cells, and GCN2 KO T-cells are also resistant to these inhibitory effects *in vitro*.[136] In line with this, we show that GCN2 KO T-cells are more resistant to MDSC-IL13 mediated suppression when compared to WT T-cells. Further, the suppressive effects are specific for L-arginine starvation, because only the addition of exogenous L-arginine to MLR cultures, and not tryptophan, had the capacity to restore T-cell proliferation.

It is known that under conditions of low concentrations of L-arginine, the reductase domain of iNOS generates superoxide ion (O_2^-),[148] which is converted to hydrogen peroxide (H_2O_2) and oxygen or, in the presence of nitric oxide, to peroxynitrite (ONOO-).[149] Peroxynitrite inhibits T-cell activation and proliferation by reducing tyrosine phosphorylation and inducing apoptosis.[150] Gabrilovich *et al*. demonstrated that peroxynitrite was involved in T-cell inhibition by Gr-1^+ MDSCs derived from tumor-bearing mice and the addition of the peroxynitrite scavenger, uric acid, completely abrogated the antigen-specific inhibitory effect of MDSC.[84] Others have also shown that the stimulation of T-cells in an L-arginine poor microenvironment results in an inhibition of T-cell proliferation, decreased CD3ζ expression, and a decreased production of IFN-

γ.[85,137,151,152] Under these circumstances, inhibiting the production of H_20_2 did not reverse these effects, and only arginase-1 inhibitors or excess L-arginine allowed for CD3ζ re-expression, indicating different MDSC types may utilize one or more distinct pathways to achieve suppression.[152] Because we have shown that MDSC-IL13 express both arg-1 and iNOS, it remains possible that these are acting synergistically and are producing toxic metabolites, such as superoxide ion or peroxynitrite, which can affect T-cell function. We attribute much but not all of the immunosuppressive capabilities of MDSC-IL13 to the consumption of L-arginine. Thus, it is not surprising that most of the MDSC-IL13 suppression occurs independent of cell contact. We favor the hypothesis that the component of MDSC-IL13 induced suppression that occurs via a contact-dependent suppression may be mediated through interactions with negative regulators of the immune response. For instance, PD1-PDL1 interactions which are known to regulate tolerance have been documented to reduce both proliferation and IFN-γ secretion by CD3 activated T-cells.[153] Indeed, MDSC-IL13 express high levels of PDL-1 (data not shown). Future studies will be needed to search for additional contributing mechanisms that can account for the residual suppression by MDSC-IL13 that does not require contact dependence or as was observed using arginase-1 KO MDSC-IL13.

Because human MDSC do not express CAT-2B transporter, and therefore cannot uptake L-arginine, MDSC release arginase-1 into the environment where it depletes L-arginine and induces T-cell dysfunction. Although recombinant human arginase-1 (rhArg-1) has been successfully cloned, the short circulatory half-life in the human body ($t_{1/2}$<30 min) makes it difficult to achieve therapeutically effective blood arginine concentrations in patients.[154] The attachment of PEG is an established technique used to

extend the circulatory half-life and increase stability of numerous proteins. Studies have shown the effectiveness of PEG-arg1 for treatment of cancers dependant on L-arginine, such as hepatocellular carcinoma and acute lymphoblastic T-cell leukemia (T-ALL).[141,155] These studies have lead us to hypothesize that we may be able to replicate the inhibitory effects of MDSC by creating an L-arginine-free microenvironment. Upon administration of PEG-arg1, we show a significant benefit in the survival of mice with lethal GVHD. This enhancement in survival is virtually the same as that seen when administering a higher ($6x10^6$) MDSC-IL13 dose. It is interesting to note that the early survival kinetics were more favorable early post-transplant for mice given PEG-arg1 than mice given MDSC-IL13. However, in contrast to the single infusion of MDSC-IL13, PEG-arg1 suppression of GVHD lethality appeared to require continuous PEG-arg1 administration since discontinuation on day 28 post-BMT was followed by GVHD-induced deaths between days 30-62. This leads us to speculate that a longer duration of PEG-arg1 treatment may have an even more significant impact on long-term survival. Whether PEG-arg1 is immune suppressive or can be considered tolerigenic is unknown at present. Although future studies will be required to optimize PEG-arg1 dose and schedule, clearly PEG-arg1 has a beneficial effect on reducing GVHD lethality.

In conclusion, MDSC-IL13 generated from murine BM have the ability to enhance GVHD survival. Arginase-1 expression contributes to the GVHD inhibitory effect of MDSC-IL13. A GVL effect was not aborted by MDSC-IL13. The administration of PEG-arg1 had similar effects of higher dose MDSC-IL13 ($6x10^6$ cells) and was modestly superior to a lower dose of MDSC-IL13 ($2x10^6$ cells; data not shown). Future studies will be needed to optimize the dose and schedule of MDSC-IL13 and

PEG-arg1. Nonetheless, these studies may hold promise for GVHD prevention and perhaps GVHD therapy in the clinic.

Acknowledgments

We thank Rachel Sutlif, Klara Noble, and Christopher Lees for technical assistance. We also thank Dr. Augusto Ochoa and Dorota Wyczechowska (Louisiana State University) for providing arginase-1 KO BM. This work was supported in part by NIH grants R01 AI34495, HL56067, and HL49997 (Bethesda, MD; to B.R.B.), and the Children's Cancer Research Fund (Minneapolis, MN; to S.L.H.).

Figure 1. Generation and phenotype of cultured MDSC. (A) FACS phenotype of B6 whole bone marrow at day 4 of culture that has been left untreated, treated with G-CSF alone (100ng/ml), treated with GM-CSF alone (250U/ml), or treated with both G-CSF and GM-CSF. All gates based on isotype controls. Ly6G/Ly6C graphs were first gated on $CD11b^{+}$ cells. Representative images of H/E stained cytospins of MDSC with combined treatment (B) and combined treatment plus IL-13 addition on day 3 (C)(40X magnification).

Figure 1

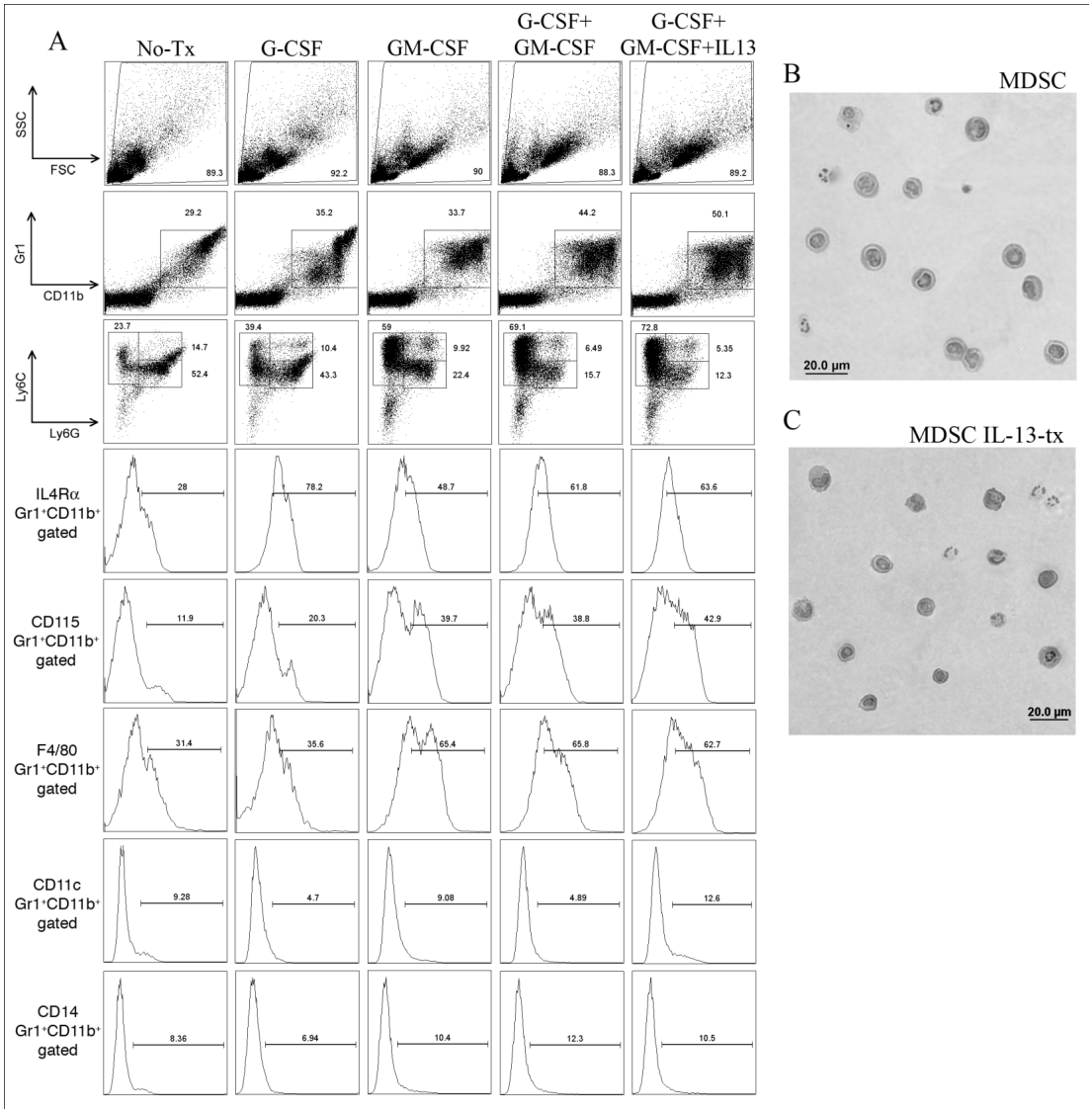
A
No-Tx
G-CSF
GM-CSF
G-CSF+ GM-CSF
G-CSF+ GM-CSF+IL13
SSC
FSC
89.3
92.2
90
88.3
89.2
Gr1
CD11b
29.2
35.2
33.7
44.2
50.1
Ly6C
Ly6G
23.7
14.7
52.4
39.4
10.4
43.3
59
9.92
22.4
69.1
6.49
15.7
72.8
5.35
12.3
IL4Rα Gr1+CD11b+ gated
28
78.2
48.7
61.8
63.6
CD115 Gr1+CD11b+ gated
11.9
20.3
39.7
38.8
42.9
F4/80 Gr1+CD11b+ gated
31.4
35.6
65.4
65.8
62.7
CD11c Gr1+CD11b+ gated
9.28
4.7
9.08
4.89
12.6
CD14 Gr1+CD11b+ gated
8.36
6.94
10.4
12.3
10.5
B
MDSC
20.0 μm
C
MDSC IL-13-tx
20.0 μm

Figure 2. MDSC inhibit T-cell allo-responses through the expression of arginase-1. (A) RTPCR showing MDSC express arginase-1 and iNOS and upregulate arginase-1 upon stimulation with IL-13. HPRT shown as endogenous control. (B) Real time RTPCR showing quantitatively the extent of arginase-1 and iNOS upregulation by IL-13 stimulated MDSC. Standardized to GAPDH endogenous control and relative expression compared to untreated BM. (C) Western blot showing arginase-1 and actin control at the protein level in untreated BM, MDSC and MDSC IL13-tx. (D) Arginase activity was determined by measuring the production of urea over time. MLR was performed by mixing B6 purified T-cells with irradiated BALB/c stimulators (1:1 ratio) and MDSC (1:10 ratio). Cultures were pulsed with ^{3}H-thymidine on the indicated days and harvested after a 16 hour incubation. (E) MLR:MDSC co-cultures were left untreated or were treated with arginase inhibitor, nor-NOHA (300uM), Nitric Oxide inhibitor, L-NMMA (300uM), or both. (F) Arginase inhibitor (nor-NOHA) was added to MLR:MDSC co-cultures at increasing concentrations (30uM, 100uM, 300uM). (G) B6 WT T-cells or GCN2 KO T-cells were used as responder cells and MDSC were added at 1:10 ratio as above. (H) Addition of excess L-arginine (5uM) or tryptophan (5uM) was added back to MLR:MDSC co-cultures and assessed for T-cell proliferation.

Figure 2

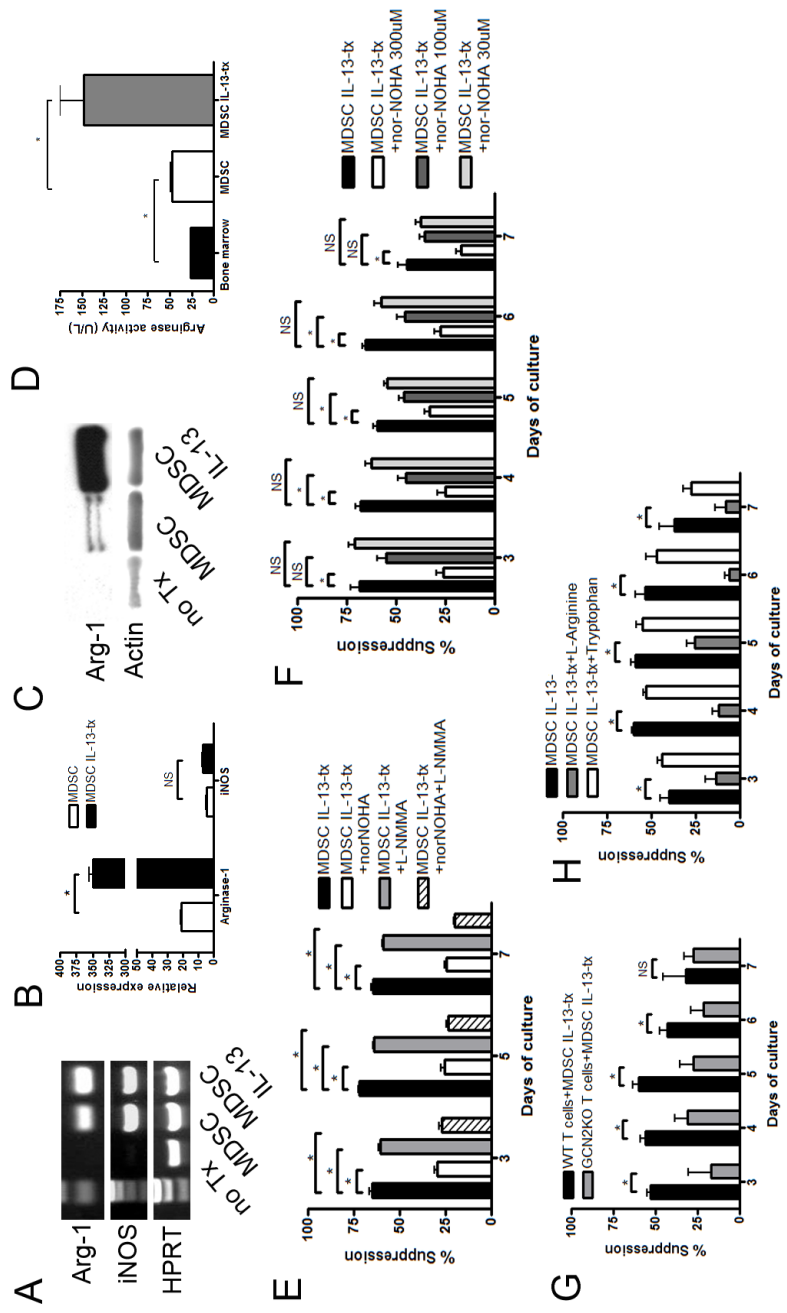
A
Arg-1
iNOS
HPRT
no Tx
MDSC
MDSC IL-13
B
Relative expression
MDSC
MDSC IL-13-tx
Arginase-1
iNOS
NS
C
Arg-1
Actin
no Tx
MDSC
MDSC IL-13
D
Arginase activity (U/L)
Bone marrow
MDSC
MDSC IL-13-tx
E
% Suppression
Days of culture
MDSC IL-13-tx
MDSC IL-13-tx +norNOHA
MDSC IL-13-tx +L-NMMA
MDSC IL-13-tx +norNOHA+L-NMMA
F
% Suppression
Days of culture
MDSC IL-13-tx
MDSC IL-13-tx +nor-NOHA 300uM
MDSC IL-13-tx +nor-NOHA 100uM
MDSC IL-13-tx +nor-NOHA 30uM
G
% Suppression
Days of culture
WT T cells+MDSC IL-13-tx
GCN2KO T cells+MDSC IL-13-tx
H
% Suppression
Days of culture
MDSC IL-13-
MDSC IL-13-tx+L-Arginine
MDSC IL-13-tx+Tryptophan

Figure 3. MDSC migrate to sites of allo-priming in a GVHD setting. (A) FACS analysis of pre-transplant MDSC were gated on $Gr1^+CD11b^+$ and analyzed for the surface expression of molecules associated with homing and recruitment. Gates are based off of isotype controls. (B) Lethally irradiated BALB/c recipients were given 10^7 BM cells plus $2x10^6$ T-cells with $6x10^6$ eGFP transgenic MDSCs. Control mice were given BM and T-cells only. On day 7 and 14, LN and spleen were harvested and imaged using macroscopic fluorescent microscopy. (C) The absolute number of $eGFP^+$ cells that had migrated to the LNs and spleen was determined using flow cytometry. (D) Spleen was harvested from day 7 transplanted mice and flow cytometry was performed to determine if MDSC retained $Gr1^+CD11b^+$ phenotype. Cells were gated on donor $CD11b^+$ cells.

Figure 3

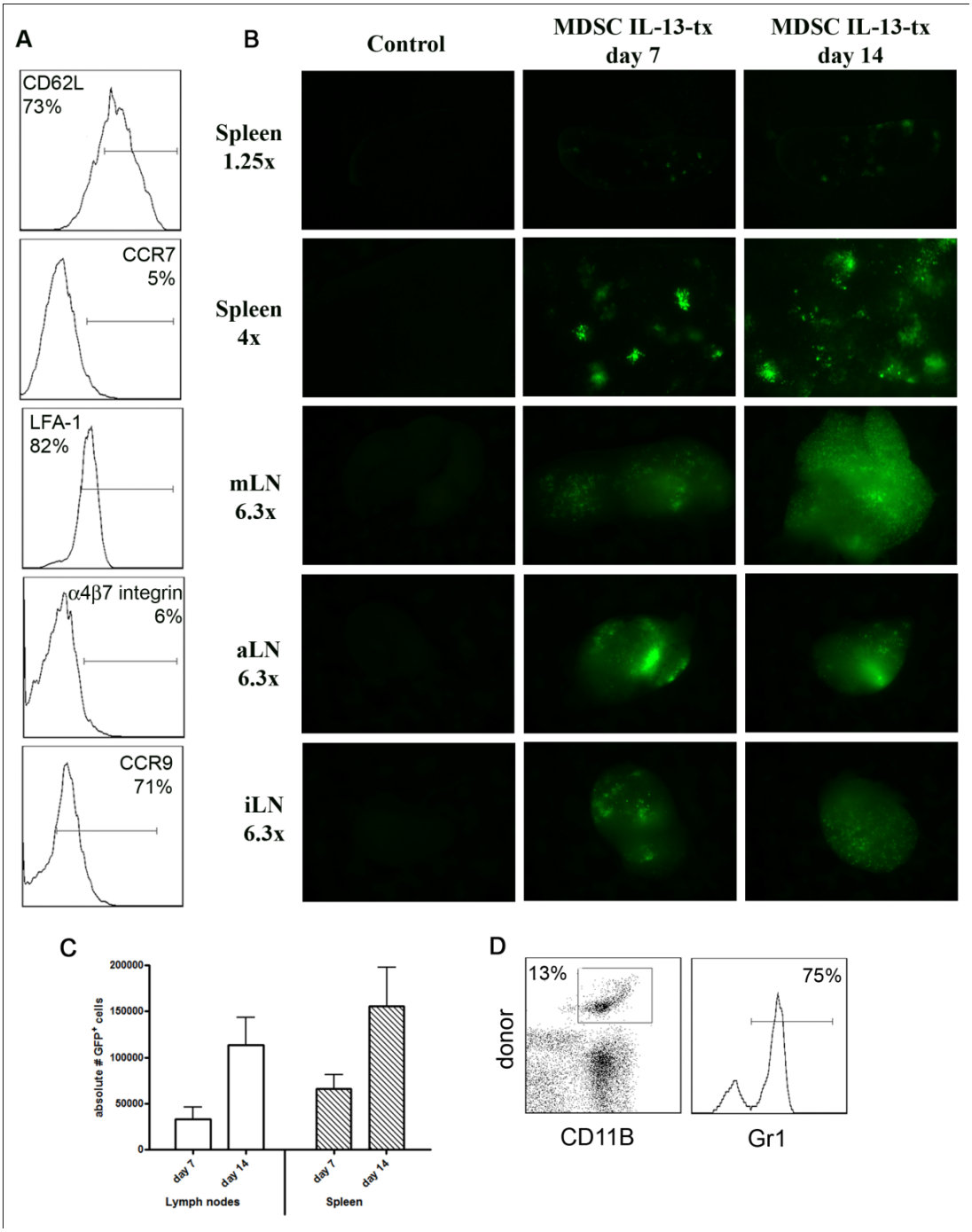
A
B
Control
MDSC IL-13-tx day 7
MDSC IL-13-tx day 14
CD62L 73%
CCR7 5%
LFA-1 82%
α4β7 integrin 6%
CCR9 71%
Spleen 1.25x
Spleen 4x
mLN 6.3x
aLN 6.3x
iLN 6.3x
C
absolute # GFP+ cells
200000
150000
100000
50000
0
day 7
day 14
day 7
day 14
Lymph nodes
Spleen
D
donor
13%
75%
CD11B
Gr1

Figure 4. Cultured MDSC enhance GVHD survival in an arginase-1 dependant fashion. Lethally irradiated BALB/c recipients were given 10^7 B6 BM cells plus $2x10^6$ purified CD25-depleted T-cells plus either $2x10^6$ MDSC or $6x10^6$ MDSC, both IL-13-tx. Kaplan-Meier survival curve of transplanted mice (A). Data represents two pooled experiments (BM only, N=18; BM+T, N=18; BM+T+$2x10^6$ MDSC IL13-tx, N=22; BM+T+ $6x10^6$ MDSC IL13-tx, N=22; BM+T vs. $2x10^6$ MDSC IL-13-tx, $P<0.001$; BM+T vs. $6x10^6$ MDSC IL13-tx, $P<0.001$; $2x10^6$ MDSC IL13-tx vs. $6x10^6$ MDSC IL13-tx, $P=0.06$). Corresponding weights are shown in (B). (C) Kaplan-Meier survival curve of BM transplant as outlined above, except using $6x10^6$ MDSC IL-13-tx generated from either WT mice or arginase-1 KO mice. Represents one experiment (BM only, N=8; BM+T, N=12; BM+T+$6x10^6$ WT MDSC, N=12; BM+T+ $6x10^6$ arginase-I KO MDSC, N=12; BM+T vs. $6x10^6$ WT MDSC, $P=0.05$; BM+T vs. $6x10^6$ arginase-I KO MDSC, $P=0.08$; arginase-1 KO MDSC vs. WT MDSC, $P=0.1$). (D) Corresponding weights are shown. (E) Tissues were harvested from experimental mice in a separate transplant on day 28 post transplant. Representative H/E images are shown (20x).

Figure 4

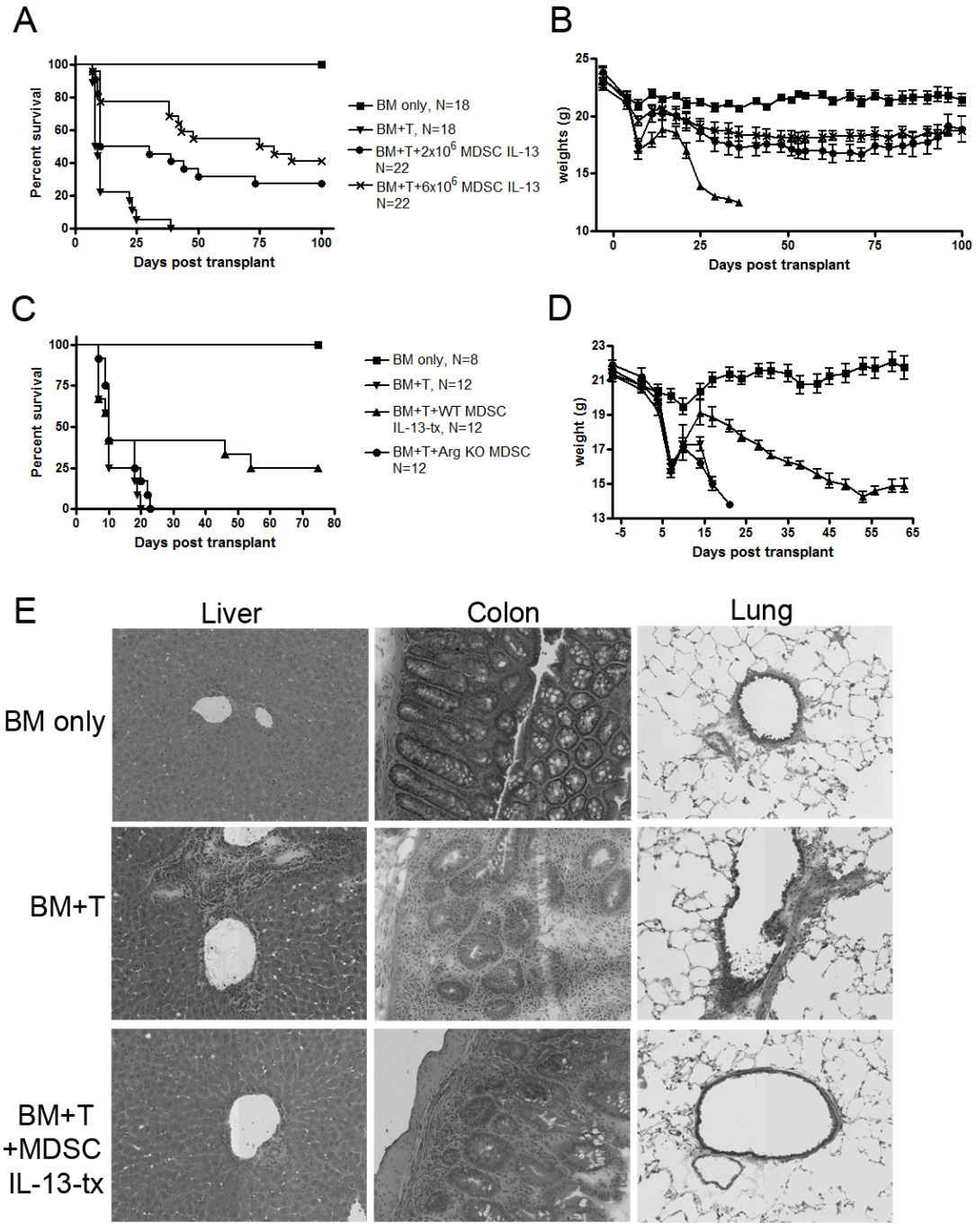
A
Percent survival
Days post transplant
BM only, N=18
BM+T, N=18
BM+T+2x10^6 MDSC IL-13 N=22
BM+T+6x10^6 MDSC IL-13 N=22
B
weights (g)
Days post transplant
C
Percent survival
Days post transplant
BM only, N=8
BM+T, N=12
BM+T+WT MDSC IL-13-tx, N=12
BM+T+Arg KO MDSC N=12
D
weight (g)
Days post transplant
E
Liver
Colon
Lung
BM only
BM+T
BM+T +MDSC IL-13-tx

Figure 5. MDSC negatively impact proliferation, activation, and effector function of donor T-cells. Lethally irradiated BALB/c mice were transplanted with $15x10^6$ CFSE-labeled CD25-depleted B6 Ly5.1 expressing T-cells alone or with $10x10^6$ CD11b purified MDSC.(A) Day 4 splenocytes were analyzed via flow cytometry for CFSE dilution on CD4 and CD8 T-cells. (B) Flow cytometry was used to detect amount of CD3ζ present on CD4 and CD8 splenic T-cells. (C) Graph of common activation markers (CD25 and CD62L) on CD4 and CD8 splenic T-cells. (D) Intracellular cytokine staining was performed on LN CD4 and CD8 T-cells to determine the percentage of cells producing IFN-γ.

Figure 5

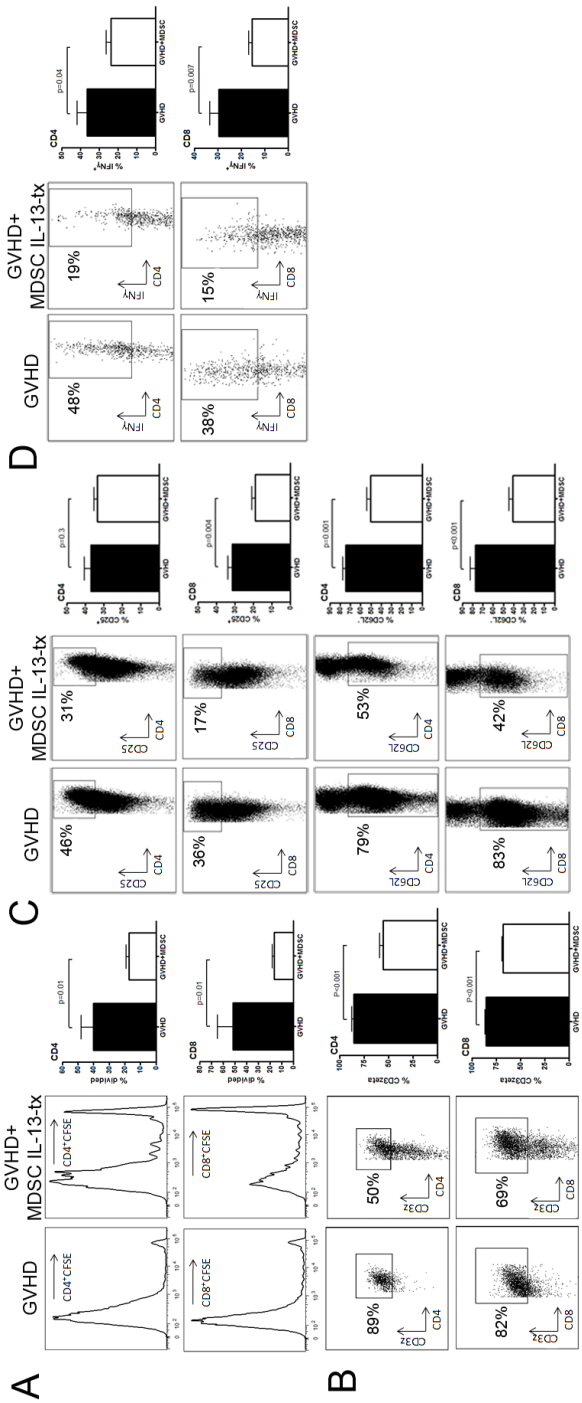
A
GVHD
GVHD+ MDSC IL-13-tx
CD4+CFSE
CD8+CFSE
% divided
p=0.01
p=0.01
CD4
CD8
GVHD
GVHD+MDSC
B
% CD3zeta
P<0.001
P<0.001
89%
82%
50%
69%
CD3z
C
46%
36%
31%
17%
79%
83%
53%
42%
CD25
CD62L
% CD25+
% CD62L-
p=0.3
p=0.004
p<0.001
p<0.001
D
48%
38%
19%
15%
IFNγ
% IFNγ+
p=0.04
p=0.007

Figure 6. MDSCs preserve graft versus leukemia effect of allogeneic donor T-cells. Lethally irradiated BALB/c mice were given $10x10^6$ B6 T-cell-depleted BM cells alone or with $2x10^6$ CD25-depleted B6 T-cells. Cohorts of mice also received $3x10^5$ A20 cells and/or $6x10^6$ B6 MDSC. All cells were given *i.v.* on day 0 of transplant. (A) Kaplan-Meier survival curve of mice receiving BM only (N=10), BM+T (N=10), or BM+T+MDSC (N=10). (B) Corresponding weights from these mice. (C) Kaplan-Meier survival curve of mice receiving BM+A20 (N=10), BM+T+A20 (N=10), or BM+T+A20+MDSC (N=10). (D) Corresponding weights from these mice. (E) Mice were monitored on days 14, 18, and 50 using bioluminescent imaging to detect Renilla luciferase-expressing A20 cells. BM+T vs. BM+T+MDSC, $P<0.001$; BM+A20 vs. BM+T+A20, $P<0.001$; BM+T+A20 vs. BM+T+A20+MDSC, $P<0.001$.

Figure 6

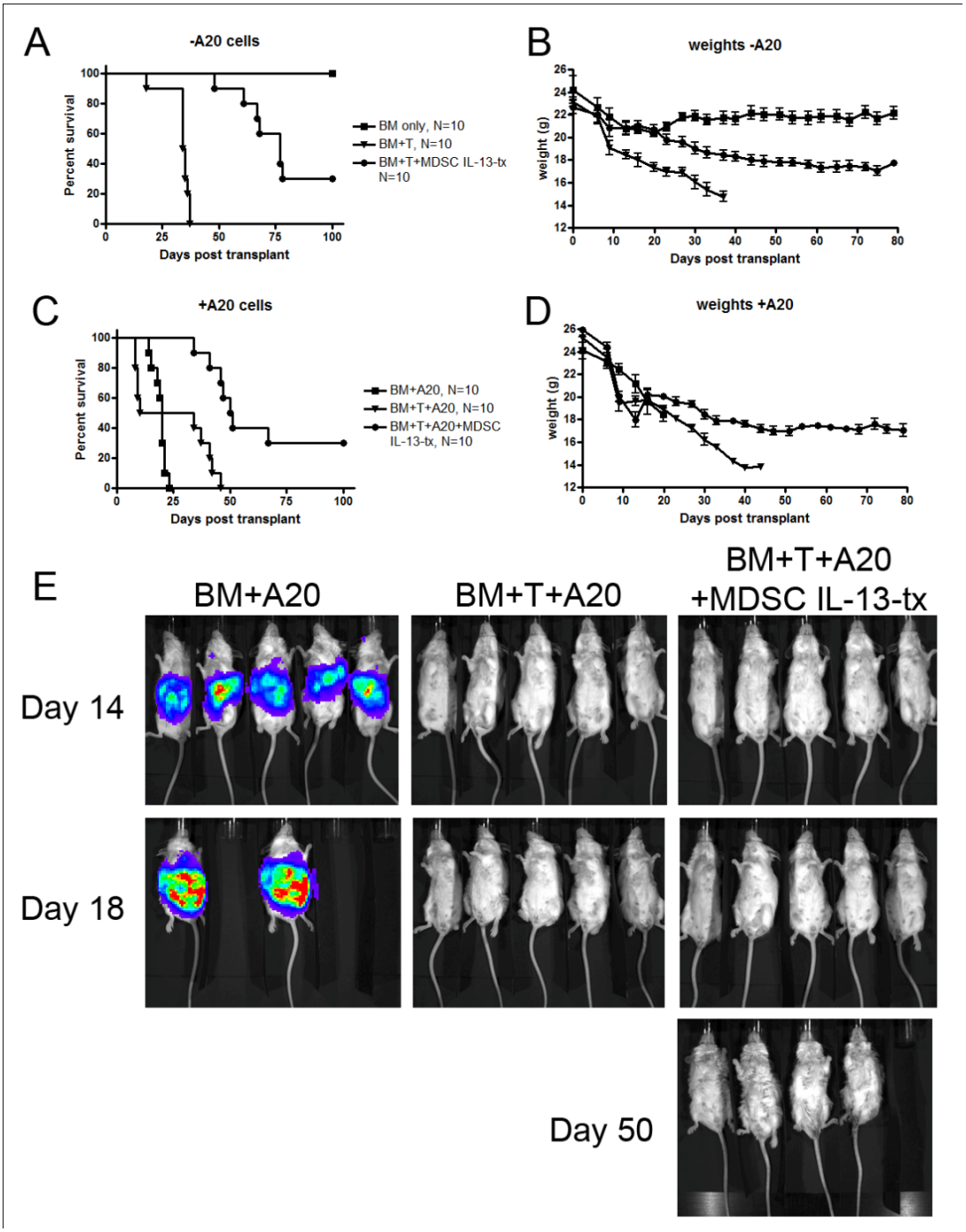
A
-A20 cells
Percent survival
Days post transplant
BM only, N=10
BM+T, N=10
BM+T+MDSC IL-13-tx N=10
B
weights -A20
weight (g)
Days post transplant
C
+A20 cells
Percent survival
Days post transplant
BM+A20, N=10
BM+T+A20, N=10
BM+T+A20+MDSC IL-13-tx, N=10
D
weights +A20
weight (g)
Days post transplant
E
BM+A20
BM+T+A20
BM+T+A20 +MDSC IL-13-tx
Day 14
Day 18
Day 50

Figure 7. PEG-arg1 has similar protective effects as MDSC IL-13-tx. Lethally irradiated BALB/c mice were given $10x10^6$ B6 BM cells alone or with $2x10^6$ CD25-depleted T-cells. In addition to this, cohorts were also given $6x10^6$ MDSC IL13-tx on day 0 or PEG-arg1 at 1mg/mouse, 2 times weekly. (A) Kaplan-Meier survival curve and (B) corresponding weights are shown. *P* values for survival are BM+T vs. $6x10^6$ MDSC, *P*=0.03; BM+T vs. PEG-arg1, *P*=0.003. (C) L-arginine was quantified using HPLC on day 14 from the peripheral blood of transplanted mice. WT B6 mice were used as controls.

Figure 7

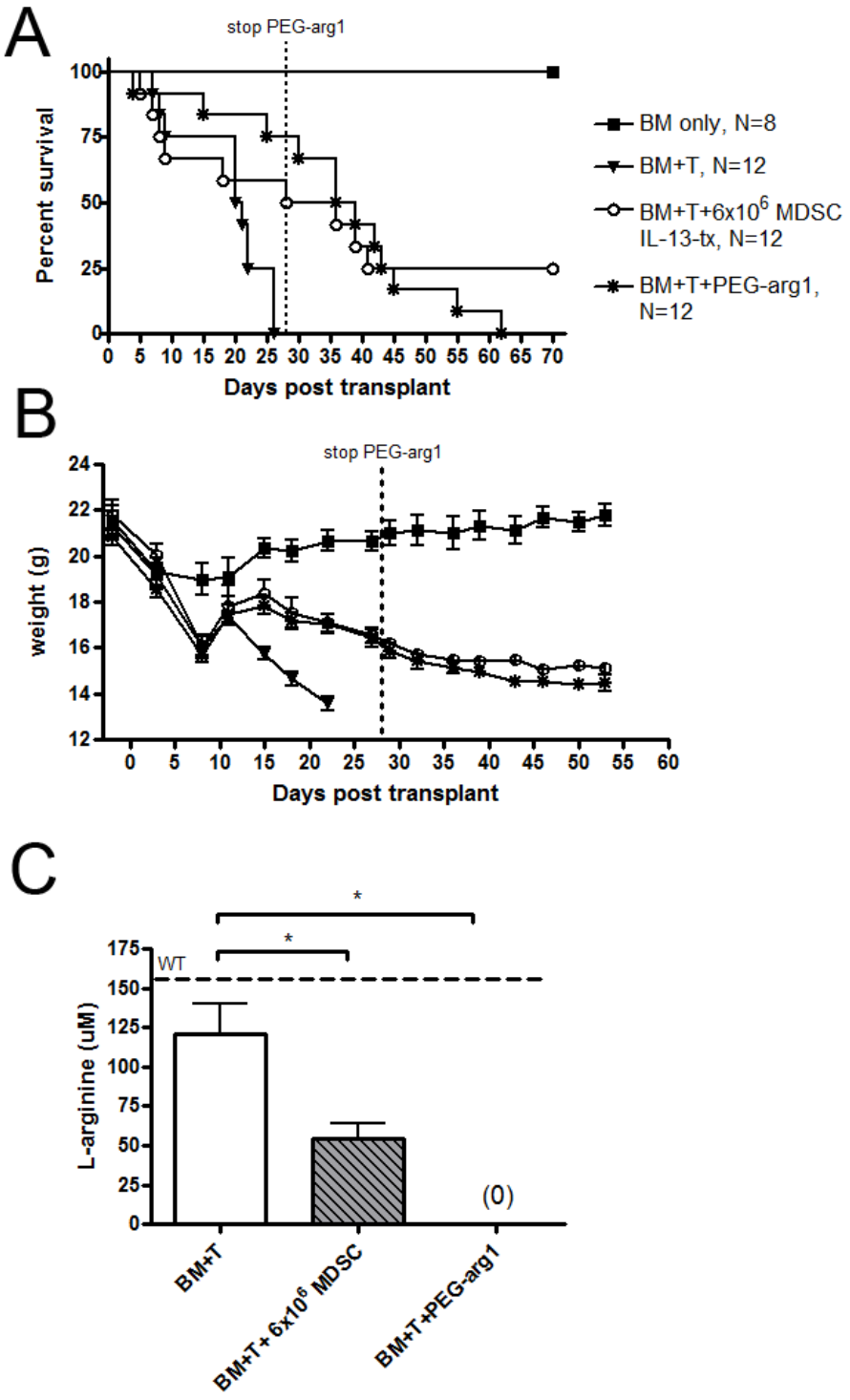
A
stop PEG-arg1
Percent survival
100
75
50
25
0
0 5 10 15 20 25 30 35 40 45 50 55 60 65 70
Days post transplant
BM only, N=8
BM+T, N=12
BM+T+6x10^6 MDSC IL-13-tx, N=12
BM+T+PEG-arg1, N=12
B
stop PEG-arg1
weight (g)
24
22
20
18
16
14
12
0 5 10 15 20 25 30 35 40 45 50 55 60
Days post transplant
C
*
*
WT
L-arginine (uM)
175
150
125
100
75
50
25
0
(0)
BM+T
BM+T+ 6x10^6 MDSC
BM+T+PEG-arg1

Supplemental Figure 1. IL-13 treated MDSCs have significantly enhanced suppressive capacity. MLR cultures were performed using B6 purified T-cells mixed with BALB/c irradiated TCD splenocytes (1:1). MDSCs were left untreated or were treated with IL-13 (80ng/ml) and added at 1:10 (MDSC:T-cell) ratio. Proliferation was assessed using 3H-thymidine uptake.

Supplemental Figure 1

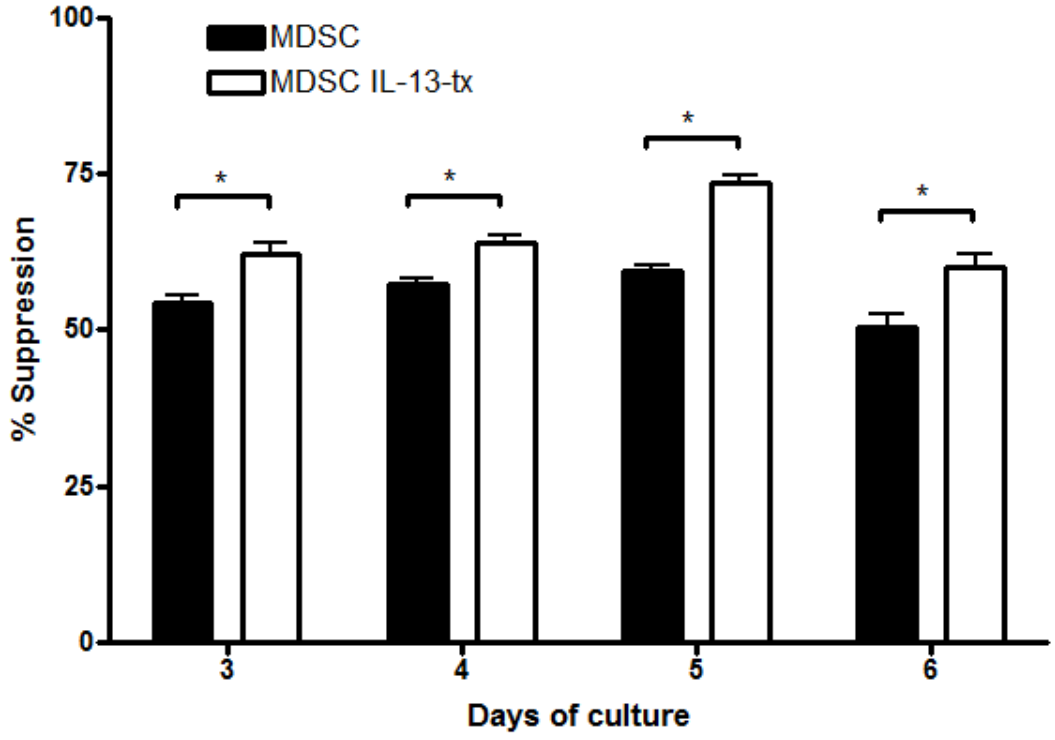

Supplemental Figure 2. MDSC IL13-tx elicit suppression mostly in a contact-independent manner. MLR cultures were performed using B6 purified T-cells mixed with BALB/c irradiated TCD splenocytes (1:1) plated on the bottom of a semi-permeable membrane. MDSC IL13-tx were placed in direct contact with MLR culture or within the top chamber of a TransWell (TW) and added at 1:10 (MDSC:T-cell) ratio. Proliferation was assessed using 3H-thymidine uptake.

Supplemental Figure 2

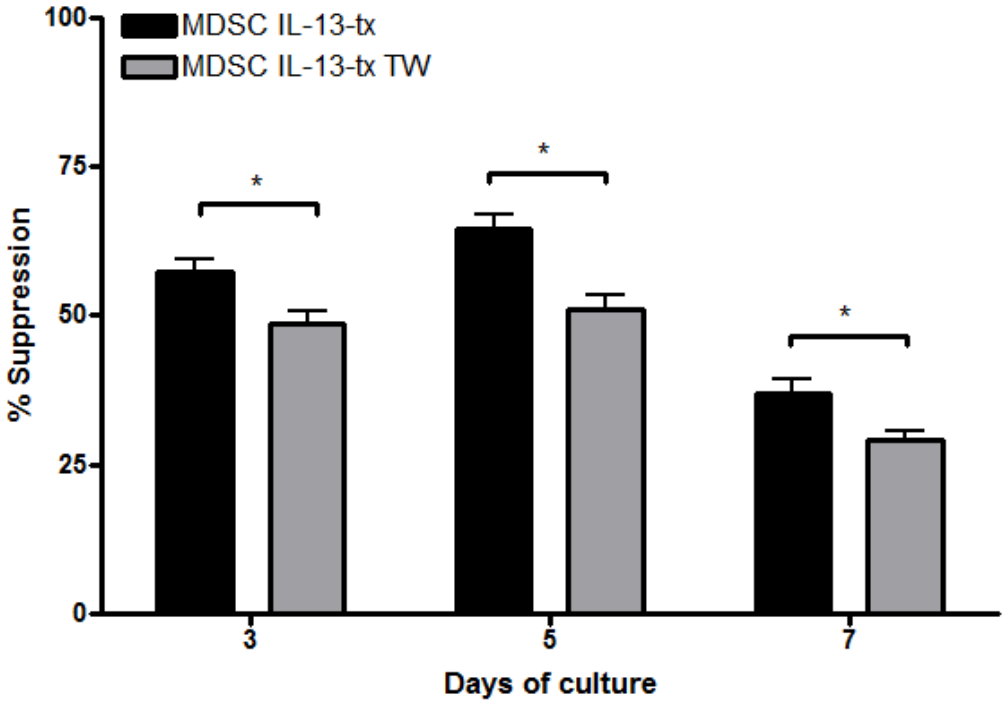

Supplemental Figure 3. IL13-tx MDSC have enhanced suppressive capacity *in vivo*. Lethally irradiated BALB/c mice were given 10^7 B6 T-cell-depleted BM cells alone or with $2x10^6$ CD25-depleted B6 T-cells. Cohorts of mice also received $6x10^6$ B6 MDSC or $6x10^6$ B6 MDSC IL-13-tx. All cells were given *i.v.* on day 0 of transplant. (A) Kaplan-Meier survival curve. (BM+T vs. $6x10^6$ MDSC, P=0.001;BM+T vs. $6x10^6$ MDSC IL13-tx, P<0.001; $6x10^6$ MDSC vs. $6x10^6$ MDSC IL13-tx, P=0.001)

Supplemental Figure 3

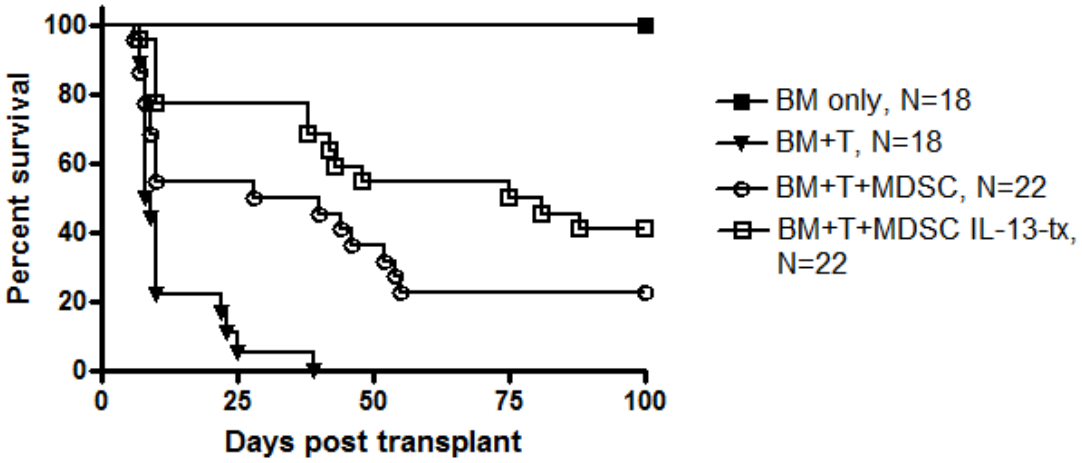

Chapter 4

Mesenchymal Stem Cell Production of Prostaglandin E_2 Amplifies Hematopoietic Stem Cell Differentiation and Expansion

Steven L. Highfill,[1] JakubTolar,[1] Bruce R. Blazar [1]

[1]University of Minnesota Masonic Cancer Center and Department of Pediatrics, Division of Bone Marrow Transplantation, Minneapolis, MN 55455, USA

Foreward

Mesenchymal stem cells (MSCs) are currently used in the clinic as treatment to improve bone marrow engraftment. Although there have been many reports which describe an improvement bone marrow engraftment following the co-infusion of MSCs with bone marrow, the mechanism(s) of action by which this occurs remains to be defined. Here, we report that the secretion of prostaglandin E_2 (PGE_2) by MSCs is likely one of the contributing factors of this phenomenon. Murine MSCs produce large amounts of PGE_2 and the incubation of BM cells with MSCs through a semi-permeable membrane increases the absolute number of LSK hematopoietic stem cells (HSCs), increases the differentiation potential of HSCs, and increases primitive CFU-S cells *in vivo*. Importantly, when the ability of MSCs to produce PGE_2 is inhibited, most of these effects are reversed. Collectively, these results uncover a novel mechanism of action employed by MSCs to enhance BM engraftment. This improved understanding will hopefully allow for effective and targeted use of MSC for this purpose in the clinic.

Introduction

Hematopoietic stem cell (HSC) transplantation has been shown to be a lifesaving procedure for a variety of malignant and hereditary diseases. There have been many advances since the first successful bone marrow transplants were carried out, but, in spite of these advances, primary BM graft failure remains a considerable limitation to the procedure. Our goal is to investigate novel cellular strategies that may enhance BM engraftment and thus promote hematopoietic reconstitution and recovery of immune function.

HSCs are a rare population of cells found in the bone marrow that give rise to all the blood cell types including myeloid and lymphoid lineages. HSCs are thought to originate in the embryonic yolk sac and seed into the marrow cavity following establishment of the stroma.[156,157] The initiation of hematopoiesis subsequent to the establishment of the stroma has underscored the importance of the hematopoietic microenvironment in the regulation of HSC homeostasis. Stromal cells present in the BM, such as fibroblasts and endothelial cells, produce numerous cytokines that support hematopoiesis.[101,158] Recent advances in the field that highlight the multifaceted roles of prostaglandins in hematopoiesis has stimulated a new flurry of research in this area.

Prostaglandins are a group of lipid compounds derived enzymatically from fatty acids. Arachidonic acid (AA) derived from membrane lipids is converted into PGG_2 and PGH_2 by the action of cyclooxygenase (COX). PGH_2 is in turn converted by specific synthases into PGI_2, PGF_2, PGD_2, and PGE_2.[159] These compounds regulate many processes in the body, including kidney function, platelet aggregation, neurotransmitter

release, and modulation of immune function.[160,161] Studies performed nearly 40 years ago show that PGE_2, in particular, had the capacity to stimulate HSC proliferation.[162] More recent research has not only affirmed the expression of PGE_2 receptors on HSCs, but has also defined a role for this signaling pathway in the context of BMT.[163,164]

In addition to HSCs, bone marrow also contains a population of pluripotent mesenchymal stem cells (MSC). MSCs represent approximately 0.01-0.001% of nucleated BM cells and are most commonly characterized by their differentiation potential which allows them to give rise to osteoblasts, adipocytes, and chondroblasts under the appropriate culture conditions.[165] The relative ease of isolating these cells from murine and human sources has allowed for studies exploring the potential use of these cells for therapeutic purposes. In this regard, numerous animal studies have shown MSCs to impart a beneficial effect on BM engraftment[64,166-168], however, the mechanisms by which this occurs remains elusive.

Here, we show that MSCs produce cytokines capable of fostering the engraftment of transplanted HSCs following myeolablative radiation. We find that MSCs enhance the differentiation capacity and proliferative capacity of HSCs. Further, we find that this enhancement effect is at least partially due to the secretion of PGE_2 by MSCs, because the inhibition of PGE_2 secretion reverses these effects. These studies bridge the gap between the known engraftment-enhancing capabilities of MSCs and the mechanism of action by which this is done and has possible consequences for the selection of clinical-grade MSCs that are to be used as cellular therapy for these purposes.

Materials and Methods

Mice. C57BL/6 ($H2^b$)(termed B6 and expressing Ly5.2) and congenic B6 Ly5.2 mice (expressing Ly5.1) were purchased from the National Institute of Health (Bethesda, MD). All mice were housed in specific pathogen-free facility in microisolator cages and used at 8-12 weeks of age in protocols approved by the Institutional Animal Care and Use Committee.

MSC generation, culture and differentiation. MSCs were generated from C57Bl/6 and BALB/c mice (NCI, Bethesda, MD) as described by others.[169] Briefly, femurs and tibia from 8-10 week old female mice were removed, cleaned of connective tissue, and flushed with ice cold RPMI (Invitrogen, Carlsbad, CA). Cells were re-suspended in complete media consisting of 10% fetal bovine serum (FBS) Hyclone Laboratories, Logan, UT), 10% horse serum (Hyclone Laboratories), 100 U/ml Penicillin (Invitrogen), 100 ug/ml streptomycin (Invitrogen), and 12 uM L-glutamine (Invitrogen). Cells were plated at $5x10^5$ cells/ml in 20ml in a $150cm^2$ tissue culture flask. After 24 hours, non-adherent cells were removed by washing with phosphate buffered saline (PBS). Fresh media was added (20ml) and cells were incubated for a period of 4 weeks. Media changes were performed every 3-4 days. After 4 weeks, cells were harvested by a 2 minute treatment with trypsin (0.25% trypsin; Invitrogen), and replated as above for a period of 1 week with media changes on day 2 and 5. These cells were harvested using trypsin as above and plated at 50 cells/cm^2 in expansion media consisting of Iscove modified Dulbecco medium (IMDM; Invitrogen), 10% FBS, 10% HS, 100 U/ml penicillin, 100 ug/ml

streptomycin, and 12 uM L-glutamine. Cells were expanded and frozen in liquid nitrogen at passages 3-6 for use in experiments described here.

For differentiation, cells were placed at 100 cells/well in a 6 well dish in expansion media for 1 week with media changes. Adipogenesis was tested by changing media to IMDM supplemented with 10% FBS, 10% HS, 1 uM dexamethasone (Sigma-Aldrich, St. Louis, MO), 5 ug/ml insulin (Sigma-Aldrich), 100 U/ml penicillin, 100 ug/ml streptomycin, 12 mM L-glutamine, 50 uM indomethacin (Sigma-Aldrich), 0.5 uM 3-isobutyl-1-methylxanthine (IBMX; Sigma-Aldrich). Cells were incubated in adipogenesis media for 3 weeks with media changes before the cells were fixed with 10% formalin for 20 minutes and stained with 0.5% Oil Red O (Sigma-Aldrich). Osteogenesis was tested by changing media to alpha-MEM (Invitrogen) supplemented with 10% FBS, 100 nM dexamethasone, 0.2 mM ascorbic acid (Sigma-Aldrich), 100 U/ml penicillin, 100 ug/ml streptomycin, and 10 mM beta-glycerophosphate (Sigma-Aldrich). Cells were incubated in osteogenesis media for 3 weeks with media changes before cells were fixed with 10% formalin and stained with Alizarian Red (Sigma-Aldrich) pH 4.1. For chondrogenesis, $2x10^5$ cells were spun down in a 15 ml conical tube at 1500 rpm for 5 minutes. Media was changed to DMEM supplemented with 1X ITS (Sigma-Aldrich), 1X linoleic acid BSA (Sigma-Aldrich), 0.1 uM dexamethasone, 50 ug/ml ascorbic acid, 10 ng/ml TGF-β (R&D Systems, Minneapolis, MN), 100 U/ml penicillin, and 100 ug/ml streptomycin. Cells were incubated in 500 ul chondrogenesis media for 3 weeks with media changes before removing and freezing the cell pellet in optimal cutting temperature (OCT) compound (Sakura, Tokyo, Japan). For microscopy, 6 uM sections were cut and stained with Toluidine blue solution (Sigma-Aldrich).

PGE_2 ELISA. Quantitative determination of PGE_2 in cell culture supernatants was performed using a commercially available PGE_2 ELISA assay (R&D Systems). This assay is based on the competitive binding of PGE_2 within the sample with a fixed amount of horseradish peroxidase (HRP)-labeled PGE_2 for sites on a mouse monoclonal antibody.

RTPCR. RNA was isolated from mesenchymal stem cells using RNAqueous 4 PCR kit (Applied Biosystems, Inc., Foster City, CA). cDNA was synthesized using Superscript III reverse transcriptase (Invitrogen). cDNA for non-quantitative RT-PCR was performed using specific primers for PGE_2 synthase (sense, 5'-CTCTGTCATCATTAGTGCCCTCAA -3'; antisense, 5'-ACTGCCAGGTCAGCAAGGTTAG -3'), IL-11 (sense, 5'-CTCTGGCCAGATAGAGTCGTTG -3'; antisense, 5'-CGCGGCGCAGCCATTGTACATG -3'), LIF (sense, 5'-TCACCCCTGTAAATGCCACC -3'; antisense, 5'-CTTCTTTGTCAGAGTGGTCG -3'), GCSF (sense, 5'-CTGCCATCCCTGCCTCT -3'; antisense, 5'-TGCACAGTAGGGGCCACCCC -3'), stem cell factor (sense, 5'-TAACCCTCAACTATGTCGCC -3'; antisense, 5'-TGAAGAGAGCACACACTCAC -3'), Flt3 Ligand (sense, 5'-ACACCTGACTGTTACTTCAGC -3'; antisense, 5'-CCTGGGCCGAGGCTCTGG -3'), angiopoietin-1(sense, 5'-AATGCTGTTCAAAACCACACGG -3'; antisense, 5'-

AATGTCTGACGAGAAACCAAGCC -3'), and thrombopoietin (sense, 5'-CAGAGCAAGGCACAGGACATTC -3'; antisense, 5'-ACTGAAGTTCGTCTCCAACAATCC -3') and amplified for 35 cycles.

Flow cytometry. Expanded MSCs were stained for surface expression of Stem cell antigen-1 (Sca-1), CD34, cKit, CD44, CD45, VCAM, CD90, CD11b, and CD31. Lineage negative cells used here were depleted of T-cells, CD3, CD4, CD8; monocytes, CD11b; dendritic cells, CD11c; myeloid cells, CD33; erythroid cells, Ter119; B-cells, B220; granulocytes, Gr-1. These were further gated on $cKit^+$ and $Sca\text{-}1^+$ high cells to obtain LSK hematopoietic stem cell population previously defined. All antibodies were purchased through Pharmingen (San Diego, Ca) or E-bioscience (San Diego, Ca) and stained according to manufacturer's instructions then analyzed using FACSLSRII or FACSCanto (Becton Dickinson, San Jose, Ca) and Flow Jo software (Treestar inc).

Colony forming unit assay (CFU assay). Bone marrow from the femurs of 8-10 week old C57Bl/6 mice were incubated in the top chamber of a TransWell insert *ex vivo* overnight with 20uM $dmPGE_2$ or $1x10^5$ MSCs plated on the bottom of the TransWell insert. MSCs were either untreated or treated overnight with 5uM indomethacin prior to the addition of BM cells. On day 0, BM was harvested, counted, and plated in methylcellulose containing M3434 media (Stem Cell Technologies). A total of 0.4 ml of cells at a $1x10^6$ cells/ml concentration was added to 4 ml MethoCult medium and 1.1 ml of this was added to a 35 mm dish. Cells were placed in a humidified incubator at 37C and 5% CO_2

for a period of 12 days. After incubation, cells were counted and colony-types were evaluated using an inverted microscope and a gridded scoring dish.

Colony forming unit- S assay (CFU-S). Bone marrow cells were harvested and treated as in CFU assay above. On day 0, lethally irradiated (950 cesium) mice received $7x10^4$ MSC-treated or untreated BM cells. Spleens were dissected on day 12, weighed and fixed in Bouin's solution. Hematopoietic colonies per spleen were counted.

Statistical analysis. Significance level was determined using Graphpad Prism software (Graphpad Software, LaJolla, CA). Student's *t* test was used to analyze differences between groups. Results were considered significant if the *P* value was ≤ 0.05.

Results

Isolation and characterization of bone marrow derived murine mesenchymal stem cells.

Murine mesenchymal stem cells (MSC) were isolated and expanded for 8 weeks, at which point the MSCs were a highly homogeneous spindle-shaped population with large round nuclei (Figure 1A). MSCs expressed Sca-1, CD34, CD44, and VCAM (CD106) and were negative for markers used to identify epitopes found on many hematopoietic and endothelial cells including CD11b, CD45, cKit, CD90, and CD31 (Figure 1C). Importantly, this cell-surface phenotype is consistent with other reports.[169] In terms of their differentiation potential, MSCs were capable of differentiation into adipocytes, osteocytes, and chondrocytes (Figure 1C).

MSCs produce cytokines that can positively influence engraftment. We next determined the expression profile of secreted proteins of MSCs, focusing the analysis to molecules known to have an influence on BM engraftment. MSCs express LIF, G-CSF, SCF, Flt3L (FL), and PGE_2 synthase (Figure 2A). Interestingly, when MSCs isolated from B6 mice were compared to MSCs isolated from BALB/c mice, only B6 MSCs expressed thrombopoietin (TPO), whereas only BALB/c MSCs express angiopoietin-1 (APO)(Figure 2A). Neither strain of MSCs expressed IL-3, IL-4, IL-6, or GM-CSF (data not shown). Recent studies by North *et al*. have shown PGE_2 to regulate HSC homeostasis;[164] therefore we chose to focus our attention primarily on PGE_2 secretion. After overnight culture, PGE_2 protein concentration within the supernatant is

significantly elevated, a finding that was nearly completely abrogated by pre-treatment of MSCs with a COX-inhibitor, indomethacin (Figure 2B). These results show that MSCs secrete copious amounts of PGE_2 in the steady state, and that production of PGE_2 is easily blocked by pretreatment of MSC with indomethacin.

Ex vivo treatment of BM with MSCs increases HSC number and is partially dependent on PGE_2 To examine the effect PGE_2 production by MSCs has on HSCs, untreated or indomethacin-treated MSCs were co-cultured with whole bone marrow cells from B6 mice that were separated by a Transwell (TW). This system allows passage of soluble molecules through the transwell, but inhibits direct contact of MSC with bone marrow cells. As a positive control for these studies, the long-acting PGE_2 derivative, 16,16-dimethyl PGE_2 ($dmPGE_2$), was incubated with BM alone. After 48 hours, BM cells incubated with $dmPGE_2$ and untreated MSCs contain approximately 4 to 5-fold higher numbers of $Lin^-Sca1^+cKit^+$ (LSK) HSCs when compared to BM incubated alone, and approximately 2-fold higher numbers of LSK HSCs when compared to MSCs incapable of producing PGE_2 (Figure 3A, B). There is, however, a slight but significant increase in LSK MSCs when comparing indomethacin-treated MSC- to BM alone, which is an indication that there may be other soluble molecules affecting LSK number in addition to PGE_2. There was no difference in the absolute numbers of B-cells, NK-cells, or macrophages between BM incubated with MSCs and BM incubated with MSCs unable to produce PGE_2 (Figure 4C). This is in accordance to our hypothesis that PGE_2 specifically targets the progenitor population of cells. Therefore, treatment of BM cells with MSCs *ex*

vivo expands LSK HSCs at early time points, an effect that is partly mediated by MSC-derived PGE_2.

MSCs increase BM CFU and differentiation capabilities. To determine whether the expansion of LSK HSCs by MSCs at early time points correlated with an increase in downstream populations at later time points, we incubated B6 BM with dmPGE2, or with untreated or indo-pre-treated MSCs for 24 hours in a TW. This was followed by harvesting and extensive washing in PBS before application in a methyl-cellulose-based colony-forming assay. On day 12, total CFCs were counted and enumerated by lineage; erythroid (E), granulocyte/monocyte (GM), or granulocyte/erythroid/monocyte/megakaryocyte (GEMM). Treatment of BM with $dmPGE_2$ and MSCs resulted in a significant increase in the total number of colonies formed in this CFU assay when compared to BM left untreated (Figure 5A). Importantly, there were also significantly more colonies within the MSC-treated group than within the indo-pretreated-MSC group (Figure 5A). When classifying by lineage, we find that MSC treatment resulted in significantly more definitive erythroid, granulocyte/monocytes, and granulocyte/erythroid/monocytes/magakaryocyte colonies than BM cells treated with indo-pretreated-MSCs (Figure 5B). In both cases, there was no statistical difference between BM left untreated and BM incubated with indo-pretreated-MSCs (Figure 5A, B). These data confirm MSCs can potently and durably regulate downstream hematopoiesis through the secretion of PGE_2.

MSCs increase primitive CFU-S number and splenic weight post transplant.

In order to test whether the above findings conferred a beneficial effect *in vivo*, we incubated BM cells alone, with $dmPGE_2$, or with untreated or indomethacin-pre-treated MSCs and analyzed effects in a CFU-S12 assay. We then transferred BM cells from each group into lethally irradiated B6 mice. Clonal colony formation of maturing hematopoietic cells was determined by counting the number of colonies within the spleens on day 12 post-transplant. The number of spleen colony-forming units and splenic weight was significantly increased in mice given BM treated with $dmPGE_2$ or MSCs (Figure 6A, B, C). Furthermore, mice given BM cells treated with MSCs unable to produce PGE_2 had significantly less CFU-S12 than mice given BM treated with normal MSCs, and there was no significant difference between BM incubated alone and BM incubated with indo-pretreated-MSCs (Figure 6A, B). These results show that MSCs enhance hematopoietic progenitor formation through the production of PGE_2.

Discussion

Previous work has shown that transferred MSCs can create a favorable environment that allows for enhanced BM engraftment. For example, Lazarus *et al*. were the first to show that infusion of autologous MSCs at the time of transplant resulted in an increased hematopoietic recovery in patients receiving high-dose chemotherapy for advanced breast cancer.[170] Here, MSCs were administered without any signs of toxicity and hematopoietic recovery, as measured by neutrophil engraftment and platelet count, was achieved in significantly less time than historical controls.[170] These encouraging results have prompted others to use MSCs as an engraftment-promoting approach and in 2007, Le Blanc *et al*. reported a successful outcome after co-transplantation of MSCs with HSCs in patients who were re-transplanted for previous graft failure.[171] Similarly, MacMillan *et al*. tested whether MSCs from parental donors could speed hematopoietic recovery after umbilical cord blood (UCB) transplant.[172] Their results show that all 8 patients receiving MSCs had a significant enhancement in neutrophil and platelet engraftment over historical control umbilical cord blood recipients, and that this therapy had potential use in cases where there are limiting numbers of stem cells.[172] Although the studies outlined here all conclude that MSCs enhance the engraftment potential of hematopoietic progenitor cells, there is no evidence suggestive of a mechanism of action by which this occurs. In this study, we evaluated the possibility that MSCs can regulate hematopoiesis through the secretion of a soluble factor that has direct effects on progenitor cells.

North *et al.* demonstrated that PGE_2 is very important in regulating HSC number and differentiation capacity. The addition of a long-acting derivative of PGE_2, $dmPGE_2$, to embryonic stem cells during embryoid body formation lead to a 3-fold increase in the number of hematopoietic colonies formed.[164] Using a murine BM transplant model, this group demonstrated that *ex vivo* exposure of purified LSK HSC ($Lin^-Sca1^+cKit^+$) to $dmPGE_2$ gave rise to a significant increase in both splenic weight and CFU-S12.[164] In both incidences, a non-specific inhibitor of PGE_2 synthesis was able to reverse the observed beneficial effects provided by $dmPGE_2$. Hoggatt *et al*. demonstrated that the action of PGE_2 was directed toward HSCs themselves, rather than a bystander effect emanating from other cell populations. They found that the mechanisms of action PGE_2 had on stem cell function was to increase BM homing by increasing CXCR4 expression, block apoptosis by upregulating Survivin expression, and increase HSC number by increasing the proportion of HSCs entering into the cell cycle.[163] These combined effects lead to a 4–fold increase in repopulating cell frequency following a competitive transplant model using untreated and $dmPGE_2$-treated congenic BM cells.[163] These studies laid the groundwork for a phase I clinical trial currently underway examining the effects of *ex vivo* treatment of UCB cells with $dmPGE_2$ prior to transplantation.[173]

In the clinical setting, MSCs are administered systemically and their capacity to influence engraftment and hematopoiesis is dependent on their ability to traffic to the appropriate microenvironment. Human and animal studies have shown that MSCs can efficiently migrate to the bone marrow compartment after transplantation.[71,170,174] We speculate that the combined ability of MSC to effectively traffic to bone marrow niche and produce copious amounts for PGE_2 allow for maximal effect for locally boosting

HSCs. It is worth mentioning that receptors for E series of prostaglandins (EP receptors) are highly expressed in the gastrointestinal (GI) tract of rodents and humans[175] and PGE_2 signaling is implicated in the pathology of various diseases involving GI tract, such as inflammatory bowel disease, entero-invasive bacterial diseases, and colorectal cancers.[176-178] *In vitro* studies using colonic epithelial cells have demonstrated that there is an increased production of the pro-inflammatory cytokine, IL-8, upon PGE_2 binding to EP4 receptor.[179] Our own unpublished studied using $dmPGE_2$ given *i.p.* in a murine model of aGVHD have shown devastating consequences. All mice given $dmPGE_2$ (4 injections at 1mg/ml) suffered severe colonic inflammation and died by day 6 post-transplant (unpublished observation, SLH and BRB). It is also well established that PGE_2 can exert anti-inflammatory effects.[69,145,180] The precise location, activation state of cells, and micro-environmental stimuli are thought to play roles in the outcome of this signaling cascade. Therefore, extreme caution must be taken when using PGE_2 systemically as therapy, especially in the context of BMT in which radio-therapy results in damage to gut epithelial cells and creates a pro-inflammatory environment. Because PGE_2 has an extremely short half-life *in vivo*[117], the exacerbation of this pro-inflammatory effect on gut epithelium may be reduced when using MSCs to deliver PGE_2 signals directly to the BM microenvironment.

In summary, we have unveiled a novel mechanism of action by which MSCs positively influence the engraftment capabilities of HSCs. We have shown that *ex vivo* treatment of BM cells with MSCs through a semi-permeable membrane increases LSK HSC number, increases BM CFU number and differentiation capabilities, and increases primitive CFU-S12 number *in vivo*. Ongoing studies are aimed at determining the

differential engraftment-promoting effects *in vivo* of WT MSCs vs. MSCs derived from COX2 KO mice, which are known to be deficient in PGE_2 production. These studies may be useful to clinicians attempting to improve BM engraftment when using limiting numbers of stem cells and, therefore, have direct translatability.

Acknowledgments

We thank Amanda Kobbs for technical assistance with isolation, expansion, and differentiation of MSCs, Cindy Eide for technical assistance with CFU assays, and Ryan Kelly and Michelle Smith for thoroughly editing this manuscript. This work was supported in part by NIH grants (Bethesda, MD; to B.R.B.), and the Children's Cancer Research Fund (Minneapolis, MN; to S.L.H.).

Figure 1. Isolation and characterization of BM-derived murine MSCs. MSCs were isolated from the femurs and tibia of B6 mice as described in 'methods'. (A) Microscopic images were taken of expanded MSCs at 20X (left) and 40X (right) magnification. (B) Surface phenotype, as determined by FACS, was performed. Shaded histograms indicate isotype control. (C) MSCs were incubated to confluency and transferred to adipogenic or osteogenic media for 21 days. Chondrogenesis was produced by incubating $2x10^5$ pelleted MSCs in chondrogenic media for 21 days. Control cells were MSCs incubated in expansion media without differentiation-inducing cytokines.

Figure 1

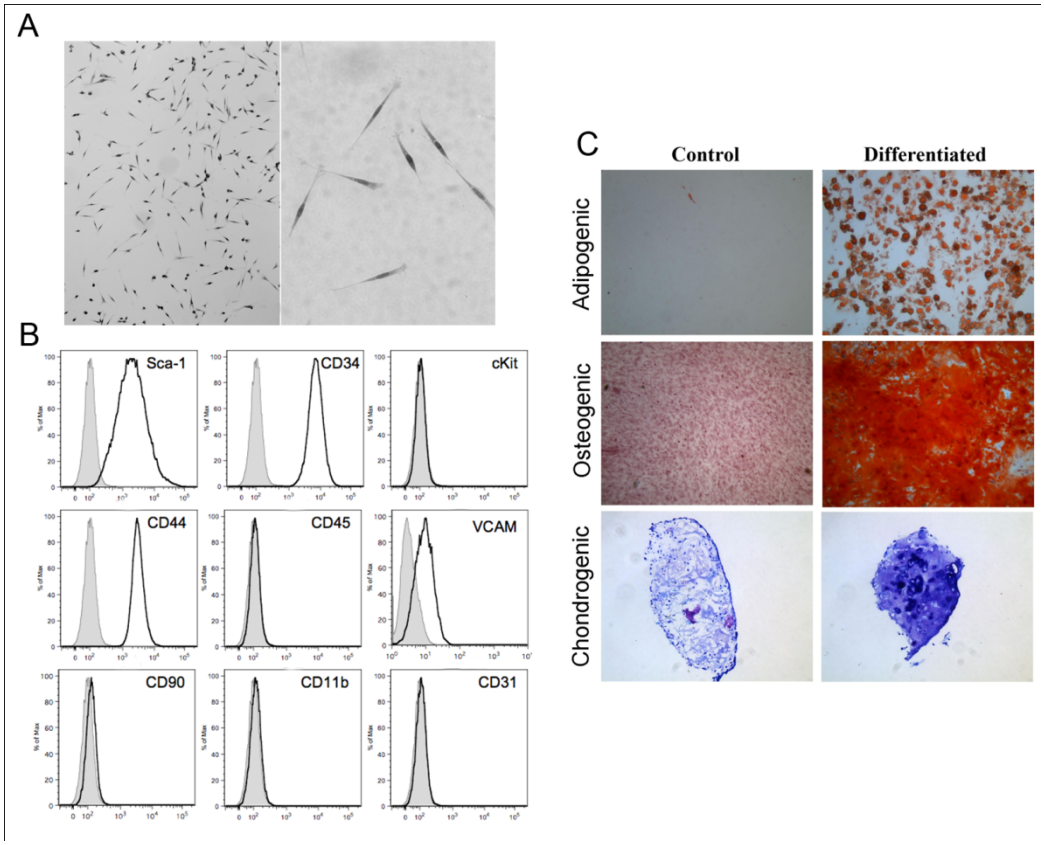
A
B
Sca-1
CD34
cKit
CD44
CD45
VCAM
CD90
CD11b
CD31
C
Control
Differentiated
Adipogenic
Osteogenic
Chondrogenic

Figure 2. MSCs produce mRNA for cytokines that can positively influence bone marrow engraftment. (A) RT-PCR showing the expression pattern of B6 and BALB/c BM-derived MSCs. HPRT, housekeeping control; NTC, no template control; IL-11, interleukin-11; LIF, leukemia inhibitory factor; GCSF, granulocyte colony stimulating factor; SCF, stem cell factor; FL, Flt3 ligand; ANG1, angiopoietin-1; TPO, thrombopoietin; PGE2 S, PGE2 synthase. (B) Supernatant was taken from cultures containing $1x10^5$ B6 MSCs 24 hours after plating and quantified for PGE2 concentration.

Figure 2

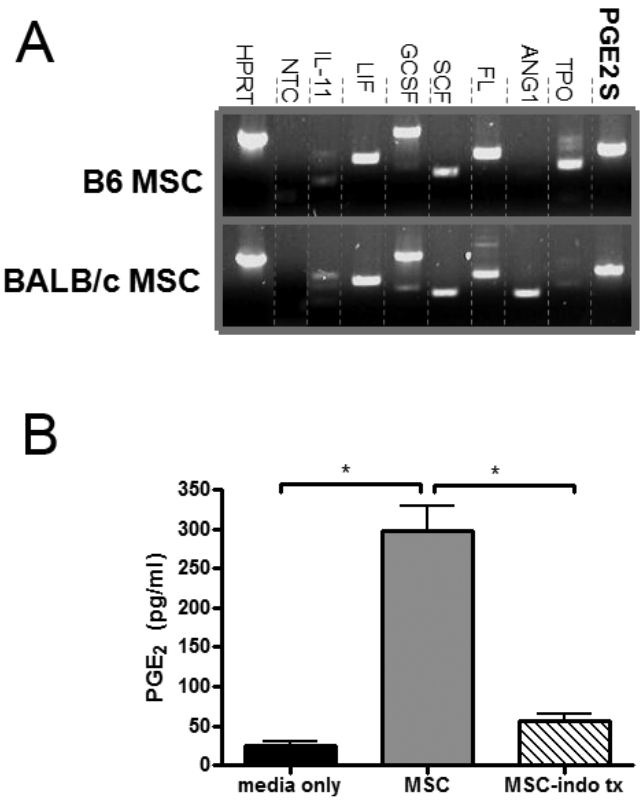
A
HPRT
NTC
IL-11
LIF
GCSF
SCF
FL
ANG1
TPO
PGE2S
B6 MSC
BALB/c MSC
B
*
*
350
300
250
200
150
100
50
0
PGE2 (pg/ml)
media only
MSC
MSC-indo tx

Figure 3. Treatment of whole BM ex vivo with MSCs increases HSC number and is partially dependant on PGE_2. BM cells ($5x10^6$) were incubated 48 hours over a semi-permeable membrane either alone or with $dmPGE_2$ (20uM), MSCs ($1x10^5$), or MSCs pretreated with indomethacin. BM cells were then harvested from each group and analyzed for the absolute number of LSK HSCs (A,B) and other downstream populations (C) by FACS.

Figure 3

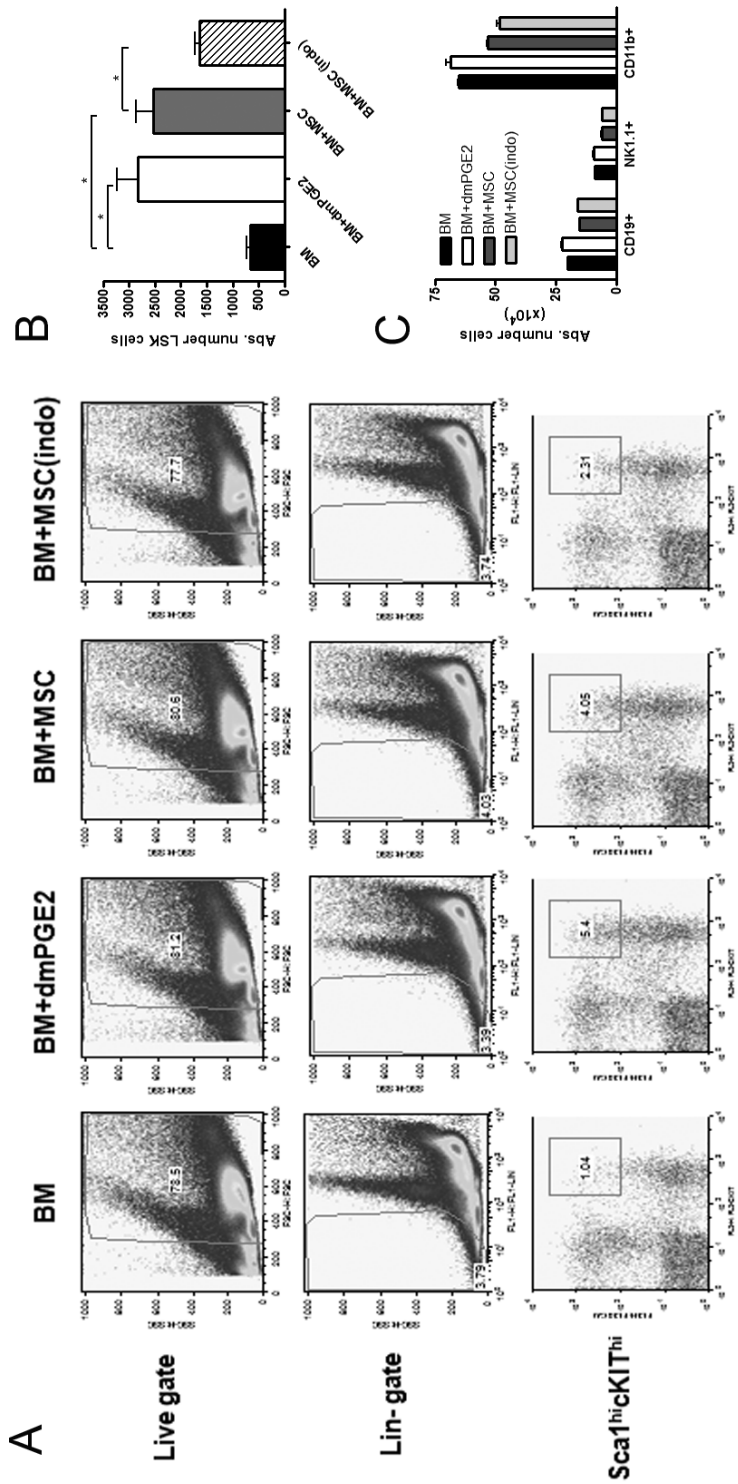
A
BM
BM+dmPGE2
BM+MSC
BM+MSC(indo)
Live gate
Lin- gate
Sca1hicKIThi
B
Abs. number LSK cells
BM
BM+dmPGE2
BM+MSC
BM+MSC (indo)
C
Abs. number cells (x10⁴)
BM
BM+dmPGE2
BM+MSC
BM+MSC(indo)
CD19+
NK1.1+
CD11b+

Figure 4. MSCs increase BM CFU and differentiation capabilities. BM cells ($5x10^6$) were incubated overnight over a semi-permeable membrane either alone or with $dmPGE_2$ (20uM), MSCs ($1x10^5$), or MSCs pretreated with indomethacin. BM cells were harvested from each group and $1x10^5$ cells were plated in methylcellulose medium for a period of 12 days. (A) Total number of colonies in each plate was counted. (B) Colony type was enumerated for each group and graphed.

Figure 4

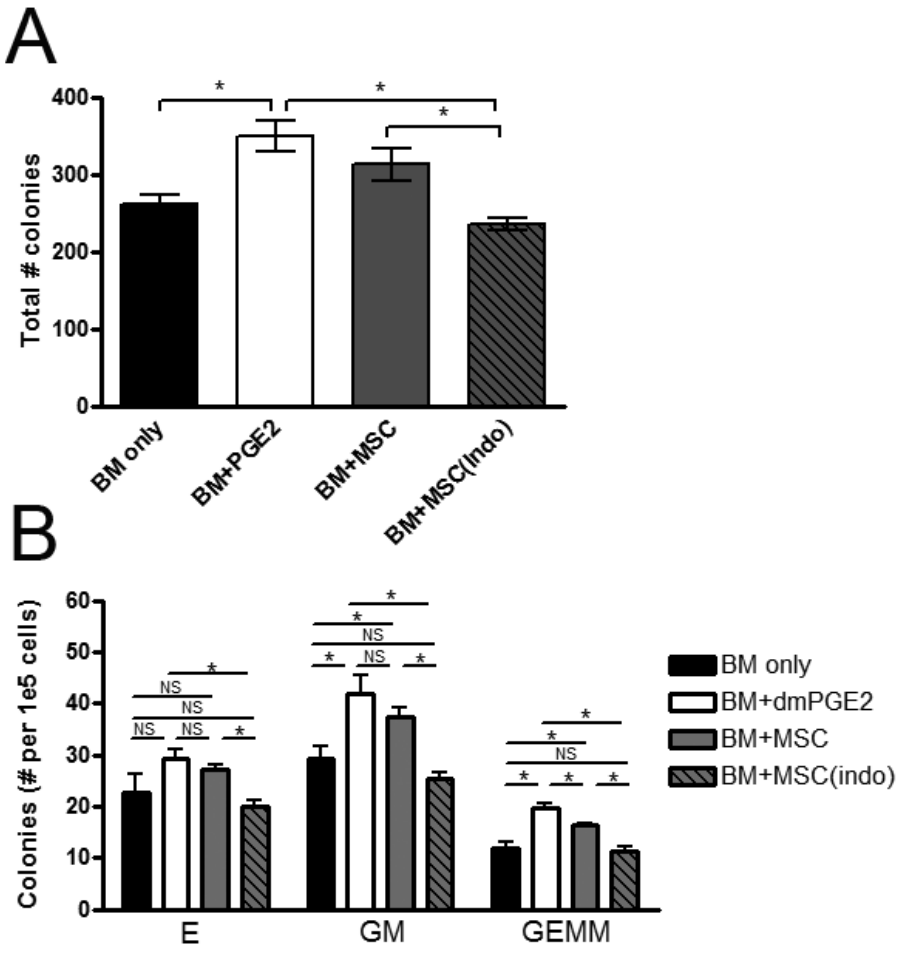
A
Total # colonies
400
300
200
100
0
BM only
BM+PGE2
BM+MSC
BM+MSC(indo)
B
Colonies (# per 1e5 cells)
60
50
40
30
20
10
0
NS
E
GM
GEMM
BM only
BM+dmPGE2
BM+MSC
BM+MSC(indo)

Figure 5. MSC increase primitive CFU-S number and splenic weight post transplant. BM cells ($5x10^6$) were incubated overnight over a semi-permeable membrane either alone or with dmPGE2 (20uM), MSCs ($1x10^5$), or MSCs pretreated with indomethacin. BM cells were harvested from each group and $7x10^4$ cells were injected into lethally irradiated B6 recipients. On day 12 post-transplant, spleens were dissected from these mice and CFU-S colonies were photographed (A) and counted (B). (C) Splenic weight was determined and graphed.

Figure 5

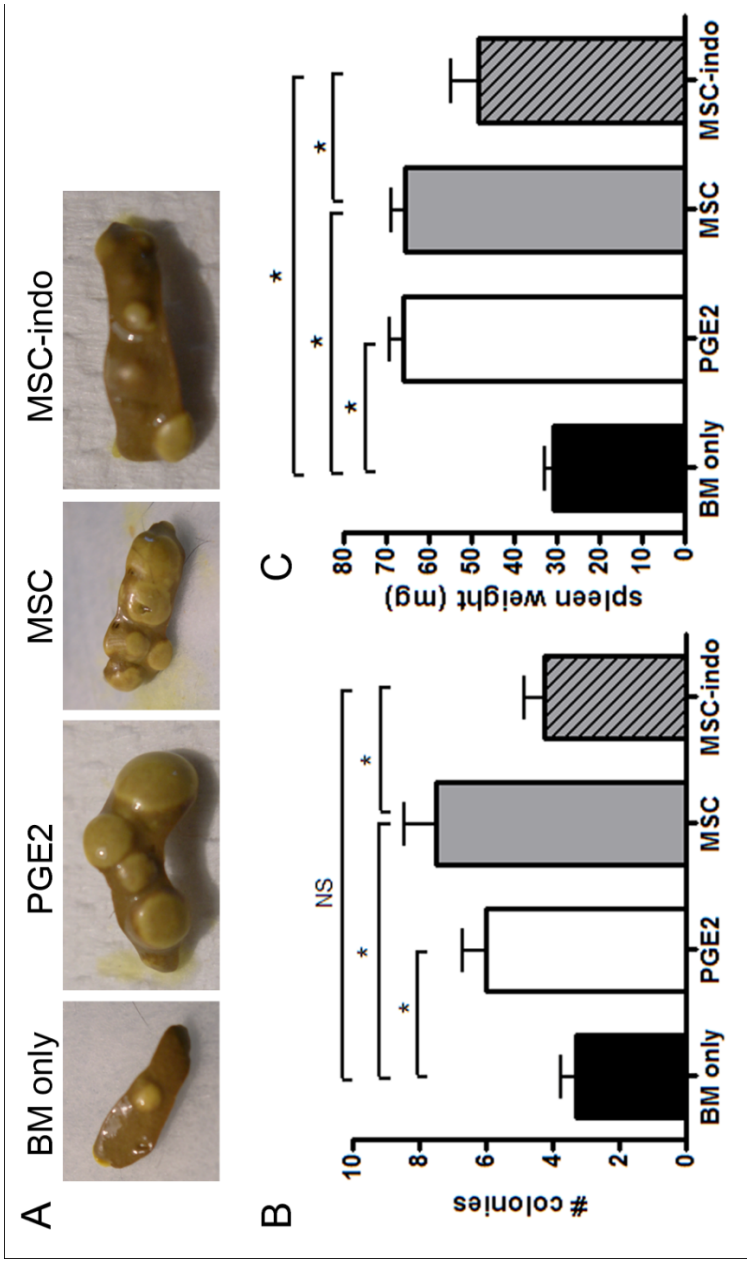
A
BM only
PGE2
MSC
MSC-indo
B
colonies
NS
*
C
spleen weight (mg)
BM only
PGE2
MSC
MSC-indo

Chapter 5:

Concluding Statements

Allogeneic bone marrow transplantation (BMT) offers hope to large number of individuals with a wide variety of malignant and non-malignant disorders. Unfortunately, the potential development of graft versus host disease (GVHD) due to antigenetic differences between donor and host constrains its wider application. Much progress has been made in the field since its conception and GVHD can now be avoided entirely through the administration of T-cell depleted BM grafts. Unfortunately, the same T-cells that cause GVHD also offer a beneficial graft versus leukemia (GVL) effect and relapse rates for patients who develop GVHD are considerably lower compared with relapse rates in patients who do not develop GVHD. Efforts are now being made to provide means by which we can dampen excessive allo-immune responses and thereby lessen the severity of GVHD but, at the same time, retain the anti-tumor properties of donor T-cells. In this regard, cellular therapy is an attractive option because it can provide this immune dampening effect without leaving the host entirely immune-compromised.

Results outlined here show cell therapy modulation of GVHD to be critically dependent on the trafficking of suppressor cells to sites of allogeneic T-cell priming. For instance, in chapter 2 we observed an attenuation of GVHD only when multipotent adult progenitor cells (MAPC) were administered directly within the spleen. In this setting we found that there were direct negative regulatory effects on donor T-cells within the same

microenvironment, which included decreased proliferation and decreased activation. In chapter 3, we found that myeloid-derived suppressor cells expressed the lymphoid homing molecule L-selectin (CD62L). This directed them to the sites of allo-priming where they exerted their immune-suppressive effects and resulted in a significant increase in GVHD survival. This is in accordance with other reports describing the ability of regulatory T-cells (Tregs) to inhibit GVHD only when they express CD62L.[53] This also agrees with results published by Sudres *et al*. in which mesenchymal stem cells (MSCs) were found to have no beneficial effect in GVHD survival despite their ability to potently inhibit allo-immune responses *in vitro*.[71] Here, MSCs were found to have preferentially migrated to the BM cavity and therefore had no contact with donor T-cells becoming primed within the secondary lymphoid organs (SLO).[71] These results highlight the importance of suppressor cell trafficking when attempting to modulate GVHD.

There are numerous inhibitory mechanisms utilized by suppressor cells that result in immune modulation. In general, these suppressive mechanisms can be divided into 3 categories: contact-mediated suppression via cell-cell interactions, secretion of inhibitory cytokines, and the depletion of growth factors necessary for survival. In the studies outlined here, we pinpoint the suppressive capacity of MAPCs primarily to the secretion of a well known anti-inflammatory cytokine, prostaglandin E_2 (PGE_2). The inhibition of T-cell proliferation by PGE_2 is well established.[110] *In vitro* inhibition of T-cell proliferation by MAPCs and enhancement of GVHD survival were both abrogated when using MAPCs unable to produce PGE_2. These were the first studies to identify a mechanism of action of MAPCs and also the first to show that in order for this

mechanism to be effective the cells needed to be located within the SLOs, presumably due to the short half-life of PGE_2 *in vivo*.

In studies using myeloid-derived suppressor cells (MDSCs), we found that suppression of GVHD was governed primarily by the expression of arginase-1. The depletion of the amino acid L-arginine by MDSCs during T-cell priming resulted in the downregulation of the intracellular signaling molecule CD3ζ in allogeneic T-cells and left them unable to mount a strong immunological response. Although most of the inhibitory attributes of MDSCs were ascribed to the depletion of L-arginine, as was evident from experiments in which L-arginine was added back to the culture medium, a significant portion of the suppressive capacity relied on cell-cell contact. Due to the high expression levels of PDL1 in MDSCs, we speculated that this negative regulatory mechanism may be important for this aspect of suppression, however, we have yet to verify this hypothesis. This observation underscores the fact that there can be, and are usually are, multiple mechanisms of action occurring simultaneously that act synergistically to restrain immune hyper-activation. It will be important to determine the precise mechanism(s) of action to help us better design potential clinical trials.

In addition to GVHD, bone marrow graft rejection is also a major complication of bone marrow transplantation. In chapter 4, we examined the potential of mesenchymal stem cells (MSCs) to influence engraftment through the secretion of PGE_2. Our findings conclude that the secretion of PGE_2 by MSCs increases the absolute number of lineage$^-$ Sca-1$^+$cKit$^+$ (LSK) hematopoietic stem cells (HSCs), increases the differentiation potential of HSCs, and increases primitive CFU-S cells *in vivo*. These exciting new findings link a mechanism of action to the well-documented engraftment-enhancing

abilities of MSCs (reviewed in [181]). The studies carried out here have all relied on the *ex vivo* treatment of BM cells with MSCs through a semi-permeable membrane. The benefit of this experimental design was that it allowed for us to specifically target PGE_2 as a potential mechanism of action by directly comparing MSCs that produce PGE_2 to MSCs in which we blocked the production of PGE_2. The fallback of this design is that it does not address the direct ability of MSCs to enhance engraftment *in vivo*. Numerous reports show that MSCs efficiently migrate to the bone marrow shortly after injection,[182] and we predict that this increases the concentration of PGE_2 within the bone marrow niche. The local increase in PGE_2 would result in a remodeling of the BM niche to better support hematopoiesis[183], and have direct effects on HSCs themselves by binding to EP receptors and enhancing their survival and proliferation.[163] Our studies provide the framework that identifies the positive impact of MSC-derived PGE_2 on HSCs using *ex vivo* treatment, however, further studies need to be performed using MSCs with and without the ability to produce PGE_2 *in vivo* (perhaps isolated from COX2 KO mice) in order to verify our hypothesis.

In summary, this dissertation research explores the use of novel cell-based methods with which we can use to prevent GVHD and enhance BM engraftment. These studies reveal that cell-based therapies can have potent inhibitory effects on GVHD-causing T-cells, and at the same time be significantly less toxic than some of the drug-based therapies currently utilized in the clinic. In addition, we explore a novel mechanism of action by which cells can positively influence BM engraftment. The body of work outlined here takes us one step closer in achieving our goal of having cellular options more readily available to patients requiring allogeneic BMT.

Bibliography:

1. Lorenz E, Uphoff D, Reid TR, Shelton E. Modification of irradiation injury in mice and guinea pigs by bone marrow injections. J Natl Cancer Inst. 1951;12:197-201

2. Barnes DW, Loutit JF. The radiation recovery factor: preservation by the Polge-Smith-Parkes technique. J Natl Cancer Inst. 1955;15:901-905

3. Billingham RE. The biology of graft-versus-host reactions. Harvey Lect. 1966;62:21-78

4. Simonsen M. Graft versus host reactions. Their natural history, and applicability as tools of research. Prog Allergy. 1962;6:349-467

5. Lindahl KF, Wilson DB. Histocompatibility antigen-activated cytotoxic T lymphocytes. II. Estimates of the frequency and specificity of precursors. J Exp Med. 1977;145:508-522

6. Robinson J, Waller MJ, Parham P, de Groot N, Bontrop R, Kennedy LJ, Stoehr P, Marsh SG. IMGT/HLA and IMGT/MHC: sequence databases for the study of the major histocompatibility complex. Nucleic Acids Res. 2003;31:311-314

7. Afzali B, Lechler RI, Hernandez-Fuentes MP. Allorecognition and the alloresponse: clinical implications. Tissue Antigens. 2007;69:545-556

8. Lechler RI, Lombardi G, Batchelor JR, Reinsmoen N, Bach FH. The molecular basis of alloreactivity. Immunol Today. 1990;11:83-88

9. Fangmann J, Dalchau R, Sawyer GJ, Priestley CA, Fabre JW. T cell recognition of donor major histocompatibility complex class I peptides during allograft rejection. Eur J Immunol. 1992;22:1525-1530

10. Simpson E, Scott D, James E, Lombardi G, Cwynarski K, Dazzi F, Millrain M, Dyson PJ. Minor H antigens: genes and peptides. Transpl Immunol. 2002;10:115-123

11. Piper KP, McLarnon A, Arrazi J, Horlock C, Ainsworth J, Kilby MD, Martin WL, Moss PA. Functional HY-specific CD8+ T cells are found in a high proportion of women following pregnancy with a male fetus. Biol Reprod. 2007;76:96-101

12. CIBMTR. Center for International Blood and Marrow Transplantation Research. Progress Report. 2009

13. Glucksberg H, Storb R, Fefer A, Buckner CD, Neiman PE, Clift RA, Lerner KG, Thomas ED. Clinical manifestations of graft-versus-host disease in human recipients of marrow from HL-A-matched sibling donors. Transplantation. 1974;18:295-304

14. Blazar BR, Taylor PA, McElmurry R, Tian L, Panoskaltsis-Mortari A, Lam S, Lees C, Waldschmidt T, Vallera DA. Engraftment of severe combined immune deficient mice receiving allogeneic bone marrow via In utero or postnatal transfer. Blood. 1998;92:3949-3959

15. Hill GR, Crawford JM, Cooke KR, Brinson YS, Pan L, Ferrara JL. Total body irradiation and acute graft-versus-host disease: the role of gastrointestinal damage and inflammatory cytokines. Blood. 1997;90:3204-3213

16. Antin JH. Acute graft-versus-host disease: inflammation run amok? J Clin Invest. 2001;107:1497-1498

17. Fietta P, Delsante G. The effector T helper cell triade. Riv Biol. 2009;102:61-74

18. Wysocki CA, Panoskaltsis-Mortari A, Blazar BR, Serody JS. Leukocyte migration and graft-versus-host disease. Blood. 2005;105:4191-4199

19. Varona R, Cadenas V, Gomez L, Martinez AC, Marquez G. CCR6 regulates CD4+ T-cell-mediated acute graft-versus-host disease responses. Blood. 2005;106:18-26

20. Duffner U, Lu B, Hildebrandt GC, Teshima T, Williams DL, Reddy P, Ordemann R, Clouthier SG, Lowler K, Liu C, Gerard C, Cooke KR, Ferrara JL. Role of CXCR3-induced donor T-cell migration in acute GVHD. Exp Hematol. 2003;31:897-902

21. Terwey TH, Kim TD, Kochman AA, Hubbard VM, Lu S, Zakrzewski JL, Ramirez-Montagut T, Eng JM, Muriglan SJ, Heller G, Murphy GF, Liu C, Budak-Alpdogan T, Alpdogan O, van den Brink MR. CCR2 is required for CD8-induced graft-versus-host disease. Blood. 2005;106:3322-3330

22. Reddy P. Pathophysiology of acute graft-versus-host disease. Hematol Oncol. 2003;21:149-161

23. Sleight BS, Chan KW, Braun TM, Serrano A, Gilman AL. Infliximab for GVHD therapy in children. Bone Marrow Transplant. 2007;40:473-480

24. Busca A, Locatelli F, Marmont F, Ceretto C, Falda M. Recombinant human soluble tumor necrosis factor receptor fusion protein as treatment for steroid refractory graft-versus-host disease following allogeneic hematopoietic stem cell transplantation. Am J Hematol. 2007;82:45-52

25. Bolitho P, Voskoboinik I, Trapani JA, Smyth MJ. Apoptosis induced by the lymphocyte effector molecule perforin. Curr Opin Immunol. 2007;19:339-347

26. Klas C, Debatin KM, Jonker RR, Krammer PH. Activation interferes with the APO-1 pathway in mature human T cells. Int Immunol. 1993;5:625-630

27. Krammer PH. CD95's deadly mission in the immune system. Nature. 2000;407:789-795

28. Jones JM, Wilson R, Bealmear PM. Mortality and gross pathology of secondary disease in germfree mouse radiation chimeras. Radiat Res. 1971;45:577-588

29. van Bekkum DW, Roodenburg J, Heidt PJ, van der Waaij D. Mitigation of secondary disease of allogeneic mouse radiation chimeras by modification of the intestinal microflora. J Natl Cancer Inst. 1974;52:401-404

30. Beelen DW, Haralambie E, Brandt H, Linzenmeier G, Muller KD, Quabeck K, Sayer HG, Graeven U, Mahmoud HK, Schaefer UW. Evidence that sustained growth suppression of intestinal anaerobic bacteria reduces the risk of acute graft-versus-host disease after sibling marrow transplantation. Blood. 1992;80:2668-2676

31. Panoskaltsis-Mortari A, Lacey DL, Vallera DA, Blazar BR. Keratinocyte growth factor administered before conditioning ameliorates graft-versus-host disease after allogeneic bone marrow transplantation in mice. Blood. 1998;92:3960-3967

32. Korngold R, Marini JC, de Baca ME, Murphy GF, Giles-Komar J. Role of tumor necrosis factor-alpha in graft-versus-host disease and graft-versus-leukemia responses. Biol Blood Marrow Transplant. 2003;9:292-303

33. Couriel DR, Hicks K, Giralt S, Champlin RE. Role of tumor necrosis factor-alpha inhibition with inflixiMAB in cancer therapy and hematopoietic stem cell transplantation. Curr Opin Oncol. 2000;12:582-587

34. Miwa K, Hashimoto H, Yatomi T, Nakamura N, Nagata S, Suda T. Therapeutic effect of an anti-Fas ligand mAb on lethal graft-versus-host disease. Int Immunol. 1999;11:925-931

35. Barnes DW, Corp MJ, Loutit JF, Neal FE. Treatment of murine leukaemia with X rays and homologous bone marrow; preliminary communication. Br Med J. 1956;2:626-627

36. Weiden PL, Flournoy N, Thomas ED, Prentice R, Fefer A, Buckner CD, Storb R. Antileukemic effect of graft-versus-host disease in human recipients of allogeneic-marrow grafts. N Engl J Med. 1979;300:1068-1073

37. Marmont AM, Horowitz MM, Gale RP, Sobocinski K, Ash RC, van Bekkum DW, Champlin RE, Dicke KA, Goldman JM, Good RA, et al. T-cell depletion of HLA-identical transplants in leukemia. Blood. 1991;78:2120-2130

38. Ringden O, Zwaan F, Hermans J, Gratwohl A. European experience of bone marrow transplantation for leukemia. Transplant Proc. 1987;19:2600-2604

39. Ringden O, Labopin M, Gorin NC, Schmitz N, Schaefer UW, Prentice HG, Bergmann L, Jouet JP, Mandelli F, Blaise D, Fouillard L, Frassoni F. Is there a graft-versus-leukaemia effect in the absence of graft-versus-host disease in patients undergoing bone marrow transplantation for acute leukaemia? Br J Haematol. 2000;111:1130-1137

40. Lundqvist A, McCoy JP, Samsel L, Childs R. Reduction of GVHD and enhanced antitumor effects after adoptive infusion of alloreactive Ly49-mismatched NK cells from MHC-matched donors. Blood. 2007;109:3603-3606

41. Miller JS, Soignier Y, Panoskaltsis-Mortari A, McNearney SA, Yun GH, Fautsch SK, McKenna D, Le C, Defor TE, Burns LJ, Orchard PJ, Blazar BR, Wagner JE, Slungaard A, Weisdorf DJ, Okazaki IJ, McGlave PB. Successful adoptive transfer and in vivo expansion of human haploidentical NK cells in patients with cancer. Blood. 2005;105:3051-3057

42. Brunkow ME, Jeffery EW, Hjerrild KA, Paeper B, Clark LB, Yasayko SA, Wilkinson JE, Galas D, Ziegler SF, Ramsdell F. Disruption of a new forkhead/winged-helix protein, scurfin, results in the fatal lymphoproliferative disorder of the scurfy mouse. Nat Genet. 2001;27:68-73

43. Ermann J, Szanya V, Ford GS, Paragas V, Fathman CG, Lejon K. CD4(+)CD25(+) T cells facilitate the induction of T cell anergy. J Immunol. 2001;167:4271-4275

44. Martin B, Banz A, Bienvenu B, Cordier C, Dautigny N, Becourt C, Lucas B. Suppression of CD4+ T lymphocyte effector functions by CD4+CD25+ cells in vivo. J Immunol. 2004;172:3391-3398

45. Takahashi T, Tagami T, Yamazaki S, Uede T, Shimizu J, Sakaguchi N, Mak TW, Sakaguchi S. Immunologic self-tolerance maintained by CD25(+)CD4(+) regulatory T cells constitutively expressing cytotoxic T lymphocyte-associated antigen 4. J Exp Med. 2000;192:303-310

46. Shimizu J, Yamazaki S, Takahashi T, Ishida Y, Sakaguchi S. Stimulation of CD25(+)CD4(+) regulatory T cells through GITR breaks immunological self-tolerance. Nat Immunol. 2002;3:135-142

47. Raimondi G, Shufesky WJ, Tokita D, Morelli AE, Thomson AW. Regulated compartmentalization of programmed cell death-1 discriminates CD4+CD25+ resting regulatory T cells from activated T cells. J Immunol. 2006;176:2808-2816

48. Sundstedt A, O'Neill EJ, Nicolson KS, Wraith DC. Role for IL-10 in suppression mediated by peptide-induced regulatory T cells in vivo. J Immunol. 2003;170:1240-1248

49. Chen ZM, O'Shaughnessy MJ, Gramaglia I, Panoskaltsis-Mortari A, Murphy WJ, Narula S, Roncarolo MG, Blazar BR. IL-10 and TGF-beta induce alloreactive CD4+CD25- T cells to acquire regulatory cell function. Blood. 2003;101:5076-5083

50. Hoffmann P, Ermann J, Edinger M, Fathman CG, Strober S. Donor-type CD4(+)CD25(+) regulatory T cells suppress lethal acute graft-versus-host disease after allogeneic bone marrow transplantation. J Exp Med. 2002;196:389-399

51. Taylor PA, Lees CJ, Blazar BR. The infusion of ex vivo activated and expanded CD4(+)CD25(+) immune regulatory cells inhibits graft-versus-host disease lethality. Blood. 2002;99:3493-3499

52. Jones SC, Murphy GF, Korngold R. Post-hematopoietic cell transplantation control of graft-versus-host disease by donor CD425 T cells to allow an effective graft-versus-leukemia response. Biol Blood Marrow Transplant. 2003;9:243-256

53. Taylor PA, Panoskaltsis-Mortari A, Swedin JM, Lucas PJ, Gress RE, Levine BL, June CH, Serody JS, Blazar BR. L-Selectin(hi) but not the L-selectin(lo) CD4+25+ T-regulatory cells are potent inhibitors of GVHD and BM graft rejection. Blood. 2004;104:3804-3812

54. Edinger M, Hoffmann P, Ermann J, Drago K, Fathman CG, Strober S, Negrin RS. CD4+CD25+ regulatory T cells preserve graft-versus-tumor activity while inhibiting graft-versus-host disease after bone marrow transplantation. Nat Med. 2003;9:1144-1150

55. Firan M, Dhillon S, Estess P, Siegelman MH. Suppressor activity and potency among regulatory T cells is discriminated by functionally active CD44. Blood. 2006;107:619-627

56. Hanash AM, Levy RB. Donor CD4+CD25+ T cells promote engraftment and tolerance following MHC-mismatched hematopoietic cell transplantation. Blood. 2005;105:1828-1836

57. Joffre O, Gorsse N, Romagnoli P, Hudrisier D, van Meerwijk JP. Induction of antigen-specific tolerance to bone marrow allografts with CD4+CD25+ T lymphocytes. Blood. 2004;103:4216-4221

58. MacMillan M. Donor T-cells in treating patients with high-risk hematologic cancer undergoing donor peripheral blood stem cell transplant. Clinical Trial NCT007250062. 2008

59. Brunstein C. T-regulatory cell infusion post umbilical blood transplant in patients with advanced hematologic cancer. Clinical Trial NCT00602693. 2008

60. Pittenger MF, Mackay AM, Beck SC, Jaiswal RK, Douglas R, Mosca JD, Moorman MA, Simonetti DW, Craig S, Marshak DR. Multilineage potential of adult human mesenchymal stem cells. Science. 1999;284:143-147

61. Ciavarella S, Dammacco F, De Matteo M, Loverro G, Silvestris F. Umbilical cord mesenchymal stem cells: role of regulatory genes in their differentiation to osteoblasts. Stem Cells Dev. 2009;18:1211-1220

62. Gronthos S, Franklin DM, Leddy HA, Robey PG, Storms RW, Gimble JM. Surface protein characterization of human adipose tissue-derived stromal cells. J Cell Physiol. 2001;189:54-63

63. Zvaifler NJ, Marinova-Mutafchieva L, Adams G, Edwards CJ, Moss J, Burger JA, Maini RN. Mesenchymal precursor cells in the blood of normal individuals. Arthritis Res. 2000;2:477-488

64. in 't Anker PS, Noort WA, Kruisselbrink AB, Scherjon SA, Beekhuizen W, Willemze R, Kanhai HH, Fibbe WE. Nonexpanded primary lung and bone marrow-derived mesenchymal cells promote the engraftment of umbilical cord blood-derived CD34(+) cells in NOD/SCID mice. Exp Hematol. 2003;31:881-889

65. Campagnoli C, Roberts IA, Kumar S, Bennett PR, Bellantuono I, Fisk NM. Identification of mesenchymal stem/progenitor cells in human first-trimester fetal blood, liver, and bone marrow. Blood. 2001;98:2396-2402

66. Prockop DJ. Marrow stromal cells as stem cells for nonhematopoietic tissues. Science. 1997;276:71-74

67. Di Nicola M, Carlo-Stella C, Magni M, Milanesi M, Longoni PD, Matteucci P, Grisanti S, Gianni AM. Human bone marrow stromal cells suppress T-lymphocyte proliferation induced by cellular or nonspecific mitogenic stimuli. Blood. 2002;99:3838-3843

68. Krampera M, Glennie S, Dyson J, Scott D, Laylor R, Simpson E, Dazzi F. Bone marrow mesenchymal stem cells inhibit the response of naive and memory antigen-specific T cells to their cognate peptide. Blood. 2003;101:3722-3729

69. Aggarwal S, Pittenger MF. Human mesenchymal stem cells modulate allogeneic immune cell responses. Blood. 2005;105:1815-1822

70. DelaRosa O, Lombardo E, Beraza A, Mancheno-Corvo P, Ramirez C, Menta R, Rico L, Camarillo E, Garcia L, Abad JL, Trigueros C, Delgado M, Buscher D. Requirement of IFN-gamma-mediated indoleamine 2,3-dioxygenase expression in the modulation of lymphocyte proliferation by human adipose-derived stem cells. Tissue Eng Part A. 2009;15:2795-2806

71. Sudres M, Norol F, Trenado A, Gregoire S, Charlotte F, Levacher B, Lataillade JJ, Bourin P, Holy X, Vernant JP, Klatzmann D, Cohen JL. Bone marrow mesenchymal stem cells suppress lymphocyte proliferation in vitro but fail to prevent graft-versus-host disease in mice. J Immunol. 2006;176:7761-7767

72. Lee ST, Jang JH, Cheong JW, Kim JS, Maemg HY, Hahn JS, Ko YW, Min YH. Treatment of high-risk acute myelogenous leukaemia by myeloablative chemoradiotherapy followed by co-infusion of T cell-depleted haematopoietic stem cells and culture-expanded marrow mesenchymal stem cells from a related donor with one fully mismatched human leucocyte antigen haplotype. Br J Haematol. 2002;118:1128-1131

73. Le Blanc K, Frassoni F, Ball L, Locatelli F, Roelofs H, Lewis I, Lanino E, Sundberg B, Bernardo ME, Remberger M, Dini G, Egeler RM, Bacigalupo A, Fibbe W, Ringden O. Mesenchymal stem cells for treatment of steroid-resistant, severe, acute graft-versus-host disease: a phase II study. Lancet. 2008;371:1579-1586

74. Osiris Therapeutics. Safety and efficacy study of adult human mesenchymal stem cells to treat acute GVHD. Clinical Trial NCT00136903. 2005

75. Wang L, Zhao RC. Mesenchymal stem cells targeting the GVHD. Sci China C Life Sci. 2009;52:603-609

76. Osiris Therapeutics. Expanded access of PROCHYMAL infusion for the treatment of pediatric patients who have failed to respond to steroid treatment for acute GVHD. Clinical Trial NCT00759018. 2008

77. Osiris Therapeutics. Osiris Therapeutics news release. Feb 24, 2010

78. Ning H, Yang F, Jiang M, Hu L, Feng K, Zhang J, Yu Z, Li B, Xu C, Li Y, Wang J, Hu J, Lou X, Chen H. The correlation between cotransplantation of mesenchymal stem cells and higher recurrence rate in hematologic malignancy patients: outcome of a pilot clinical study. Leukemia. 2008;22:593-599

79. Jiang Y, Vaessen B, Lenvik T, Blackstad M, Reyes M, Verfaillie CM. Multipotent progenitor cells can be isolated from postnatal murine bone marrow, muscle, and brain. Exp Hematol. 2002;30:896-904

80. Jiang Y, Jahagirdar BN, Reinhardt RL, Schwartz RE, Keene CD, Ortiz-Gonzalez XR, Reyes M, Lenvik T, Lund T, Blackstad M, Du J, Aldrich S, Lisberg A, Low WC, Largaespada DA, Verfaillie CM. Pluripotency of mesenchymal stem cells derived from adult marrow. Nature. 2002;418:41-49

81. Bronte V, Wang M, Overwijk WW, Surman DR, Pericle F, Rosenberg SA, Restifo NP. Apoptotic death of CD8+ T lymphocytes after immunization: induction of a suppressive population of Mac-1+/Gr-1+ cells. J Immunol. 1998;161:5313-5320

82. Kusmartsev S, Cheng F, Yu B, Nefedova Y, Sotomayor E, Lush R, Gabrilovich D. All-trans-retinoic acid eliminates immature myeloid cells from tumor-bearing mice and improves the effect of vaccination. Cancer Res. 2003;63:4441-4449

83. Terabe M, Matsui S, Park JM, Mamura M, Noben-Trauth N, Donaldson DD, Chen W, Wahl SM, Ledbetter S, Pratt B, Letterio JJ, Paul WE, Berzofsky JA. Transforming growth factor-beta production and myeloid cells are an effector mechanism through which CD1d-restricted T cells block cytotoxic T lymphocyte-mediated tumor immunosurveillance: abrogation prevents tumor recurrence. J Exp Med. 2003;198:1741-1752

84. Kusmartsev S, Nefedova Y, Yoder D, Gabrilovich DI. Antigen-specific inhibition of CD8+ T cell response by immature myeloid cells in cancer is mediated by reactive oxygen species. J Immunol. 2004;172:989-999

85. Rodriguez PC, Quiceno DG, Zabaleta J, Ortiz B, Zea AH, Piazuelo MB, Delgado A, Correa P, Brayer J, Sotomayor EM, Antonia S, Ochoa JB, Ochoa AC. Arginase I production in the tumor microenvironment by mature myeloid cells inhibits T-cell receptor expression and antigen-specific T-cell responses. Cancer Res. 2004;64:5839-5849

86. Peranzoni E, Marigo I, Dolcetti L, Ugel S, Sonda N, Taschin E, Mantelli B, Bronte V, Zanovello P. Role of arginine metabolism in immunity and immunopathology. Immunobiology. 2007;212:795-812

87. Gabrilovich D. Mechanisms and functional significance of tumour-induced dendritic-cell defects. Nat Rev Immunol. 2004;4:941-952

88. Lee J, Ryu H, Ferrante RJ, Morris SM, Jr., Ratan RR. Translational control of inducible nitric oxide synthase expression by arginine can explain the arginine paradox. Proc Natl Acad Sci U S A. 2003;100:4843-4848

89. Zhang P, McGrath BC, Reinert J, Olsen DS, Lei L, Gill S, Wek SA, Vattem KM, Wek RC, Kimball SR, Jefferson LS, Cavener DR. The GCN2 eIF2alpha kinase is required for adaptation to amino acid deprivation in mice. Mol Cell Biol. 2002;22:6681-6688

90. El-Gayar S, Thuring-Nahler H, Pfeilschifter J, Rollinghoff M, Bogdan C. Translational control of inducible nitric oxide synthase by IL-13 and arginine availability in inflammatory macrophages. J Immunol. 2003;171:4561-4568

91. Fibbe WE, Nauta AJ, Roelofs H. Modulation of immune responses by mesenchymal stem cells. Ann N Y Acad Sci. 2007;1106:272-278

92. Uccelli A, Moretta L, Pistoia V. Immunoregulatory function of mesenchymal stem cells. Eur J Immunol. 2006;36:2566-2573

93. Rasmusson I, Ringden O, Sundberg B, Le Blanc K. Mesenchymal stem cells inhibit lymphocyte proliferation by mitogens and alloantigens by different mechanisms. Exp Cell Res. 2005;305:33-41

94. Meisel R, Zibert A, Laryea M, Gobel U, Daubener W, Dilloo D. Human bone marrow stromal cells inhibit allogeneic T-cell responses by indoleamine 2,3-dioxygenase-mediated tryptophan degradation. Blood. 2004;103:4619-4621

95. Sato K, Ozaki K, Oh I, Meguro A, Hatanaka K, Nagai T, Muroi K, Ozawa K. Nitric oxide plays a critical role in suppression of T-cell proliferation by mesenchymal stem cells. Blood. 2007;109:228-234

96. Di Ianni M, Del Papa B, De Ioanni M, Moretti L, Bonifacio E, Cecchini D, Sportoletti P, Falzetti F, Tabilio A. Mesenchymal cells recruit and regulate T regulatory cells. Exp Hematol. 2008;36:309-318

97. Augello A, Tasso R, Negrini SM, Amateis A, Indiveri F, Cancedda R, Pennesi G. Bone marrow mesenchymal progenitor cells inhibit lymphocyte proliferation by activation of the programmed death 1 pathway. Eur J Immunol. 2005;35:1482-1490

98. Yanez R, Lamana ML, Garcia-Castro J, Colmenero I, Ramirez M, Bueren JA. Adipose tissue-derived mesenchymal stem cells have in vivo immunosuppressive properties applicable for the control of the graft-versus-host disease. Stem Cells. 2006;24:2582-2591

99. Tisato V, Naresh K, Girdlestone J, Navarrete C, Dazzi F. Mesenchymal stem cells of cord blood origin are effective at preventing but not treating graft-versus-host disease. Leukemia. 2007;21:1992-1999

100. Bruder SP, Jaiswal N, Haynesworth SE. Growth kinetics, self-renewal, and the osteogenic potential of purified human mesenchymal stem cells during extensive subcultivation and following cryopreservation. J Cell Biochem. 1997;64:278-294

101. Deans RJ, Moseley AB. Mesenchymal stem cells: biology and potential clinical uses. Exp Hematol. 2000;28:875-884

102. Tolar J, Osborn M, Bell S, McElmurry R, Xia L, Riddle M, Panoskaltsis-Mortari A, Jiang Y, McIvor RS, Contag CH, Yant SR, Kay MA, Verfaillie CM, Blazar BR. Real-time in vivo imaging of stem cells following transgenesis by transposition. Mol Ther. 2005;12:42-48

103. Gudmundsdottir H, Wells AD, Turka LA. Dynamics and requirements of T cell clonal expansion in vivo at the single-cell level: effector function is linked to proliferative capacity. J Immunol. 1999;162:5212-5223

104. Song HK, Noorchashm H, Lieu YK, Rostami S, Greeley SA, Barker CF, Naji A. In vivo MLR: a novel method for the study of alloimmune responses. Transplant Proc. 1999;31:834-835

105. Breyer A, Estharabadi N, Oki M, Ulloa F, Nelson-Holte M, Lien L, Jiang Y. Multipotent adult progenitor cell isolation and culture procedures. Exp Hematol. 2006;34:1596-1601

106. Tolar J, O'Shaughnessy M J, Panoskaltsis-Mortari A, McElmurry RT, Bell S, Riddle M, McIvor RS, Yant SR, Kay MA, Krause D, Verfaillie CM, Blazar BR. Host

factors that impact the biodistribution and persistence of multipotent adult progenitor cells. Blood. 2006;107:4182-4188

107. Prevosto C, Zancolli M, Canevali P, Zocchi MR, Poggi A. Generation of CD4+ or CD8+ regulatory T cells upon mesenchymal stem cell-lymphocyte interaction. Haematologica. 2007;92:881-888

108. Casiraghi F, Azzollini N, Cassis P, Imberti B, Morigi M, Cugini D, Cavinato RA, Todeschini M, Solini S, Sonzogni A, Perico N, Remuzzi G, Noris M. Pretransplant infusion of mesenchymal stem cells prolongs the survival of a semiallogeneic heart transplant through the generation of regulatory T cells. J Immunol. 2008;181:3933-3946

109. Takahashi HK, Iwagaki H, Yoshino T, Mori S, Morichika T, Itoh H, Yokoyama M, Kubo S, Kondo E, Akagi T, Tanaka N, Nishibori M. Prostaglandin E(2) inhibits IL-18-induced ICAM-1 and B7.2 expression through EP2/EP4 receptors in human peripheral blood mononuclear cells. J Immunol. 2002;168:4446-4454

110. Harris SG, Padilla J, Koumas L, Ray D, Phipps RP. Prostaglandins as modulators of immunity. Trends Immunol. 2002;23:144-150

111. Ruggeri P, Nicocia G, Venza I, Venza M, Valenti A, Teti D. Polyamine metabolism in prostaglandin E2-treated human T lymphocytes. Immunopharmacol Immunotoxicol. 2000;22:117-129

112. Brown DM, Warner GL, Ales-Martinez JE, Scott DW, Phipps RP. Prostaglandin E2 induces apoptosis in immature normal and malignant B lymphocytes. Clin Immunol Immunopathol. 1992;63:221-229

113. Ikegami R, Sugimoto Y, Segi E, Katsuyama M, Karahashi H, Amano F, Maruyama T, Yamane H, Tsuchiya S, Ichikawa A. The expression of prostaglandin E receptors EP2 and EP4 and their different regulation by lipopolysaccharide in C3H/HeN peritoneal macrophages. J Immunol. 2001;166:4689-4696

114. Harizi H, Juzan M, Grosset C, Rashedi M, Gualde N. Dendritic cells issued in vitro from bone marrow produce PGE(2) that contributes to the immunomodulation induced by antigen-presenting cells. Cell Immunol. 2001;209:19-28

115. Krause P, Bruckner M, Uermosi C, Singer E, Groettrup M, Legler DF. Prostaglandin E(2) enhances T-cell proliferation by inducing the costimulatory molecules OX40L, CD70, and 4-1BBL on dendritic cells. Blood. 2009;113:2451-2460

116. Li H, Guo Z, Jiang X, Zhu H, Li X, Mao N. Mesenchymal Stem Cells Alter Migratory Property of T and Dendritic Cells to Delay the Development of Murine Lethal Acute Graft-Versus-Host Disease. Stem Cells. 2008

117. Fitzpatrick FA, Aguirre R, Pike JE, Lincoln FH. The stability of 13,14-dihydro-15 keto-PGE2. Prostaglandins. 1980;19:917-931

118. Pabst R, Westermann J. The role of the spleen in lymphocyte migration. Scanning Microsc. 1991;5:1075-1079; discussion 1079-1080

119. Anderson BE, Taylor PA, McNiff JM, Jain D, Demetris AJ, Panoskaltsis-Mortari A, Ager A, Blazar BR, Shlomchik WD, Shlomchik MJ. Effects of donor T-cell trafficking and priming site on graft-versus-host disease induction by naive and memory phenotype CD4 T cells. Blood. 2008;111:5242-5251

120. Beilhack A, Schulz S, Baker J, Beilhack GF, Nishimura R, Baker EM, Landan G, Herman EI, Butcher EC, Contag CH, Negrin RS. Prevention of acute graft-

versus-host disease by blocking T-cell entry to secondary lymphoid organs. Blood. 2008;111:2919-2928

121. Clouthier SG, Ferrara JL, Teshima T. Graft-versus-host disease in the absence of the spleen after allogeneic bone marrow transplantation. Transplantation. 2002;73:1679-1681

122. Ermann J, Hoffmann P, Edinger M, Dutt S, Blankenberg FG, Higgins JP, Negrin RS, Fathman CG, Strober S. Only the CD62L+ subpopulation of CD4+CD25+ regulatory T cells protects from lethal acute GVHD. Blood. 2005;105:2220-2226

123. Wysocki CA, Jiang Q, Panoskaltsis-Mortari A, Taylor PA, McKinnon KP, Su L, Blazar BR, Serody JS. Critical role for CCR5 in the function of donor CD4+CD25+ regulatory T cells during acute graft-versus-host disease. Blood. 2005;106:3300-3307

124. Zhang N, Schröppel B, Lal G, Jakubzick C, Mao X, Chen D, Yin N, Jessberger R, Ochando JC, Ding Y, Bromberg JS. Regulatory T Cells Sequentially Migrate from Inflamed Tissues to Draining Lymph Nodes to Suppress the Alloimmune Response. 2009;30:458-469

125. Aranguren XL, McCue JD, Hendrickx B, Zhu XH, Du F, Chen E, Pelacho B, Penuelas I, Abizanda G, Uriz M, Frommer SA, Ross JJ, Schroeder BA, Seaborn MS, Adney JR, Hagenbrock J, Harris NH, Zhang Y, Zhang X, Nelson-Holte MH, Jiang Y, Billiau AD, Chen W, Prosper F, Verfaillie CM, Luttun A. Multipotent adult progenitor cells sustain function of ischemic limbs in mice. J Clin Invest. 2008;118:505-514

126. Pelacho B, Nakamura Y, Zhang J, Ross J, Heremans Y, Nelson-Holte M, Lemke B, Hagenbrock J, Jiang Y, Prosper F, Luttun A, Verfaillie CM. Multipotent adult progenitor cell transplantation increases vascularity and improves left ventricular function after myocardial infarction. J Tissue Eng Regen Med. 2007;1:51-59

127. Tolar J, Wang X, Braunlin E, McElmurry RT, Nakamura Y, Bell S, Xia L, Zhang J, Hu Q, Panoskaltsis-Mortari A, Zhang J, Blazar BR. The host immune response is essential for the beneficial effect of adult stem cells after myocardial ischemia. Exp Hematol. 2007;35:682-690

128. Kovacsovics-Bankowski M, Streeter PR, Mauch KA, Frey MR, Raber A, Hof WV, Deans R, Maziarz RT. Clinical scale expanded adult pluripotent stem cells prevent graft-versus-host disease. Cell Immunol. 2008

129. Ghansah T, Paraiso KH, Highfill S, Desponts C, May S, McIntosh JK, Wang JW, Ninos J, Brayer J, Cheng F, Sotomayor E, Kerr WG. Expansion of myeloid suppressor cells in SHIP-deficient mice represses allogeneic T cell responses. J Immunol. 2004;173:7324-7330

130. Nagaraj S, Gabrilovich DI. Myeloid-derived suppressor cells. Adv Exp Med Biol. 2007;601:213-223

131. Movahedi K, Guilliams M, Van den Bossche J, Van den Bergh R, Gysemans C, Beschin A, De Baetselier P, Van Ginderachter JA. Identification of discrete tumor-induced myeloid-derived suppressor cell subpopulations with distinct T cell-suppressive activity. Blood. 2008;111:4233-4244

132. Youn JI, Nagaraj S, Collazo M, Gabrilovich DI. Subsets of myeloid-derived suppressor cells in tumor-bearing mice. J Immunol. 2008;181:5791-5802

133. Gallina G, Dolcetti L, Serafini P, De Santo C, Marigo I, Colombo MP, Basso G, Brombacher F, Borrello I, Zanovello P, Bicciato S, Bronte V. Tumors induce a

subset of inflammatory monocytes with immunosuppressive activity on CD8+ T cells. J Clin Invest. 2006;116:2777-2790

134. Huang B, Pan PY, Li Q, Sato AI, Levy DE, Bromberg J, Divino CM, Chen SH. Gr-1+CD115+ immature myeloid suppressor cells mediate the development of tumor-induced T regulatory cells and T-cell anergy in tumor-bearing host. Cancer Res. 2006;66:1123-1131

135. Bronte V, Zanovello P. Regulation of immune responses by L-arginine metabolism. Nat Rev Immunol. 2005;5:641-654

136. Rodriguez PC, Quiceno DG, Ochoa AC. L-arginine availability regulates T-lymphocyte cell-cycle progression. Blood. 2007;109:1568-1573

137. Rodriguez PC, Zea AH, Culotta KS, Zabaleta J, Ochoa JB, Ochoa AC. Regulation of T cell receptor CD3zeta chain expression by L-arginine. J Biol Chem. 2002;277:21123-21129

138. Zhou Z, French DL, Ma G, Eisenstein S, Chen Y, Divino CM, Keller G, Chen SH, Pan PY. Development and Function of Myeloid-Derived Suppressor Cells Generated from Mouse Embryonic and Hematopoietic Stem Cells. Stem Cells. 2010

139. Munn DH, Sharma MD, Baban B, Harding HP, Zhang Y, Ron D, Mellor AL. GCN2 kinase in T cells mediates proliferative arrest and anergy induction in response to indoleamine 2,3-dioxygenase. Immunity. 2005;22:633-642

140. Serody JS, Burkett SE, Panoskaltsis-Mortari A, Ng-Cashin J, McMahon E, Matsushima GK, Lira SA, Cook DN, Blazar BR. T-lymphocyte production of macrophage inflammatory protein-1alpha is critical to the recruitment of CD8(+) T cells to the liver, lung, and spleen during graft-versus-host disease. Blood. 2000;96:2973-2980

141. Cheng PN, Lam TL, Lam WM, Tsui SM, Cheng AW, Lo WH, Leung YC. Pegylated recombinant human arginase (rhArg-peg5,000mw) inhibits the in vitro and in vivo proliferation of human hepatocellular carcinoma through arginine depletion. Cancer Res. 2007;67:309-317

142. Abe F, Dafferner AJ, Donkor M, Westphal SN, Scholar EM, Solheim JC, Singh RK, Hoke TA, Talmadge JE. Myeloid-derived suppressor cells in mammary tumor progression in FVB Neu transgenic mice. Cancer Immunol Immunother. 2010;59:47-62

143. Bronte V, Chappell DB, Apolloni E, Cabrelle A, Wang M, Hwu P, Restifo NP. Unopposed production of granulocyte-macrophage colony-stimulating factor by tumors inhibits CD8+ T cell responses by dysregulating antigen-presenting cell maturation. J Immunol. 1999;162:5728-5737

144. Shojaei F, Wu X, Qu X, Kowanetz M, Yu L, Tan M, Meng YG, Ferrara N. G-CSF-initiated myeloid cell mobilization and angiogenesis mediate tumor refractoriness to anti-VEGF therapy in mouse models. Proc Natl Acad Sci U S A. 2009;106:6742-6747

145. Highfill SL, Kelly RM, O'Shaughnessy MJ, Zhou Q, Xia L, Panoskaltsis-Mortari A, Taylor PA, Tolar J, Blazar BR. Multipotent adult progenitor cells can suppress graft-versus-host disease via prostaglandin E2 synthesis and only if localized to sites of allopriming. Blood. 2009;114:693-701

146. Munder M, Eichmann K, Modolell M. Alternative metabolic states in murine macrophages reflected by the nitric oxide synthase/arginase balance: competitive regulation by CD4+ T cells correlates with Th1/Th2 phenotype. J Immunol. 1998;160:5347-5354

147. Munn DH, Mellor AL. Indoleamine 2,3-dioxygenase and tumor-induced tolerance. J Clin Invest. 2007;117:1147-1154

148. Xia Y, Roman LJ, Masters BS, Zweier JL. Inducible nitric-oxide synthase generates superoxide from the reductase domain. J Biol Chem. 1998;273:22635-22639

149. Squadrito GL, Pryor WA. The formation of peroxynitrite in vivo from nitric oxide and superoxide. Chem Biol Interact. 1995;96:203-206

150. Groves JT. Peroxynitrite: reactive, invasive and enigmatic. Curr Opin Chem Biol. 1999;3:226-235

151. Zea AH, Rodriguez PC, Atkins MB, Hernandez C, Signoretti S, Zabaleta J, McDermott D, Quiceno D, Youmans A, O'Neill A, Mier J, Ochoa AC. Arginase-producing myeloid suppressor cells in renal cell carcinoma patients: a mechanism of tumor evasion. Cancer Res. 2005;65:3044-3048

152. Rodriguez PC, Zea AH, DeSalvo J, Culotta KS, Zabaleta J, Quiceno DG, Ochoa JB, Ochoa AC. L-arginine consumption by macrophages modulates the expression of CD3 zeta chain in T lymphocytes. J Immunol. 2003;171:1232-1239

153. Freeman GJ, Long AJ, Iwai Y, Bourque K, Chernova T, Nishimura H, Fitz LJ, Malenkovich N, Okazaki T, Byrne MC, Horton HF, Fouser L, Carter L, Ling V, Bowman MR, Carreno BM, Collins M, Wood CR, Honjo T. Engagement of the PD-1 immunoinhibitory receptor by a novel B7 family member leads to negative regulation of lymphocyte activation. J Exp Med. 2000;192:1027-1034

154. Ash DE. Structure and function of arginases. J Nutr. 2004;134:2760S-2764S; discussion 2765S-2767S

155. Hernandez CP, Morrow K, Lopez-Barcons LA, Zabaleta J, Sierra R, Velasco C, Cole J, Rodriguez PC. Pegylated arginase I: a potential therapeutic approach in T-ALL. Blood First Edition Paper. April 2010

156. Cumano A, Godin I. Ontogeny of the hematopoietic system. Annu Rev Immunol. 2007;25:745-785

157. Orkin SH, Zon LI. Hematopoiesis: an evolving paradigm for stem cell biology. Cell. 2008;132:631-644

158. Devine SM. Mesenchymal stem cells: will they have a role in the clinic? J Cell Biochem Suppl. 2002;38:73-79

159. Harizi H, Corcuff JB, Gualde N. Arachidonic-acid-derived eicosanoids: roles in biology and immunopathology. Trends Mol Med. 2008;14:461-469

160. Goetzl EJ, An S, Smith WL. Specificity of expression and effects of eicosanoid mediators in normal physiology and human diseases. FASEB J. 1995;9:1051-1058

161. Phipps RP, Stein SH, Roper RL. A new view of prostaglandin E regulation of the immune response. Immunol Today. 1991;12:349-352

162. Feher I, Gidali J. Prostaglandin E2 as stimulator of haemopoietic stem cell proliferation. Nature. 1974;247:550-551

163. Hoggatt J, Singh P, Sampath J, Pelus LM. Prostaglandin E2 enhances hematopoietic stem cell homing, survival, and proliferation. Blood. 2009;113:5444-5455

164. North TE, Goessling W, Walkley CR, Lengerke C, Kopani KR, Lord AM, Weber GJ, Bowman TV, Jang IH, Grosser T, Fitzgerald GA, Daley GQ, Orkin SH, Zon LI. Prostaglandin E2 regulates vertebrate haematopoietic stem cell homeostasis. Nature. 2007;447:1007-1011

165. Dazzi F, Ramasamy R, Glennie S, Jones SP, Roberts I. The role of mesenchymal stem cells in haemopoiesis. Blood Rev. 2006;20:161-171

166. Kim DH, Yoo KH, Yim YS, Choi J, Lee SH, Jung HL, Sung KW, Yang SE, Oh WI, Yang YS, Kim SH, Choi SY, Koo HH. Cotransplanted bone marrow derived mesenchymal stem cells (MSC) enhanced engraftment of hematopoietic stem cells in a MSC-dose dependent manner in NOD/SCID mice. J Korean Med Sci. 2006;21:1000-1004

167. Noort WA, Kruisselbrink AB, in't Anker PS, Kruger M, van Bezooijen RL, de Paus RA, Heemskerk MH, Lowik CW, Falkenburg JH, Willemze R, Fibbe WE. Mesenchymal stem cells promote engraftment of human umbilical cord blood-derived CD34(+) cells in NOD/SCID mice. Exp Hematol. 2002;30:870-878

168. Park SK, Won JH, Kim HJ, Bae SB, Kim CK, Lee KT, Lee NS, Lee YK, Jeong DC, Chung NG, Kim HS, Hong DS, Park HS. Co-transplantation of human mesenchymal stem cells promotes human CD34+ cells engraftment in a dose-dependent fashion in NOD/SCID mice. J Korean Med Sci. 2007;22:412-419

169. Peister A, Mellad JA, Larson BL, Hall BM, Gibson LF, Prockop DJ. Adult stem cells from bone marrow (MSCs) isolated from different strains of inbred mice vary in surface epitopes, rates of proliferation, and differentiation potential. Blood. 2004;103:1662-1668

170. Koc ON, Gerson SL, Cooper BW, Dyhouse SM, Haynesworth SE, Caplan AI, Lazarus HM. Rapid hematopoietic recovery after coinfusion of autologous-blood stem cells and culture-expanded marrow mesenchymal stem cells in advanced breast cancer patients receiving high-dose chemotherapy. J Clin Oncol. 2000;18:307-316

171. Le Blanc K, Samuelsson H, Gustafsson B, Remberger M, Sundberg B, Arvidson J, Ljungman P, Lonnies H, Nava S, Ringden O. Transplantation of mesenchymal stem cells to enhance engraftment of hematopoietic stem cells. Leukemia. 2007;21:1733-1738

172. Macmillan ML, Blazar BR, DeFor TE, Wagner JE. Transplantation of ex-vivo culture-expanded parental haploidentical mesenchymal stem cells to promote engraftment in pediatric recipients of unrelated donor umbilical cord blood: results of a phase I-II clinical trial. Bone Marrow Transplant. 2009;43:447-454

173. Cutler C. Reduced Intensity, Sequential Double Umbilical Cord Blood Transplantation Using Prostaglandin E2 (PGE2). NCT00890500. 2009

174. Horwitz EM, Gordon PL, Koo WK, Marx JC, Neel MD, McNall RY, Muul L, Hofmann T. Isolated allogeneic bone marrow-derived mesenchymal cells engraft and stimulate growth in children with osteogenesis imperfecta: Implications for cell therapy of bone. Proc Natl Acad Sci U S A. 2002;99:8932-8937

175. Dey I, Lejeune M, Chadee K. Prostaglandin E2 receptor distribution and function in the gastrointestinal tract. Br J Pharmacol. 2006;149:611-623

176. Ahrenstedt O, Hallgren R, Knutson L. Jejunal release of prostaglandin E2 in Crohn's disease: relation to disease activity and first-degree relatives. J Gastroenterol Hepatol. 1994;9:539-543

177. Eberhart CE, Coffey RJ, Radhika A, Giardiello FM, Ferrenbach S, DuBois RN. Up-regulation of cyclooxygenase 2 gene expression in human colorectal adenomas and adenocarcinomas. Gastroenterology. 1994;107:1183-1188

178. Resta-Lenert S, Barrett KE. Enteroinvasive bacteria alter barrier and transport properties of human intestinal epithelium: role of iNOS and COX-2. Gastroenterology. 2002;122:1070-1087

179. Belley A, Chadee K. Prostaglandin E(2) stimulates rat and human colonic mucin exocytosis via the EP(4) receptor. Gastroenterology. 1999;117:1352-1362

180. Klingemann HG, Tsoi MS, Storb R. Inhibition of prostaglandin E2 restores defective lymphocyte proliferation and cell-mediated lympholysis in recipients after allogeneic marrow grafting. Blood. 1986;68:102-107

181. Battiwalla M, Hematti P. Mesenchymal stem cells in hematopoietic stem cell transplantation. Cytotherapy. 2009;11:503-515

182. Karp JM, Leng Teo GS. Mesenchymal stem cell homing: the devil is in the details. Cell Stem Cell. 2009;4:206-216

183. Frisch BJ, Porter RL, Gigliotti BJ, Olm-Shipman AJ, Weber JM, O'Keefe RJ, Jordan CT, Calvi LM. In vivo prostaglandin E2 treatment alters the bone marrow microenvironment and preferentially expands short-term hematopoietic stem cells. Blood. 2009;114:4054-4063